Oil & Natural Gas Technology

DOE Award No.: DE-FE0024311

Final Report

Progress Report (Period Ending 30/09/2017)

Maximize Liquid Oil Production from Shale Oil and Gas Condensate Reservoirs by Cyclic Gas Injection

Project Period (01/01/2014 to 30/09/2017)

Submitted by:
James J. Sheng

Signature

Texas Tech University
DUNS #: 041367053
P.O. Box 43111
Lubbock, TX 79409-3111
Email: james.seng@ttu.edu
Phone number: (806) 834-8477

Prepared for:
United States Department of Energy
National Energy Technology Laboratory

Nov. 17, 2017

Office of Fossil Energy

Final Report:

Maximize Liquid Oil Production from Shale Oil and Gas Condensate Reservoirs by Cyclic Gas Injection

Texas Tech University (TTU)

Los Alamos National Laboratory (LANL)

Apache Corporation

Contributing authors:

TTU: Lei Li, Yang Yu, Xingbang Meng, Sharanya Sharma, Siyuan Huang, Ziqi Shen, Yao Zhang, Xiukun Wang

LANL: Bill Carey, Phong Nguyen, Mark Porter, Joaquin Jiménez-Martínez and Hari Viswanathan

Apache: Fersheed Mody, Warren Barnes, Tim Cook, Paul Griffith

DOE Award No.: DE-FE0024311

Abstract

The current technology to produce shale oil reservoirs is the primary depletion using fractured wells (generally horizontal wells). The oil recovery is less than 10%. The prize to enhance oil recovery (EOR) is big. Based on our earlier simulation study, huff-n-puff gas injection has the highest EOR potential. This project was to explore the potential extensively and from broader aspects. The huff-n-puff gas injection was compared with gas flooding, water huff-n-puff and waterflooding. The potential to mitigate liquid blockage was also studied and the gas huff-n-puff method was compared with other solvent methods. Field pilot tests were initiated but terminated owing to the low oil price and the operator's budget cut. To meet the original project objectives, efforts were made to review existing and relevant field projects in shale and tight reservoirs. The fundamental flow in nanopores was also studied.

Table of Contents

Executive Summary

The current technology to produce shale oil reservoirs is by primary depletion using fractured wells (generally horizontal wells). The oil recovery is less than 10%. The prize to enhance oil recovery (EOR) is big. This project was to explore the potential of gas injection extensively and from broader aspects. The research work completed in this project is summarized in more details below.

Extensive experimental work was performed to evaluate the EOR potentials of gas huff-n-puff injection, gas flooding, and water huff-n-puff injection in shale oil cores. Nitrogen (N_2) was used as the gas. For the huff-n-puff gas injection mode, soaking time increased oil recovery within a single cycle. However, with the same period of time, a longer soaking time resulted in less time for injection and production, and as a result, less total oil could be produced. More oil was produced when the pressure was depleted faster.

The N2 flooding produced oil rapidly during the early injection period until gas breakthrough. Gas flooding showed similar recovery efficiency as huff-n-puff before breakthrough. After that, the production rate declined sharply. But huff-n-puff began to show more oil produced. As a result, the recovery performance of gas huff-n-puff injection was superior to gas flooding.

Water huff-n-puff had limited shale oil recovery potential with a low ultimate recovery factor (RF). It had fewer number of cycles to recover oil effectively than gas huff-n-puff process. Within a certain range, the incremental RF from a single water huff-n-puff cycle increased with the soaking period, extra longer time could not contribute to additional oil recovery. Increasing injection pressure of water huff-n-puff was beneficial to increase oil recovery. However, the recovery performance of the N2 huff-n-puff outperformed water huff-n-puff greatly when operating the two processes under the same conditions.

Shale cores of different diameters and lengths were used to study huff-n-puff EOR performance. With smaller cores, more oil was produced. To be able to predict the field performance based on experimental data, an upscale theory was developed. It is a type curve of oil recovery factor versus a dimensionless time.

For the huff-n-puff gas injection in shale, an MMP was first determined using a sand-packed slimtube. Then an MMP was determined based on the plot of oil recovery factor vs. injection pressure for a series of huff-n-puff injection in a shale core. It was found that the MMP determined from the huff-n-puff tests was about 200 psi lower than that determined from the slimtube. Our analysis revealed that during the huff period, the pressure in most parts of the shale core was lower than the injection pressure because of ultra-low permeability; as a result the injection pressure did not represent the actual pressure within the core; therefore, the MMP is lower than that from the slimtube.

Because of the limited CT resolution, the gas penetration depth could not be directly observed. Instead, huff-n-puff experiments were history-matched and the model results were analyzed to investigate the gas penetration depth. Although the gas penetration was high relatively to the core size, it is very shallow (< 1 ft.) in field scale. And it is strongly dependent on natural fracture density; with higher fracture density, more gas can penetrate into the matrix.

The pores in shale rock are in the order of nanometers. It is well known that gas injection can result in asphaltene deposition, thus reducing rock permeability. Such permeability reduction in shale and tight formation may be relatively significant. The experiments and simulation analysis showed that the shale permeability reduction could be from 26.8% in the first cycle to 48.5% in the 6^{th} cycle.

In gas condensate reservoirs, as the pressure decreases lower than the dew point pressure, condensate forms. This liquid dropout reduces gas relative permeability. As a consequence, gas production is decreased and liquid dropout-condensate remains in the reservoir. To mitigate this liquid blockage, several methods were studied: gas huff-n-puff injection, gas flooding, and solvent (methanol and isopropanol) injection. It was found that gas huff-n-puff injection is more effective than gas flooding. A very important mechanism is vaporization. In addition, gas huff-n-puff is more effective than solvent huff-n-puff injection. Ethane was determined to be the best among hydrocarbon gases and solvents.

In terms of the field pilot test in a shale oil reservoir, a sector model was built using the reservoir and fluid properties in the Wolfcamp formation in the Apache's Lin field. A typical production gas and oil rate histories and the well bottom-hole flowing pressure were reasonably matched. Facility injection capacity was considered in the design of a pilot test, such as compressor capacity, injection and production capacities. A typical huff-n-puff injection scheme was 1 month injection and 3 month production. For the field test in a gas condensate reservoir, we used the PVT data from an Apache gas condensate reservoir to conduct a simulation study to prepare for the field test. However, due to the spending budget cuts within Apache, Apache terminated the field tests. Because of that, efforts were made to collect existing project data to understand field performance.

It is much easier to inject gas in shale and tight reservoirs than to inject water or other liquids. In addition, air has immerse availability and free resources, and air injection may have heat effect. We initiated a study to explore the feasibility and effects of air injection in shale and tight reservoirs. Although simulation data demonstrated the benefit of incremental oil recovery of air injection over flue gas injection, the preliminary results from our experimental work did not show significant heat benefits from air injection.

Because of nanopores, the interactions between shale rock and fluids become very important. We studied such interactions result in several phenomena in terms of flow transport: slip flow which enhances permeability, and low-velocity non-Darcy flow.

To further study gas injection in nanopores, a microfluidic system was used to observe pore-scale fluid displacement and mobilization. The experiments at reservoir conditions compared the relative efficiency of energized fluids (supercritical carbon dioxide and nitrogen) with incompressible water. The experiments revealed the importance of gas dissolution into the hydrocarbon phase and the role of gas exsolution and gas expansion during hydrocarbon recovery (i.e., depressurization). Supercritical CO2 was particularly effective and could remove almost all of the oil from inter-connected fracture networks and substantial portions of dead-end fractures. Nitrogen was also effective but due to lower solubility was not as efficient as CO2 in the displacement and recovery of hydrocarbon.

List of Acronyms

BOE	Barrel of Oil Equivalent
BT	breakthrough
C	unit conversion factor
CH_4	methane
CO_2	Carbon dioxide
c_t	total compressibility
DSC	Differential Scanning Calorimetry
EOR	enhanced oil recovery
GC	gas chromatograph
HTO	high temperature oxidation
ITO	intermediate temperature oxidation
k	permeability
L	characteristic length
L	characteristic length
LANL	Los Alamos National Laboratory
LB	Lattice-Boltzmann
LTO	low temperature oxidation
MS	Mass Spectrometer
N_2	Nitrogen
NTC	negative temperature coefficient
p	pressure
p_D	dimensionless pressure
PDR	pressure depletion rate
PDT	pressure depletion time
PV	pore volume
r	radius
RF	recovery factor
S	saturation
SBR	small batch reactor
$scCO_2$	supercritical carbon dioxide
t	time
t_D	dimensionless time
TGA	Thermogravimetry Analysis
TPG	Threshold Pressure Gradient
TTU	Texas Tech University
t	time
t_D	dimensionless time
V	bulk volume
W	weight
x	length
Greek symbols	
φ	porosity
μ	viscosity
Subscript	
d	dry

D	Darcy or dimensionless
i	initial or element i
s	saturated

Summary of Technology Transfer

First, the project team published more than 50 papers. These papers are published in academic journals and presented in conferences. Several PhD and Master's students graduated with their theses on the project topics, and several students are continuing the research to improve oil recovery in shale reservoirs. Their theses are available for the public.

Second, the PI, James Sheng, was invited to present the project work on the following occasions:

1. Invited Discussion Leader in the SPE Forum: Enhanced Oil Recovery in Unconventional Reservoirs, San Antonia, Texas, Nov. 5-10, 2017.

2. Invited presentation at Applied Geoscience Annual Conference, Houston Geological Society (American Association of Petroleum Geologists (AAPG)), Houston, Texas, March 7-8, 2017. Presentation title: What Are We Doing about EOR in Shale and Tight Formations?

3. Invited presentation at the SPE Liquid-Rich Basins Conference – North America, Midland, Texas, 2-3 September, 2015. Presentation title: What Can We Do about Shale Resources after Frac?

4. Invited presentation at Pioneer Natural Resources EOR/IOR Workshop, Irving, Texas, Aug. 26, 2015.
5. Invited presentations by several Chinese Petroleum Universities and Petroleum companies in 2015 and 2016.

Third, one workshop was held to present our results to the delegates from Pioneer Natural Resources.

Chapter 1 Introduction

The current technology to produce shale oil reservoirs is by primary depletion using fractured wells. The oil recovery is less than 10%. The overall objective of this research was to evaluate the oil recovery potentials of cyclic gas injection.

The presentation of the research work from this project is organized in the following chapters.

1. Introduction (this chapter)
2. Experimental Study of Enhanced Shale Oil Recovery Potential by Gas (N2) Injection and Water injection
3. Effect of core sizes on huff-n-puff gas injection
4. Effect of MMP
5. Gas penetration depth in oil reservoirs
6. Upscale of huff-n-puff oil recovery from lab scale to field scale
7. Asphaltene deposition in huff-n-puff gas injection
8. EOR potential of huff-n-puff gas injection in gas condensate reservoirs
9. Comparative study of gas injection and solvent injection for shale gas condensate reservoirs
10. Design of a field pilot test
11. EOR potential of air injection
12. Non-Darcy flow mechanisms in shale and tight formations
13. Gas injection pore-scale experiments and simulation

The contents of each chapter are from several papers. These papers are already in the public domain and thus it is not necessary to repeat the presentation in detail. Therefore, for each chapter, the methodology, results and main conclusion are briefly summarized. At the proper points in the middle of each chapter or at the end of each chapter, the relevant papers are listed. The readers may refer those papers if more details are needed. At the end of this final report, those papers which were written based on this research project are listed.

Chapter 2 Experimental Study of Enhanced Shale Oil Recovery Potential by Gas (N2) Injection and Water injection

2.1 Introduction

During the past decade, the rapid shale oil production growth is attributed to horizontal drilling with multi-stage hydraulic fracturing technique. Those wells drilled into tight formations tend to have high initial production rates, but they also have steep initial decline rates over the first year or two of production. In order to extend the productive life of existing wells, enhanced oil recovery (EOR) techniques must be applied. Recent experimental and simulation studies have confirmed the EOR potential of gas injection in tight/shale reservoirs, among which the process of gas huff-n-puff injection was highlighted. However, limited experimental work has been conducted in-depth to investigate the recovery performance of gas injection, including gas flooding and gas huff-n-puff processes, in shale rocks with an ultra-low matrix permeability (less than 1 μD). Moreover, a comparative study needs to be performed on the use of various EOR strategies.

This chapter will discuss extensive experimental work that was performed to evaluate the EOR potential of gas huff-n-puff injection, gas flooding, and water huff-n-puff injection in liquid-rich shale core plugs. The experimental results reveal that the recovery performance of gas huff-n-puff injection is superior to gas flooding and much more effective than cyclic water injection. The findings will be valuable for shale oil operators when designing gas injection EOR projects. Theoretically, this study enriches the EOR mechanism of gas injection in shale reservoirs.

The research work were performed is summarized as follows.

- Investigated the oil recovery process of gas huff-n-puff injection in shale plug samples.
- Evaluated the EOR potential of gas flooding in shale plug samples.
- Compared the oil recovery performances between gas huff-n-puff and gas flooding.
- Compared the oil recovery performances between gas huff-n-puff and water huff-n-puff.

2.2 Materials and methodology

The core samples used in this study were cut from the Eagle Ford outcrop with the dimensions of 1.5-in diameter, and 2-in or 4-in length, based on the test requirements. The measured average helium porosity was 10% and the nitrogen permeability ranges 300 nD to 500 nD. The oil sample used for core plug saturation was dead oil from the Wolfcamp shale play with a density of 0.81

g/cm^3 and a viscosity of 8.7 cP, both of which were measured at the temperature of 71°F and atmospheric pressure of 13.0 psia. Nitrogen gas with a high purity of 99.999% was used as the gas source in gas injection tests.

Prior to performing an oil recovery test, the core sample was placed in an oven for drying for 1-day, and then it was placed in a vessel and vacuumed for 1-day. After that, the sample was saturated with shale oil under a constant pressure of 1,000 psi for 1-day for maximum saturation. Subsequently, the fully shale oil saturated core samples were used to conduct EOR tests.

For the N_2 huff-n-puff injection test, the effects of soaking time and pressure depletion rate on the recovery efficiency were examined and analyzed in detail. For the N_2 flooding test, the effects of operation time and injection pressure on the oil recovery factor were studied. The core-scale simulation model was built to history match experimental data to predict future oil recovery at different injection pressures. For the water huff-n-puff test, the effects of soaking time and injection pressure on the recovery performance were examined.

2.3 Investigation of N_2 huff-n-puff injection process

Gas huff-n-puff process has been demonstrated as the most effective and promising EOR solution in fractured shale reservoirs. Such process involves many operating parameters that affect the recovery performance in different degrees. This study aimed to investigate the roles of soaking time and pressure depletion rate (PDR) in the oil recovery process of huff-n-puff injection.

With the injection pressure (P_{in}) of 1,000 psi, two groups of tests were conducted in a matrix-fracture system: 1) under a constant PDR in blowout and five soaking periods changed from 0.25-hr to 48-hr; 2) under a constant soaking time of 12-hr and four pressure depletion times changed from 0.05-hr to 48-hr. For each group, two plugs were employed to go through the N_2 huff-n-puff process simultaneously. The experimental setup is shown in Fig. 2.1.

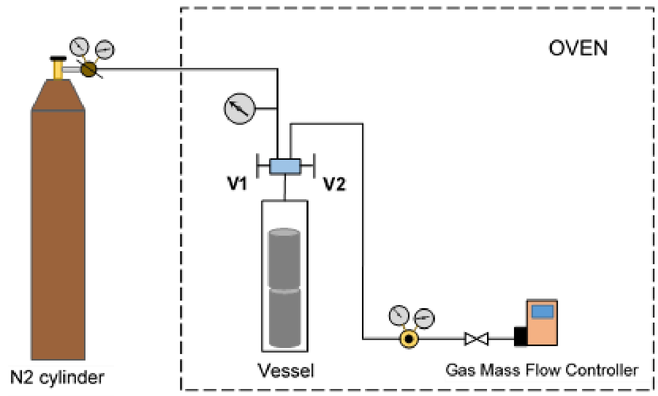

Fig. 2.1 – Schematic of gas huff-n-puff injection setup for matrix-fracture system

For more details, read these papers:

1. Wan, T., Yu, Y., and Sheng, J.J. 2015. Experimental and numerical study of the EOR potential in liquid-rich shales by cyclic gas injection, Journal of Unconventional Oil and Gas Resources, 12, 56-67.
2. Yu, Y., Sheng, J.J., Barnes, W., and Mody, F. 2015. Evaluation of Cyclic Gas Injection EOR Performance on Shale Core Samples Using X-Ray CT Scanner, paper 407411 presented at the 2015 AIChE Annual Meeting, Salt Lake City, UT, 8-13 November.

2.3.1 Effect of soaking time

Fig. 2.2 shows the effect of soaking time on the shale oil recovery factor. For the first two cycles of huff-n-puff, the oil recovered from each cycle increased with the increase of soaking time. Applying soaking period from 0.25-hr to 48-hr, the RFs in cycle one raised from 2% to 5.6% for core LEF_1 and from 1.8% to 4.8% for core LEF_2. After 10 cycles, it shows that a longer soaking time (greater than 12-hr) has no significant impact on the ultimate RF; when a soaking time less than 12 hr was applied, the ultimate RF increased with the soaking time.

Soaking time affects the RF in a certain range. When applying soaking times of 0.25-hr, 3-hr, and 12-hr, a longer duration caused more oil yielded in a single cycle, thus enhancing the ultimate RF. However, the impact of longer soaking time became less significant when the soaking periods of 24-hr and 48-hr used. After 4 cycles of huff-n-puff processes, such longer time has no significant effect on improving oil recovery. Therefore, for this study case, a soaking period is necessary in huff-n-puff process to improve oil recovery, and 12-hr is recommended to apply to achieve the optimum RF.

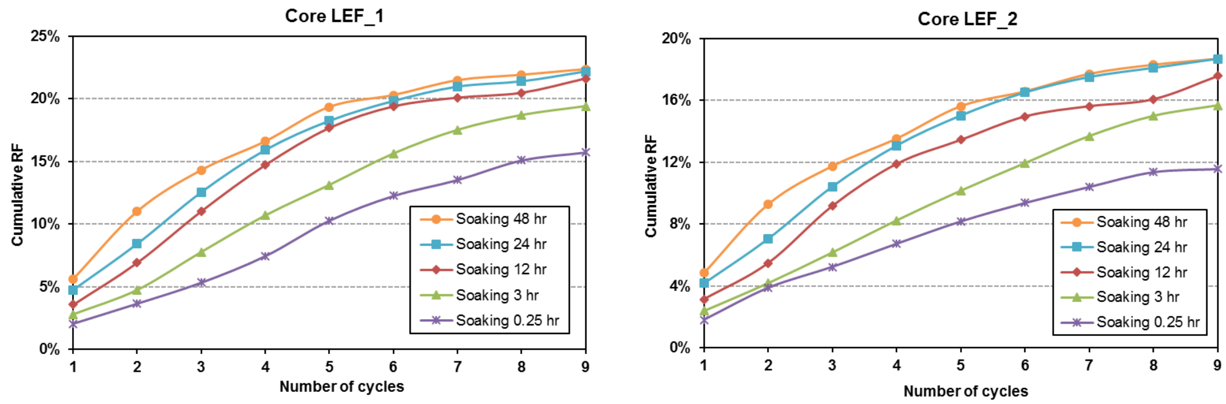

Fig. 2.2 – Effect of soaking time on shale oil recovery factor

2.3.2 Effect of pressure depletion rate

Fig. 2.3 illustrates the effect of pressure depletion rate on the RF. The experimental results from two samples consistently indicate that a shorter pressure depletion period (faster depletion rate) led to a higher oil RF in the first cycle, and also increased the incremental RF in the subsequent operated cycles. Therefore, a rapid pressure depletion has positive effect on oil recovery for each cycle, and more effective cycles can be performed than the case with a longer depletion period. Therefore, a greater ultimate RF can be achieved under the condition of a faster pressure depletion rate.

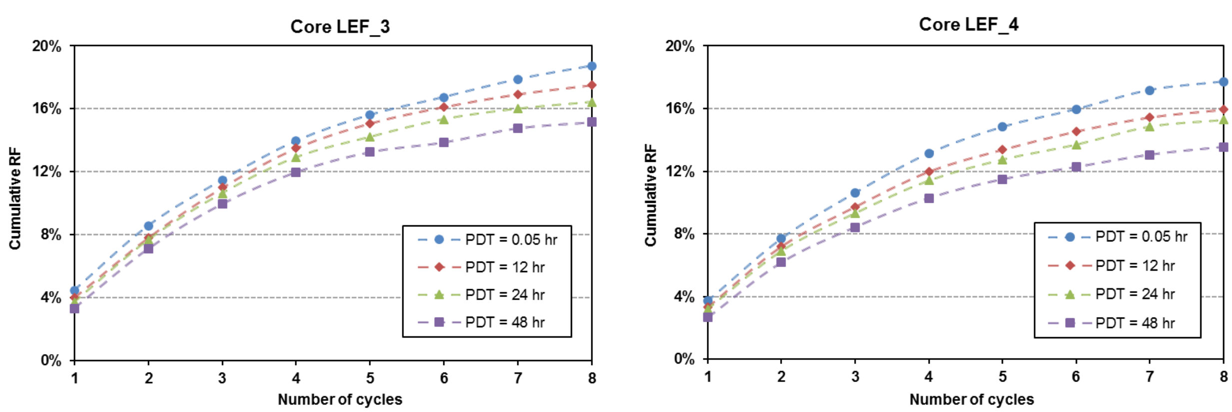

Fig. 2.3 – Effect of pressure depletion rate on shale oil recovery factor

For more details, read this paper:

3 Yu, Y., Li, L., and Sheng, J.J. 2016. Further Discuss the Roles of Soaking Time and Pressure Depletion Rate in Gas Huff-n-Puff Process in Fractured Liquid-rich Shale Reservoirs. Paper

SPE-181471-MS presented at the SPE Annual Technical Conference and Exhibition held in Dubai, UAE, 26-28 September.

2.4 Evaluation of N_2 flooding process

The N_2 flooding process were performed at different injection pressures of 1,000 psi, 3,000 psi, and 5,000 psi, respectively. Two samples were applied to experience the tests at same conditions. A core-scale simulation model was built to match the experimental data and to evaluate the injection pressure effect on RF and predict the oil recovery. Fig. 2.4 shows the experimental setup.

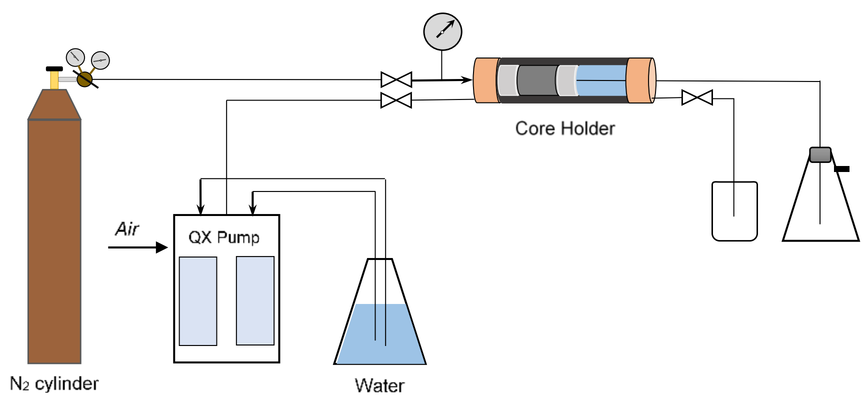

Fig. 2.4 – Schematic of gas flooding test setup

The experimental and simulation results are presented in Fig. 1.5. For all three cases, noticeable shale oil was recovered at the initial period of the recovery process with a high and constant production rate, before gas breakthrough reached. After that, the incremental RF decreased with the increase of flooding period, and a long flooding time extracted little more oil.

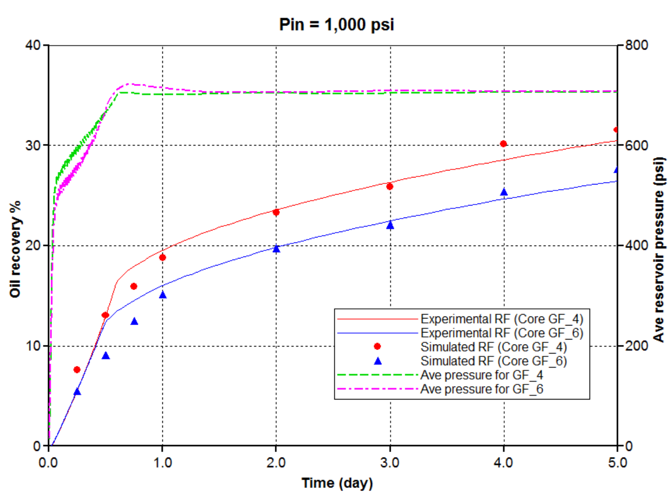

(a)

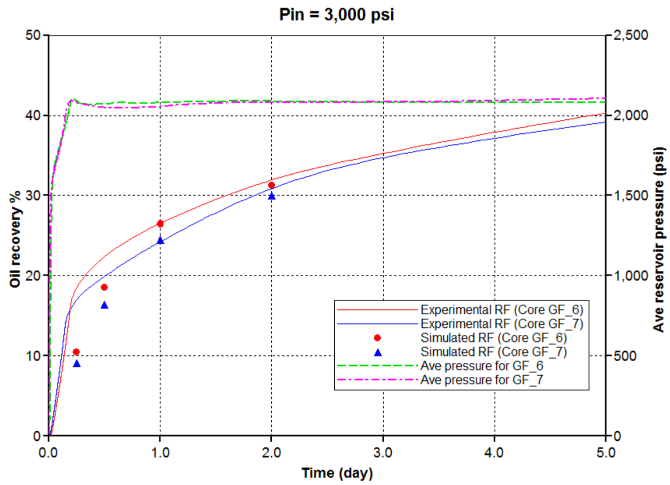

(b)

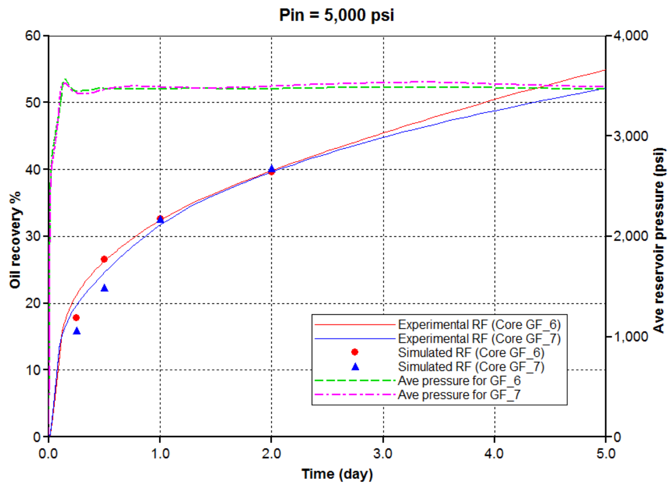

(c)

Fig. 2.5 – Experimental and simulated oil recovery by N_2 flooding at different injection pressures

Fig. 2.6 investigated the effect of injection pressure on recovery factor of the N_2 flooding for a period of 5 days, with a constant P_{in} ranging from 500 psi to 5,000 psi. It shows that P_{in} affects the oil recovery throughout the flooding process. Before gas breakthrough (BT), recovery rate increases with the increase of P_{in}, which is obviously reflected in the medium-low pressure range (500 psi to 3,000 psi). The turning point position of each recovery curve illustrated that a higher P_{in} not only makes gas flow faster through the plug but also contributes to a greater RF at the BT point.

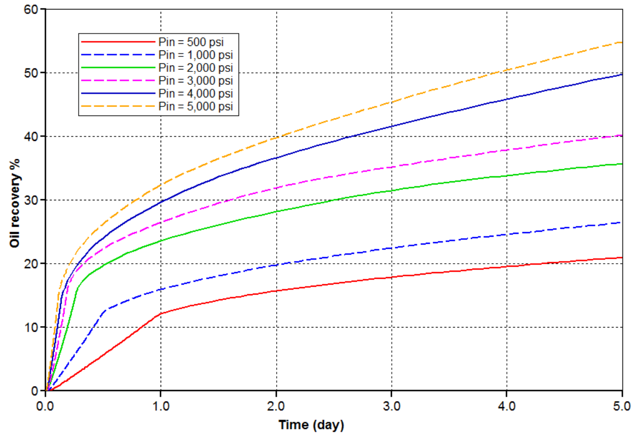

Fig. 2.6 – Effect of injection pressure on oil recovery by N_2 flooding

The simulated oil recovery for 300-day operation is presented in Fig. 2.7. We found that when increasing P_{in} from 1,000 psi to 5,000 psi, an increment of only 4.5% oil RF is yielded from the lab-scale simulation results. The distinct advantage of employing high P_{in} is to boost the production rate and shorten the development period, while it will also increase the cost of injecting the high pressure gas. By contrast, the utilization of a lower P_{in} is more suitable for the shale plays that need to be a long-term, sustainable development.

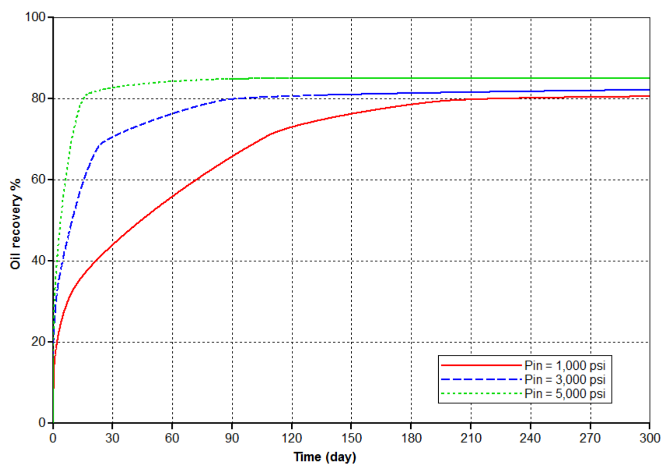

Fig. 2.7 – Estimation of the ultimate oil recovery

For more details, read these papers:

4 Yu, Y., and Sheng, J.J. 2015. An Experimental Study of the Potential of Improving Shale Oil Recovery By Gas-Flooding, paper 418166 presented at the 2015 AIChE Annual Meeting, Salt Lake City, UT, 8-13 November.

5 Yu, Y., and Sheng, J.J. 2016. Experimental Evaluation of Shale Oil Recovery from Eagle Ford Core Samples by Nitrogen Gas Flooding, paper SPE 179547 presented at the SPE Improved Oil Recovery Conference held in Tulsa, Oklahoma, USA, 11–13 April.

6 Yu, Y., Meng, X., and Sheng, J.J. 2016. Experimental and Numerical Evaluation of the Potential of Improving Oil Recovery From Shale Plugs by Nitrogen Gas Flooding. *Journal of Unconventional Oil and Gas Resources* 15: 56-65.

2.5 Comparison of EOR potential between N_2 huff-n-puff and N_2 flooding

Gas injection has been demonstrated as the most effective solution to maintain the shale oil recovery from existing wells. As gas can be injected into the subsurface by two modes: continuous injection (flooding) and cyclic injection (huff-n-puff), this study aimed to compare the recovery efficiencies of such two processes in shale core plugs.

The experimental setup for the gas huff-n-puff injection process is shown in Fig. 2.8, and the setup for gas flooding test remains is shown in Fig. 2.4. Gas injection tests were conducted on the same plug orderly by both modes under the same operating conditions. Two core samples were used to operate the gas injection processes for a total of 48-hr and 72-hr, respectively. For all tests, the injection pressure was 1,000 psi.

When performing the huff-n-puff test, for the first sample, tests were conducted at three soaking times of 0.5-hr, 2-hr, and 5-hr, respectively; production time was 1-hr, and the total operation time was 48-hr. For the second sample, 1-hr was selected as the soaking time, 3-hr as the production time, and the total operation time was 72-hr.

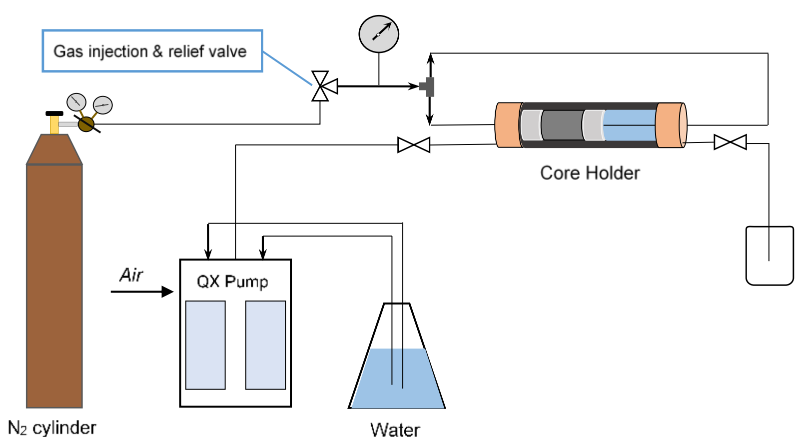

Fig. 2.8 – Schematic of gas huff-n-puff injection setup

Fig. 2.9 shows the recovery histories by the N_2 flooding and the N_2 huff-n-puff (with different soaking times) processes at a total operation period of 48-hr. The case with 0.5-hr soaking time yielded the most oil compared with the flooding process, and the cases with other soaking times. The RF achieved by huff-n-puff process was sensitive to soaking time. Under the same operating time, the test with a shorter soaking duration allows more cycles to be performed. With the increase of cycle number, it leads to the increase of cumulative RF. However, it does not imply that with shorter soaking time, more oil could be produced at the end. The reason is that if the soaking period is too short, only little oil could be extracted from a single cycle. Although an adequate number of cycles are available to be operated, the cumulative RF may be less than that from the case with a longer soaking time. A soaking period is necessary for huff-n-puff that allows the injected gas to transport pressure to the inner area of the core and diffuse into the matrix.

Fig. 2.10 shows that similar amounts of oil were produced by flooding and huff-n-puff in 18 hr, while after that, the production rate by flooding decreased greatly because the gas had broken through the plug in 24 hr. The majority of injected gas passed through the established flow channels, thus the flooding recovery performance became less positive. The huff-n-puff process offered consistent injection energy for each cycle, which recharged the matrix cyclically and maintained a relatively longer effective recovery performance.

The experimental results show that at the same operating conditions of injection pressure and total operation time, an optimized gas huff-n-puff process recovered more oil than gas flooding process in shale plugs.

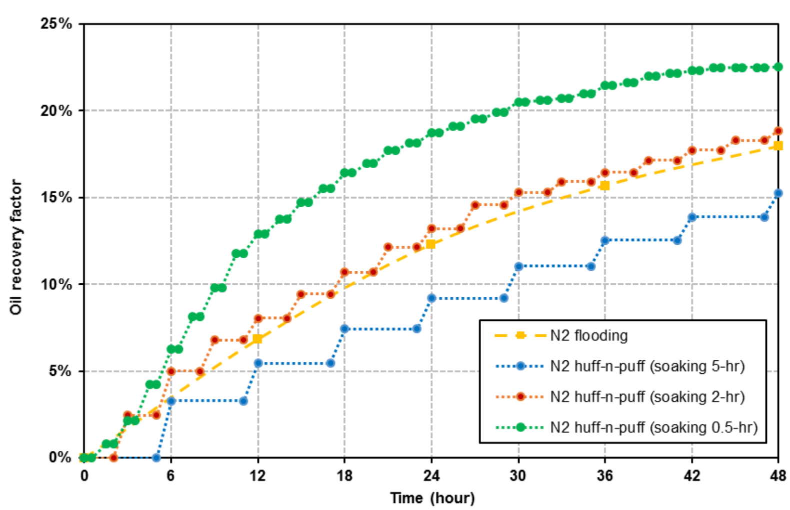

Fig. 2.9 – Recovery history by N_2 flooding and N_2 huff-n-puff in 48 hr

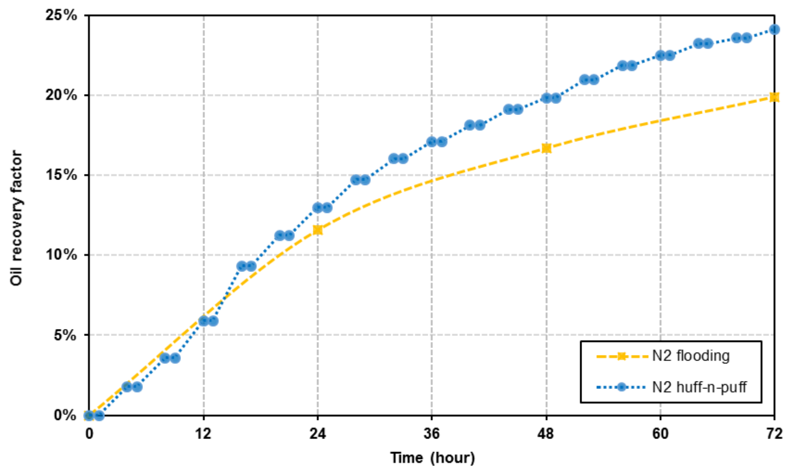

Fig. 2.10 – Recovery history by N_2 flooding and N_2 huff-n-puff in 72 hr

For more details, read this paper:

7 Yu, Y., Li, L., and Sheng, J.J. 2017. A Comparative Experimental Study of Gas Injection in Shale Plugs by Flooding and Huff-N-Puff Processes. Journal of Natural Gas Science and Engineering 38: 195-202.

2.6 Comparison of EOR potential between N_2 huff-n-puff and water huff-n-puff

Several recent studies have evaluated the potential of gas injection in shale plays. However, few studies discussed the feasibility of water huff-n-puff process. This study aims to evaluate the potential of water huff-n-puff injection process in shale plugs and compared it with the performance of the N_2 huff-n-puff injection process at the same operation conditions.

To reduce clay swelling, 5 wt.% of potassium chloride (KCl) solution was used as the injection fluid in water huff-n-puff tests. Two groups of tests were performed to examine the effects of soaking time and injection pressure (P_{in}) on the recovery performance. Fig. 2.11 shows the experimental setup. For one cycle of water huff-n-puff process, after reaching the P_{in}, the core sample was soaked with water for a certain time, then the surrounding pressure was released to enter the production period. Under the same operating conditions, the N_2 huff-n-puff tests were conducted to compare the two EOR performances.

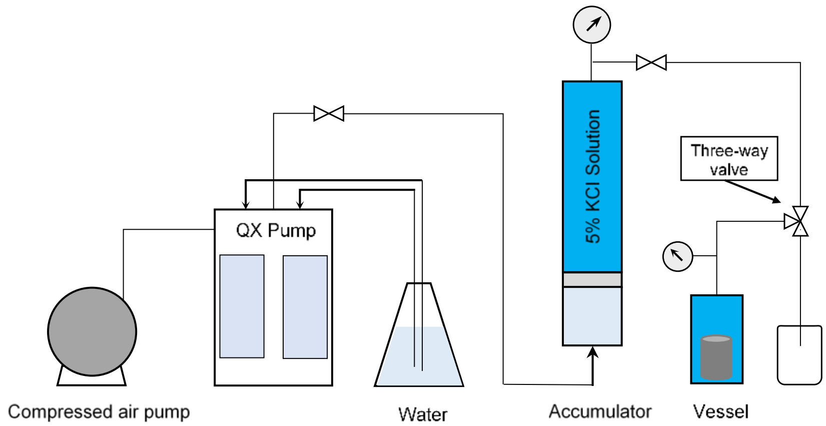

Fig. 2.11 – Schematic of water huff-n-puff injection setup

Fig. 2.12 exhibits that soaking time in water huff-n-puff process impacts the recovery factor (RF) of a single cycle within a certain range. A certain soaking period is essential for extracting oil but an extra longer during has no obvious effect on improving oil recovery, which was similarly concluded from the gas huff-n-puff tests.

Injection pressure affects the shale oil RF significantly, shown as Fig. 2.13. The recovered oil increased greatly with the injection pressure, especially for the initial five cycles. When applying 5,000 psi, after seven cycles, it was observed that fractures were created on the plug and the size enlarged with further cycles operated.

Comparing the two huff-n-puff processes by using water and N_2, as Fig. 2.14 shown, different recovery characters can be observed. Water huff-n-puff showed the recovery potential at the first four cycles, and then the incremental oil recovery decreased dramatically in the subsequent cycles. By contrast, the N_2 huff-n-puff process presented a more continuous and steady recovery performance with high incremental RF, and then gradually diminished after seven cycles of huff-n-puff processes.

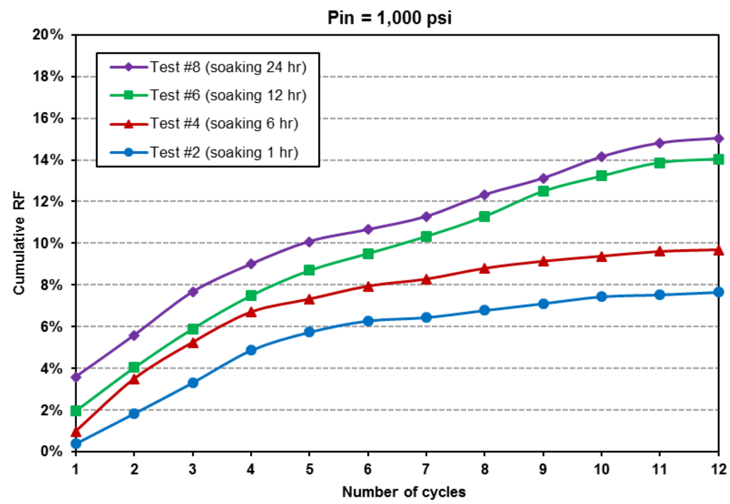

Fig. 2.12 – Oil recovery performance of water huff-n-puff with different soaking times

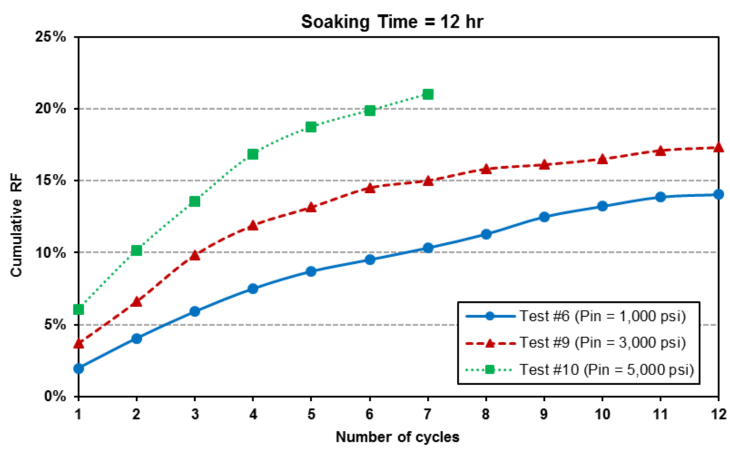

Fig. 2.13 – Oil recovery performance of water huff-n-puff with different injection pressures

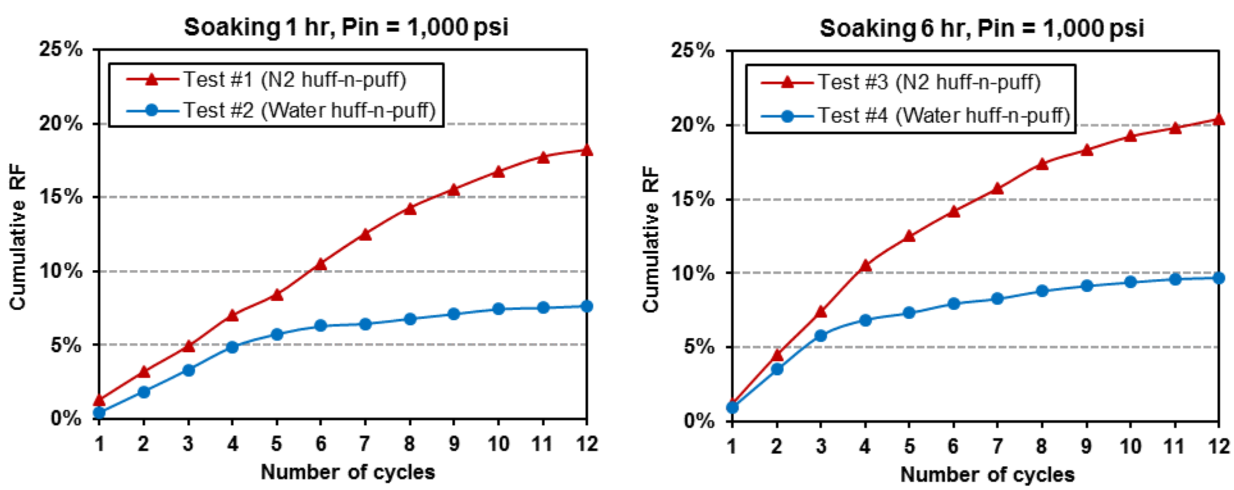

(a) (b)

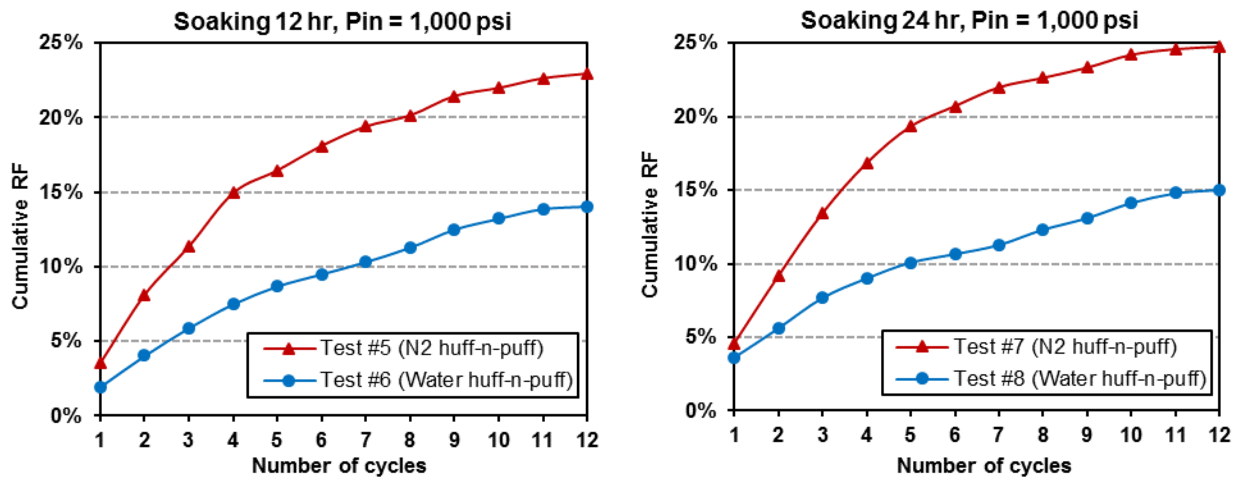

(b) (d)

Fig. 2.14 Comparison of recovery performance between the water huff-n-puff and the N2 huff-n-puff processes under different soaking times

For more details, read these papers:

8 Yu, Y. and Sheng, J.J. 2016. Experimental Investigation of Light Oil Recovery from Fractured Shale Reservoirs by Cyclic Water Injection, paper SPE 180378 presented at the SPE Western Regional Meeting held in Anchorage, Alaska, USA, 23–26 May.

9 Yu, Y. and Sheng, J.J. 2017. A Comparative Experimental Study of IOR Potential in Fractured Shale Reservoirs by Cyclic Water and Gas Injection. Journal of Petroleum Science and Engineering 149: 844-850.

2.7 Summary

Investigation of N_2 huff-n-puff process

- The experimental results demonstrate that gas huff-n-puff recovery process has a promising IOR potential in shale reservoirs.
- Soaking time influences the RF of a single cycle within a certain range. With the condition of rapid pressure injection, a "soak" period is crucial to recover oil effectively. From this study, when soaking period less than 12-hr, the incremental RF increased with the soaking period. An extra longer duration has no significant effect on improving the RF.

- Cumulative RF increases with the increase of pressure depletion rate, and same for the incremental RF of each cycle. The highest RF can be obtained under the pressure blowout condition.

EOR potential of N_2 flooding process

- The N_2 flooding presented the recovery potential and produced oil rapidly during the early injection period until gas breakthrough.
- After the gas breakthrough, the production rate declines sharply and the outlet gas flow rate become stabilized gradually.
- Injection pressure is an important factor in gas flooding process. Injecting gas with a higher pressure can shorten the breakthrough time, increase the RF at the time of BT, and improve the ultimate RF.

Compare N_2 huff-n-puff with N_2 flooding

- The experimental results show that the gas injection mode of huff-n-puff is superior to the flooding mode in shale core plugs, with a higher cumulative oil recovery during the same operation period.
- Gas flooding showed similar recovery efficiency as huff-n-puff before breakthrough. After that, the production rate by flooding declined with the operation period, and huff-n-puff began to show more oil produced.
- Compared with gas flooding, gas huff-n-puff process presented more durable and steadier EOR performance.
- For the huff-n-puff process, optimization design of key operating parameters, such as soaking time and cycle number, is crucial to achieve the maximum production, compared with the flooding process.

Compare water huff-n-puff with N_2 huff-n-puff

- Water huff-n-puff has limited shale oil recovery potential with a low ultimate RF. It has fewer number of cycles to recover oil effectively than the gas huff-n-puff process.
- Within a certain range, the incremental RF from a single water huff-n-puff cycle increased with the soaking period, and longer time cannot contribute to additional oil recovery.
- Increasing injection pressure of water huff-n-puff is beneficial to increase oil recovery. With the increase of P_{in}, RF increased after the first cycle. The higher pressure results in a

generation of fractures in the matrix, thus the extended stimulated volume contributed to additional oil recovery.

- The recovery performance of the N_2 huff-n-puff outperformed water huff-n-puff greatly when operating the two processes under the same conditions.

Chapter 3 Effect of core sizes on huff-n-puff gas injection

3.1 Introduction

Gas huff-n-puff, which avoids viscous fingering phenomenon between connected wells, is a new method to efficiently enhance oil recovery in liquid-rich shale oil cores. The previous study conducted gas huff-n-puff with 1.5 inches core samples and found this EOR method is effective. However, the other important parameter when applying this EOR approach to field study is the size effect. Will the core size affect the oil recovery result? In this study, a further experimental study about core size effect on gas huff-n-puff was implemented by using two groups of cores from the Wolfcamp formation in West Texas. The first group contains core plugs with the same length of 2 inches but different diameters varying from 1 to 4 inches. The second group core plugs have the same diameter of 1.5 inches but differ in length varying from 1 to 3.5 inches. The cores were first analyzed for their pore size distributions. Then methane huff-n-puff EOR experiments with injection pressure of 2000 psi were conducted to analyze the size effects.

3.2 Experiment study

Crude oil and core plugs are from the Wolfcamp formation in Apache's Lin field. The core plugs can be divided into two groups. One contains six core samples with the same length of 2” but with different diameters of 1”, 1.5”, 2”, 3”, 3.5”, and 4”, respectively, as shown in Fig. 3.1. Fig. 3.2 presents the four core samples with the same diameters of 1.5” but different lengths of 1”, 2”, 2.75”, and 3.5”. The injection gas in these huff-n-puff experiments is methane with purity larger than 99%.

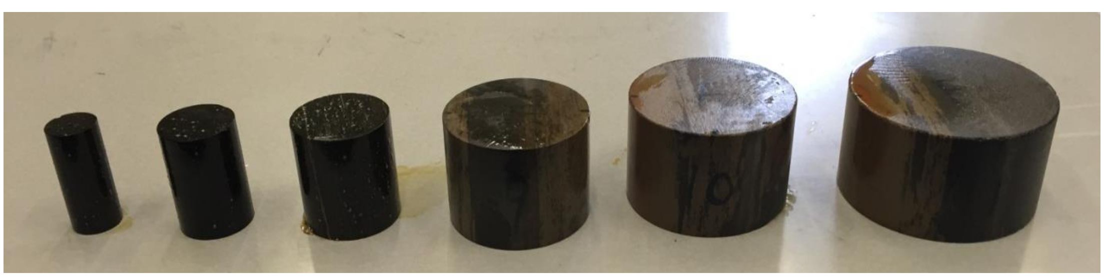

Fig. 3.1 – Shale oil cores in group 1 (the picture taken after first cycle).

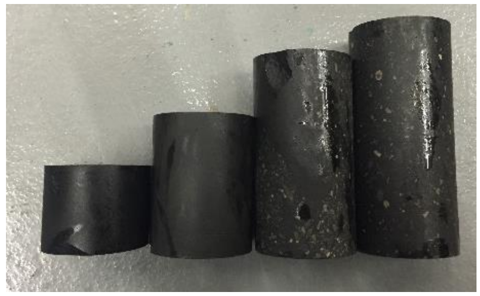

Fig. 3.2 – Shale oil cores in group 2 (the picture taken after first cycle).

All the experiments were performed at the temperature of 95°F in an oven. The experiment can be divided into two sections including the oil saturation section and the huff-n-puff gas injection section. Considering that traditional saturation method for conventional reservoir cores is not suitable to be used in these shale cores, a special saturation method applied in our previous experiments was used in this study.

Experimental Procedures of Core saturation (shown in Fig. 3.3):

1. Core samples are named and dried in the oven for one day.
2. Turn off the oven and leave the sample in the oven to cool to the lab temperature, then weigh and record the sample as W_d.
3. Then place the core samples in the stainless steel vessel shown in Fig. 3.3, connect the vessel to a vacuum pump and vacuumed the cores for three days.
4. Stop the vacuum pump and delivery water using the Quizix QX pump to push the crude oil in the accumulator, making sure the core is completely soaked in crude oil and the saturation pressure in the vessel reaches the requirement of 2000 psi.
5. After saturating for 2 days or a longer time, relieve the soaking pressure and keep the cores inside of the vessel for one day to make sure the internal and external pressures of the cores reach an equilibrium condition.
6. Saturation process is finished. Weigh and record the saturated sample as W_s.

Experimental Procedures of huff-n-puff gas injection (shown in Fig. 3.4):

1. After oil saturation, put the core sample into the core holder in the oven with temperature of 95°F. Inject methane to the core holder. When the pressure gauge installed on the top of the container shows 2,000 psi, it means gas injection has completed and soaking period starts.
2. Maintain the internal pressure of 2000 psi for one day. This certain period of soaking time

allows gas to dissolve into the oil.

3. After the soak period is finished, release the internal pressure to the atmosphere pressure of 14.7psi. Weigh and record the core sample again as W_i. The oil is produced as the pressure is released.

4. Repeat 8 cycles and weigh the core after each cycle.

The same procedure is repeated in subsequent cycles using the similar manner to the first one. Each sample was weighed and recorded after each cycle to calculate the oil recovery with its weight differences using the following equation.

$$Accumulative\ Oil\ Recovery\ in\ cycle\ i = \frac{W_s - W_i}{W_s - W_d} \times 100\% \qquad (2\text{-}1)$$

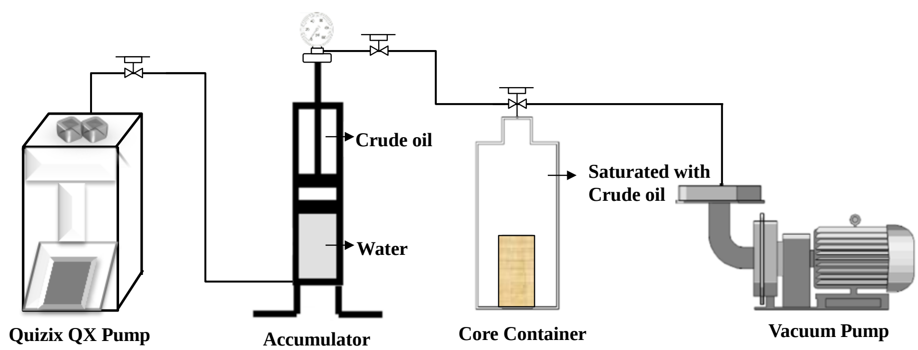

Fig. 3.3 – Schematic diagram of the experimental equipment for oil saturation.

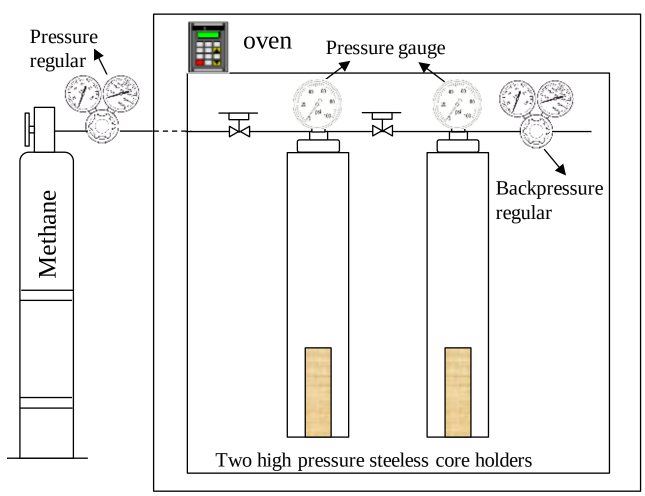

Fig. 3.4 – Schematic diagram of the experimental equipment for huff-n-puff gas injection.

3.3 Experiment Results

***Effect of core diameter size*:** After eight huff-n-puff cycles, as shown in Fig. 3.5, the oil recovery of the core plugs with diameter of 1”, 1.5”, 2”, 3”, 3.5” and 4” are 49.65%, 48.57%, 47.76%, 46.15%, 43.55% and 42.64%, respectively. The results illustrate that the core with a bigger diameter has a lower oil recovery in the same injection cycle under the same operation schedule. One important factor causing the oil recovery difference is the apparent surface-to-volume ratio (AS/V). A smaller core has a relative larger AS/V than that of a larger core. Another parameter that will affect the oil recovery of different diameter cores is the pressure gradient ($\Delta P/\Delta r$). With the same pressure drop, a smaller diameter core has relatively higher pressure gradient during production stage than that of a larger core.

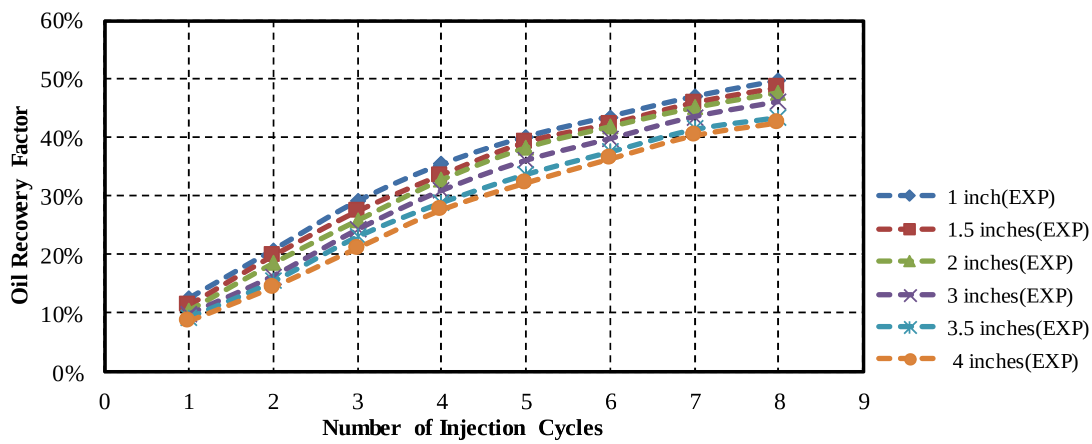

Fig. 3.5 – R.F. data of different cores diameters for 5 injection cycles under the conditions of 2000psi with crude oil and Methane injection.

Effect of core length size: Fig. 3.6 shows the relative oil recovery results of the experiments for different core length sizes. After eight huff-n-puff cycles, the oil recovery differences are only 0.26% for the core plugs with lengths of 1” and 2”, and 0.23% for the ones with lengths of 2.75” and 3.5”. This means the lengths do not have significant influence on oil recovery of shale core during huff-n-puff process. The AS/V is the same value for all the different length cores. As all the cores have the same diameter, $\Delta P/\Delta r$ is also the same for different core plugs during the experiment process. With the same AS/V and $\Delta P/\Delta r$, the core plugs yield the similar oil recovery in each gas huff-n-puff cycle. As the length does not affect the oil recovery, the structure parameters such as permeability and heterogeneity will cause some minor difference in the oil recovery during gas huff-n-puff process.

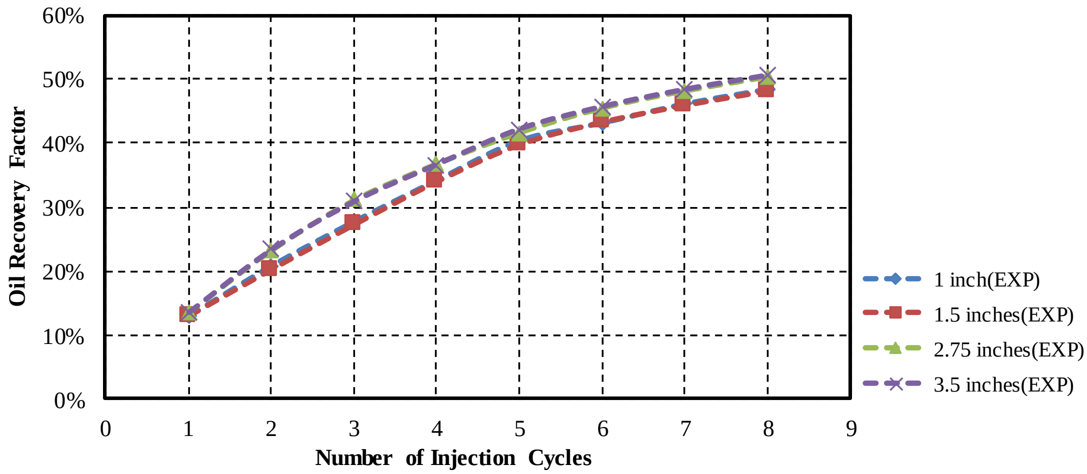

Fig. 3.6 – R.F. data of different core lengths for 8 injection cycles under the conditions of 2000psi with crude oil and CH_4 injection.

Effect of core diameter size on soaking time: Fig. 3.7 and Fig. 3.8 describe the EOR results with different soaking time on two different diameters core sizes. The result illustrate that the larger core sample needs a longer soaking time to allow pressure equilibrium inside the core to achieve the maximized oil recovery in a single cycle.

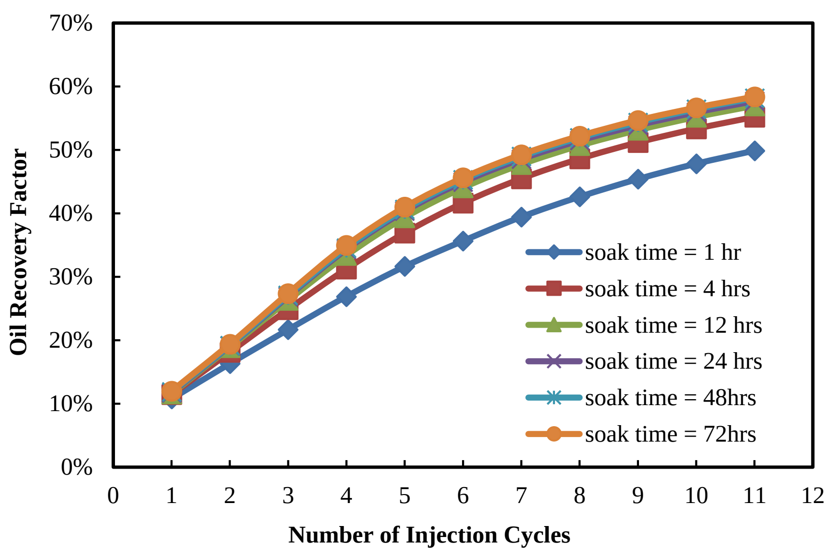

Fig. 3.7 – Effect of soaking time on oil recovery factor (Core diameter = 1.5 inches).

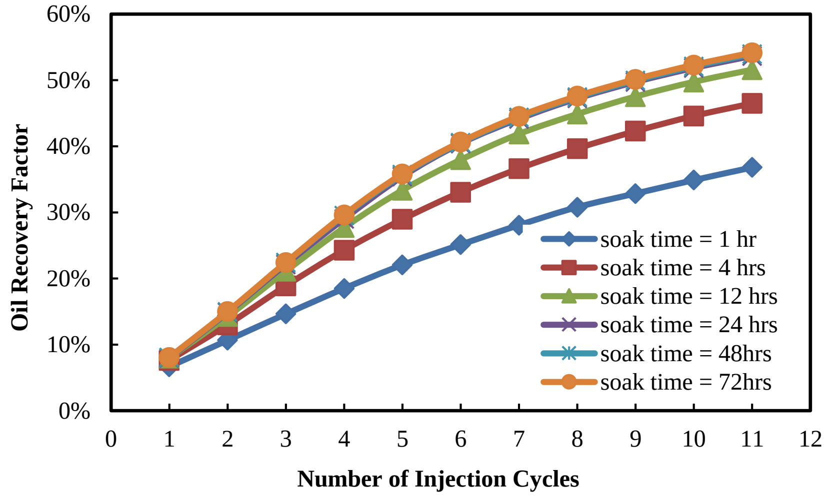

Fig. 3.8 – Effect of soaking time on oil recovery factor (Core diameter = 4 inches).

For more details, read the following papers:

10 Li, L. and Sheng, J. J. Experimental study of core size effect on CH_4 huff-n-puff enhanced oil recovery in liquid-rich shale reservoirs. Journal of Natural Gas Science and Engineering, 2016, 34, 1392-1402.

11 Li, L. and Sheng, J. J. Numerical Analysis of Cyclic CH_4 Injection in Liquid-rich Shale Reservoirs Based on the Experiments Using Different-diameter Shale Cores and Crude Oil. Journal of Natural Gas Science and Engineering, 2017, 39, 1-14.

Chapter 4 Effect of MMP

4.1 Introduction

It is known that in a conventional reservoir, once the minimum miscible pressure (MMP) is reached, the extra increased pressure will not significantly enhance oil recovery. This experimental study aims to investigate the role of MMP in oil recovery in shale cores during the huff-n-puff process.

The displacement of oil by CO_2 can occur by two main mechanisms: immiscible and multi-contact miscible flooding. During the miscible displacement, a mass transfer between oil and CO_2 occurs by vaporization, extraction, or condensation. For miscible displacements to occur, CO_2 has to be injected at a certain pressure called minimum miscibility pressure (MMP), at which oil and CO_2 become one phase. Every oil has a unique MMP with CO_2 because each oil has a distinctive oil composition. Therefore, it is required to measure the MMP for Wolfcamp crude oil in order to investigate the CO_2 miscible flooding effect in shale oil reservoirs in the Wolfcamp oilfield. This section includes results from the experimental study and the simulation study.

- Slimtube tests to determine the MMP between Wolfcamp crude oil and CO_2
- CO_2 huff-n-puff experiments at different injection pressures
- Simulation study of MMP effect on EOR

4.2 Main methodology

4.2.1 Experimental study

Slimtube Experiments. A sand packed slimtube apparatus was utilized to perform the experiments as shown in Fig. 4.1. To determine the MMP pressure, normally at least two tests are performed at pressures below the expected MMP and two tests are performed above the MMP. The data was plotted for oil recovery versus pressure and where the two lines intercept is the MMP point. To prepare and conduct each experiment, three main tasks were followed: slimtube cleaning, saturating with oil, and solvent injection.

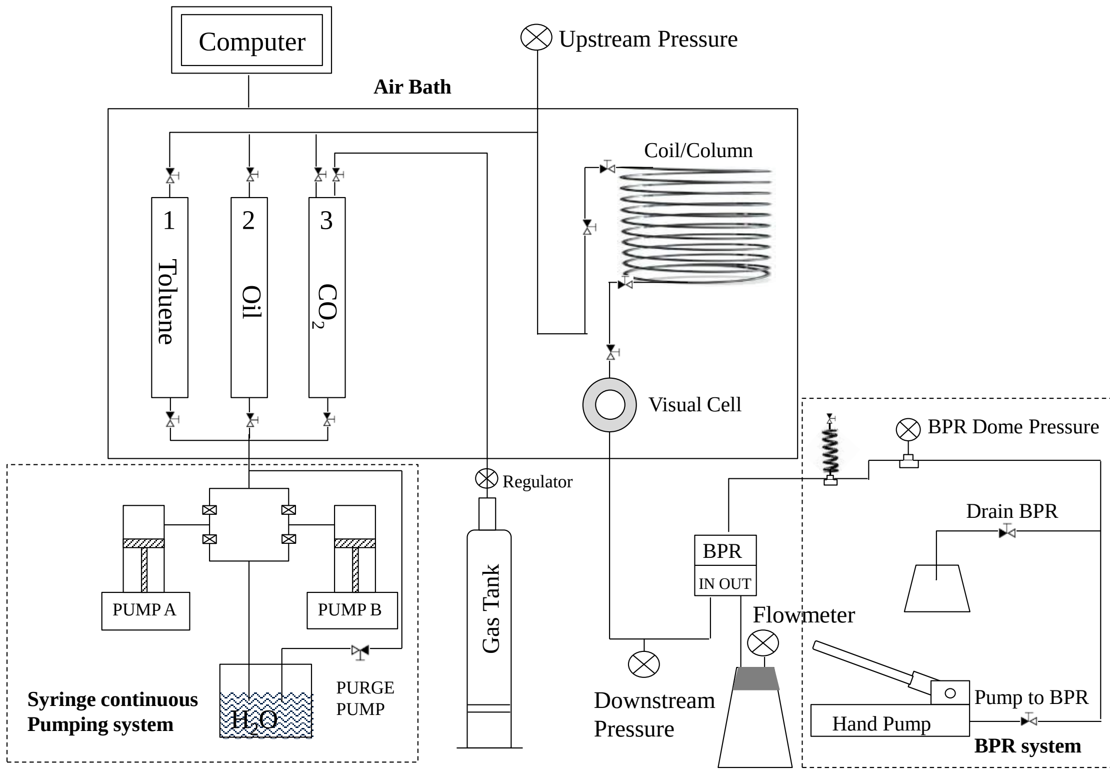

Fig. 4.1 – Schematic of the set up for the MMP determination apparatus using the slimtube technique.

Gas Huff-n-Puff Experiments. Based upon the result of MMP, fifteen series of CO_2 huff-n-puff experiments were implemented on three different Wolfcamp shale core samples at the pressures below and above MMP, which were 1200, 1600, 1800, 2000, and 2400 psi. Each huff-n-puff test had seven cycles. The cores were saturated with Wolfcamp crude oil. The huff-n-puff experiment, similar to the one in our previous research (Li and Sheng, 2016) was divided into two sections including saturating the core sample with crude oil, and conducting the gas huff-n-puff test.

4.2.2 Simulation study

A radial coordinate model with a two-dimensional radial cross section (r-z) and compositional reservoir simulator (CMG-GEM) were used to simulate the cyclic CO_2 injection experiment. The accumulator had a diameter of 2.4-inches and height of 5.6-inches. The surrounding annular volume between the accumulator and core represented the fracture volume. All faces of the core sample were open during the gas injection, soaking, and production stages. Fig. 4.2 shows the process of the model build up.

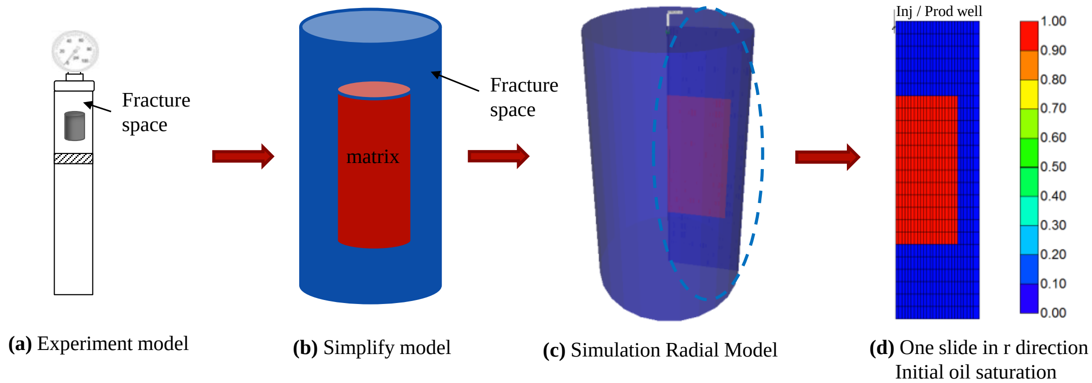

Fig. 4.2 – Model build up process and radial simulation model with logarithmic refinement (legend is initial oil saturation).

4.3 Main Results

Seven slimtube tests at pressures of 1000, 1350, 1660, 1750, 1800, and 2000 psi were conducted and the cumulative recovery was measured after 1.2 pore volumes (PV) of CO_2 was injected. The results are shown in Fig. 4.3. The point where the slope changed occurred at 91% recovery, when the test pressure was 1620 psi. Therefore, this pressure is considered as the MMP for the CO_2-Wolfcamp crude oil system.

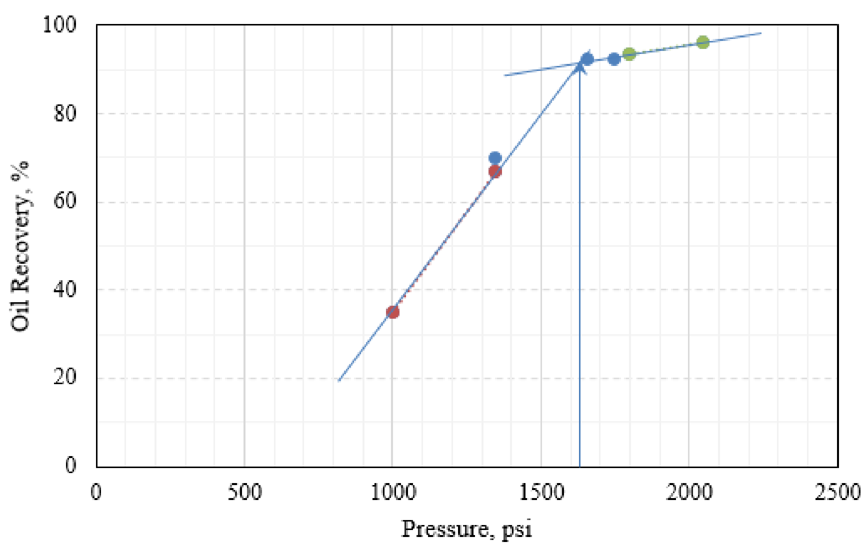

Fig. 4.3 – Results of slimtube experiments showing MMP at 1620 psi

The huff-n-puff experiment results are shown in Fig. 4.4. This figure illustrates that below the MMP, the oil recovery increases significantly with the increase of injection pressure. And the oil recovery still increases when the pressures are higher than the MMP. The estimated MMP from slimtube experiments is 1620 psi. In the gas huff-n-puff experiments, when the injection pressure increases from 1600 to 1800 psi, 10% more oil can be produced after 7 huff-n-puff cycles. However, when the pressure is higher than 1800 psi, the increase of pressure is unable to enhance the oil recovery in shale cores significantly.

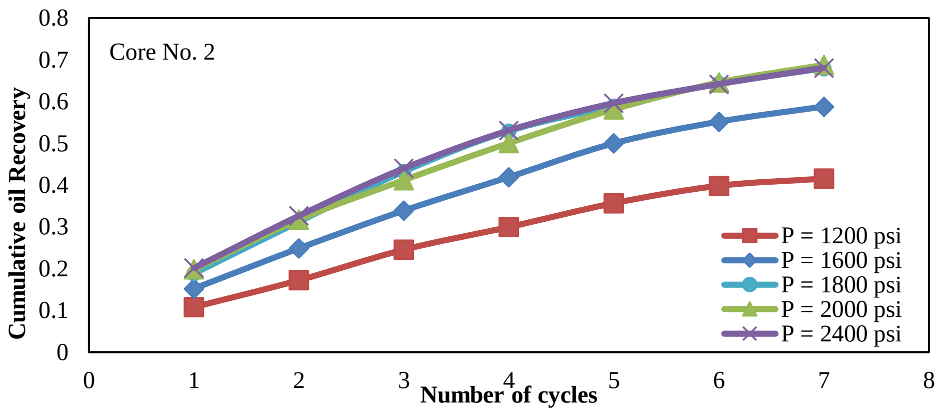

Fig. 4.4 – Pressure effect on CO_2 huff-n-puff performance

The simulated pressure distribution inside the core at different times are described in Fig. 4.5. When the injection pressure is 1800 psi, the pressure inside the core builds slowly. It takes 100 mins to allow the pressure inside the core to reach the MMP. At the end, the system equilibrium pressure is about 20 psi less than the injection pressure.

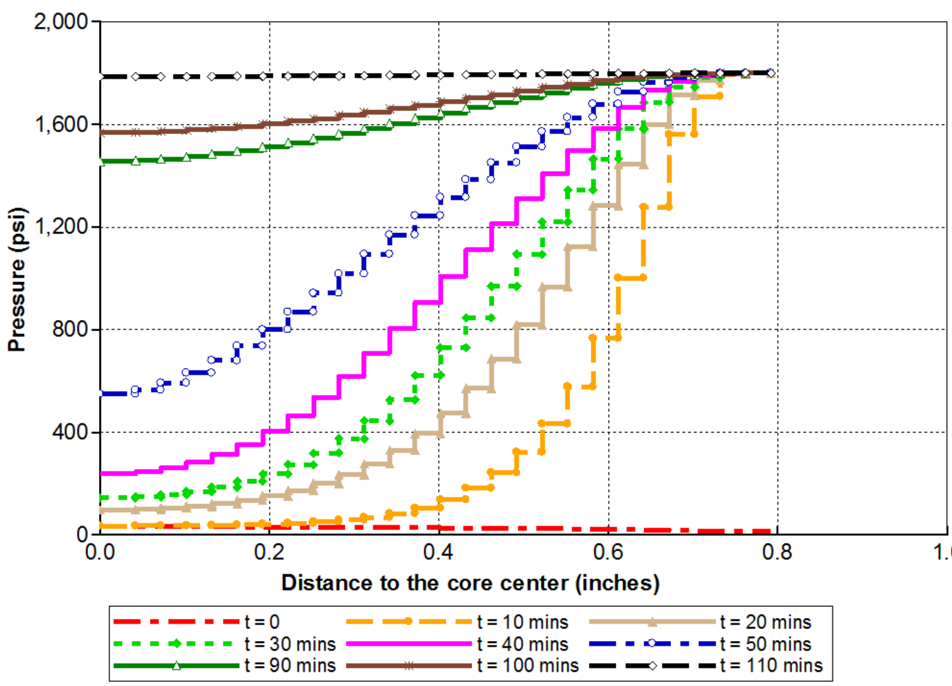

Fig. 4.5 – Pressure distribution inside the core vs. soaking time in the seventh huff-n-puff cycle.

The pressure distribution inside the core during the soaking time from numerical simulation clearly demonstrates the significant pressure difference between the core surface and the center. A high injection pressure near the core surface is needed to help gas diffusion and gas-oil miscibility, leading higher oil recovery during huff-n-puff CO_2 injection. And this pressure is higher than the MMP as shown from the simulation results. This study helps explain the pressure effect during gas huff-n-puff process in shale oil reservoirs and provides a guide to design injection pressure to produce shale oil efficiently based upon the conventional MMP.

For more details, read the following paper:

12 Li, L., Zhang, Y., Sheng, J. J. Effect of the Injection Pressure on Enhancing Oil Recovery in Shale Cores during the CO2 Huff-n-Puff Process When It Is above and below the Minimum Miscibility Pressure. Energy & Fuels, 2017, 31(4), 3856-3867.

Chapter 5 Gas penetration depth in oil reservoirs

5.1 Introduction

Gas huff-n-puff injection has been proven to be a potential EOR method after horizontal well hydraulic fracturing in shale oil reservoirs. However, the EOR mechanism of gas huff-n-puff is still not clear. During the huff period, the injected gas penetrates reservoir matrix, swelling the oil, reducing oil viscosity and increasing the reservoir pressure. This gas penetration is a fundamentally important mechanism to enhance oil recovery during gas huff-n-puff process. The purpose of this study was to investigate the gas penetration depth.

The lab scale numerical simulation model was built and validated with the experimental data. The model was employed to quantitatively describe the gas penetration process and measure the penetration depth in the core during the huff period. Diffusion effect was also investigated. As previous TTU study stated that the core size will affect the oil recovery, a history matched field scale model was applied to evaluate the field production performance. The effects of different parameters on gas penetration depth were investigated including reservoir properties such as permeability, natural fracture spacing, and operation properties such as huff-n-puff start time, number of huff-n-puff cycles, injection pressure, and huff and puff time.

5.2 Main methodology

For lab scale simulation, a radial model was developed using a commercial simulator, CMG-GEM to simulate the C1 huff-n-puff experiment. The radial grids are used to represent the core container and the cylindrical core as shown in Fig. 5.1. The distribution of porosity, absolute permeability, and oil saturation are assumed to be homogeneous in the core and the empty space.

For field scale simulation, a history matched dual permeability compositional model was used to simulate the huff-n-puff process in a horizontal well with hydraulic fractures and natural fractures as described in Fig. 5.2. A half fracture model was used in the simulation to describe changes of gas penetration in the field model because of flow symmetry.

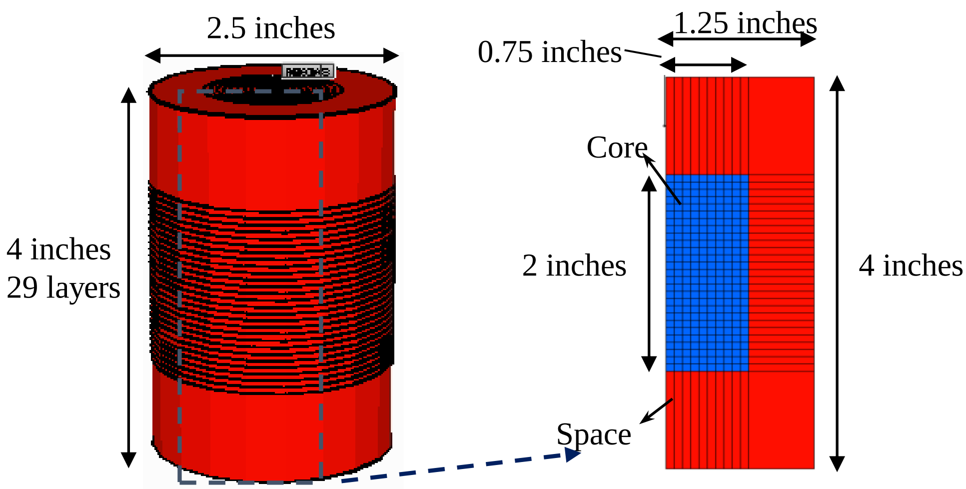

Fig. 5.1 – C1 huff-n-puff lab experimental model.

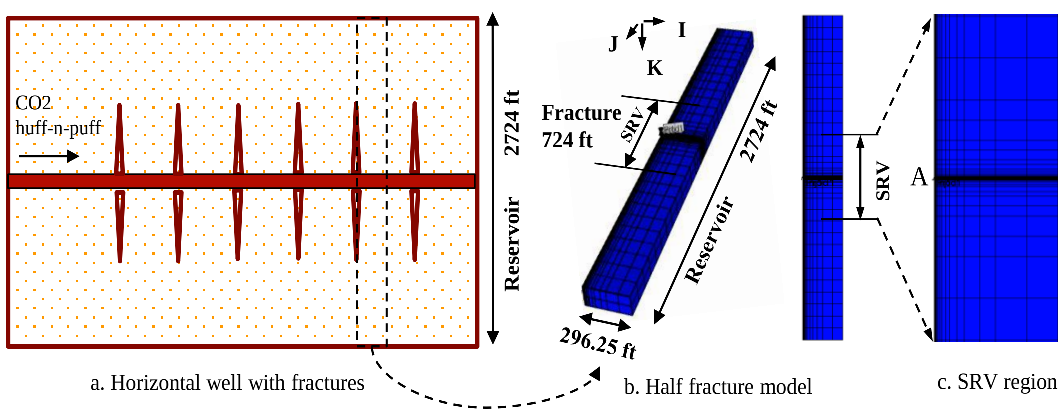

Fig. 5.2 – Field simulation model.

Sensitivity studies were conducted by using different natural fracture spaces and diffusion rate. The penetration depth is defined by the mass conservation equation.

$$\sum V_i \emptyset S_{oi} x_i = LWH \frac{\sum \emptyset V_i S_{oi}}{\sum \emptyset V_i} \times \frac{\sum \emptyset V_i x_i}{\sum \emptyset V_i} \qquad (5\text{-}1)$$

5.3 Main Results

The lab model simulation indicated that the gas penetration depth for cycles 1 to 4 are 0.15, 0.45, 0.675, and 0.75 inches, respectively. During one huff-n-puff cycle, gas penetrated fast during the injection time and slowly during the soaking time, which illustrates that longer soaking time is not necessary. With diffusion, injected gas will penetrate deeper area during huff period. Without diffusion effect, the oil viscosity, gas saturation, and injected gas model fraction in oil phase do not change during the huff period, resulting in slow gas penetration rate. Compared C1 and CO_2

huff-n-puff injection, CO_2 can dissolve more into the oil, leading to higher gas mole fraction in oil phase, lower oil viscosity, higher gas saturation, and higher oil recovery.

Fig. 5.3 presents the distribution of CO_2 mole fraction in oil phase in the X-Z cross section in the field model at the end of the huff time (100 days) of the first huff-n-puff cycle. The gas mainly penetrated the stimulated reservoir volume (SRV) region. For the reservoir with the hydraulic fracture spacing of 600ft, the CO_2 penetration depth is about 105.6 ft at 100 days' huff time in the first huff-n-puff cycle, covering about 36% of the SRV region. Fig. 5.4 shows that in the gas penetrated region, the oil viscosity decreases by 30% to 70%, and the average injected CO_2 mole fraction in oil phase reaches about 40%. A sensitivity study result shows that the most important parameter that can affect penetration depth is natural fracture spacing, followed by injection pressure, injected gas diffusivity in oil phase, huff-n-puff time, huff-n-puff start time, and reservoir permeability. Gas diffusion rate in the gas phase has little effect on penetration depth.

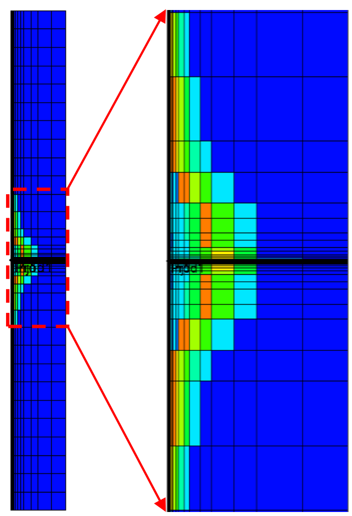

Fig. 5.3 – The distribution of CO_2 mole fraction in oil phase in field model at the end of huff period in field.

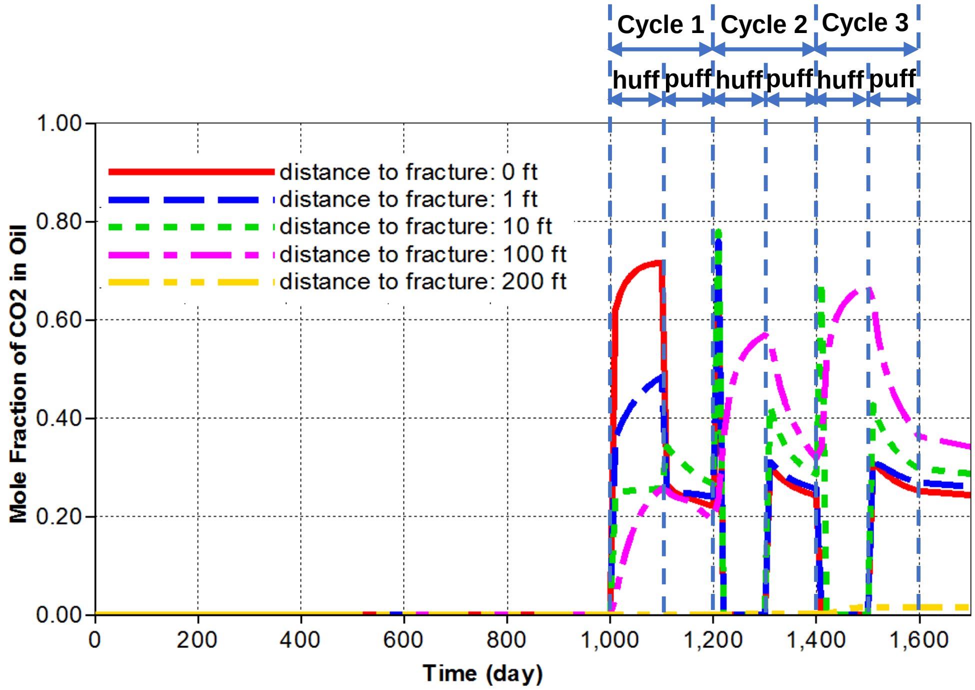

a. CO_2 mole fraction in oil phase

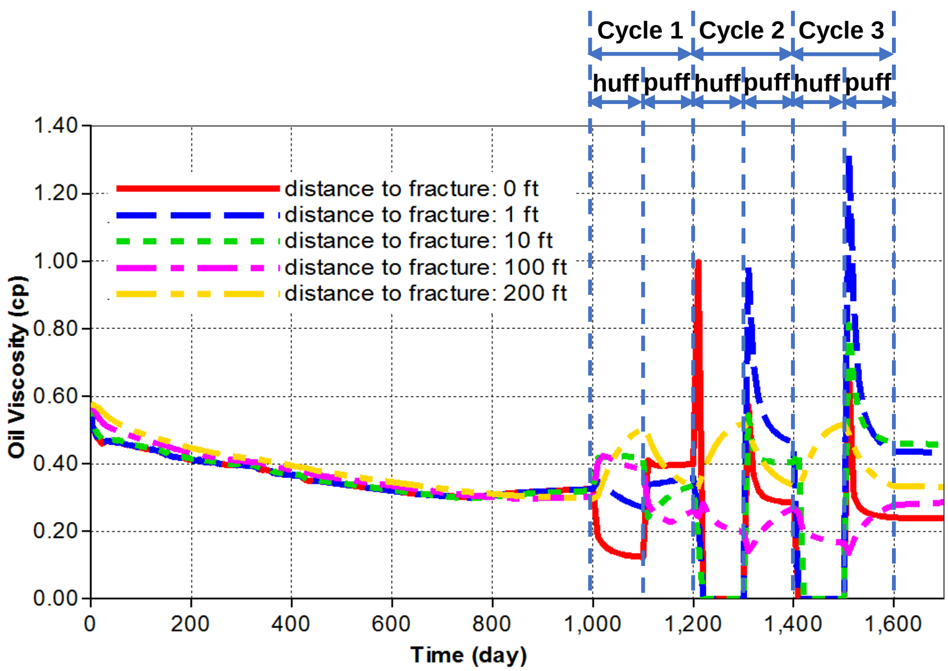

b. oil viscosity

Fig. 5.4 – Changes of CO_2 mole fraction in oil phase and oil viscosity at different distances during huff-n-puff process.

Chapter 6 Upscale of huff-n-puff oil recovery from lab scale to field scale

6.1 Introduction

Recent laboratory studies prove that the gas huff-n-puff holds a great potential for increased oil recovery in shale oil cores. However, field-scale tests of gas huff-n-puff in shale reservoirs are very limited. In order to predict the oil recovery in field scale production, an upscale method would need to be developed. After examining the literature, one way for upscaling is to generate a single curve which can describe the relationship of oil recovery with dimensionless time for different scales. For gas huff-n-puff in shale oil reservoirs, it is also needed to generate one single curve to upscale lab experiment to field production. And this theory should be confirmed by test data. This part includes the following research work.

- Scale up theory development
- Parameter validation tests

6.1 Scale up theory development

A general upscaling approach for gas huff-n-puff was developed based upon assumptions that the matrix is homogeneous and isotropic, and that the fracture and matrix permeabilities are constant. As the oil recovery is mostly dependent on the pressure change during the huff-n-puff cycle, we need to get a pressure related parameter to describe the huff-n-puff process. To start with the Gringarten et al.'s equations which address viscous drive (pressure drive) mechanism was modified by taking the time effect into consideration to describe the huff-n-puff efficiency.

After analyzing Fig. 6.1 which shows the oil recovery and average pressure changes with time, the time dependent term P_{huff} was a reasonable choice to describe the efficiency of the huff process. It describes the pressure build up efficiency of huff period. The higher the P_{huff} value is, the faster the reservoir is re-pressurized.

$$P_{\text{huff}} = \frac{S1}{S2} = \frac{\int_0^{t_{\text{huff}}} P_{\text{avg}}}{S_{\text{huff}}} = \frac{\int_0^{t_{\text{huff}}} P_{\text{avg}}}{P_{\max} \times t_{\text{huff}}} \tag{7-1}$$

Use the term P_{puff} to describe puff efficiency is:

$$P_{\text{puff}} = \frac{S3}{S4} = \frac{\int_0^{t_{\text{puff}}} P_{\text{avg}}}{S_{\text{puff}}} = \frac{\int_0^{t_{\text{puff}}} P_{\text{avg}}}{P_{\max} \times t_{\text{puff}}} \tag{7-2}$$

The dimensionless pressure is defined as the huff efficiency subtracted by puff efficiency and represents the efficiency in one huff-n-puff cycle.

$$P_D = P_{huff} - P_{puff} = \frac{\int_0^{t_{huff}} P_{avg}}{S_{huff}} - \frac{\int_0^{t_{puff}} P_{avg}}{S_{puff}} \tag{7-3}$$

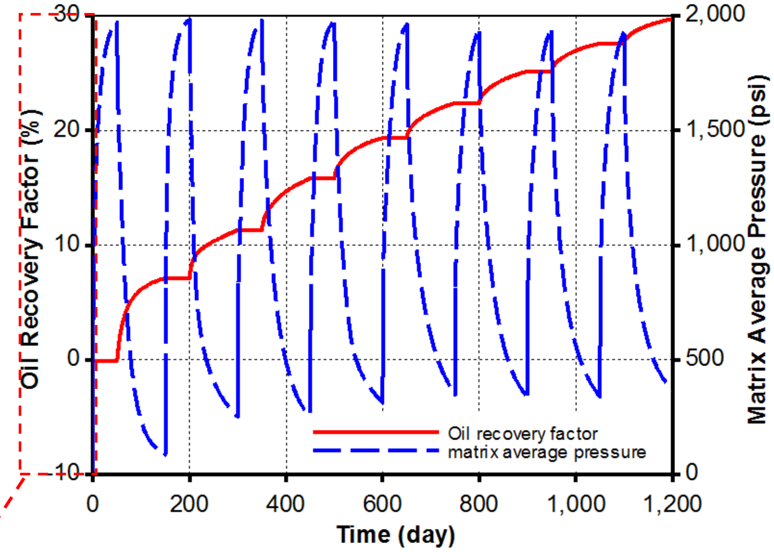

(a). Oil recovery factor & Matrix average pressure vs. operation time

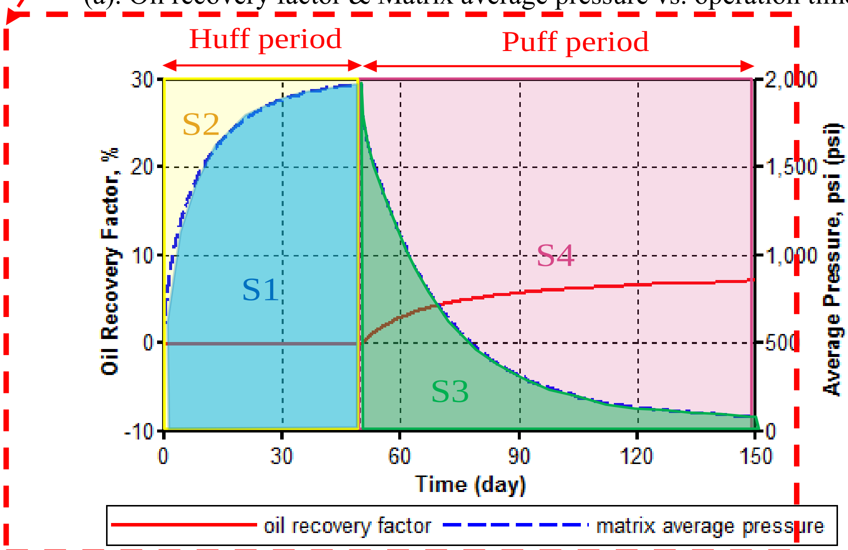

(b). Oil recovery factor & Matrix average pressure vs. operation time in the first cycle

Fig. 6.1 – Oil recovery factor, average pressure change during huff-n-puff cycle

The dimensionless time with response to the dimensionless pressure and other factors such as permeability, porosity, viscosity, and core length is expressed in equation (7-4):

$$t_D = \frac{Ckt}{\emptyset \mu c_t (L^2)({P_D}^2)} \tag{7-4}$$

6.2 Parameter validation tests

A simulation approach was applied to confirm the theory of dimensionless time and dimensionless pressure, the parameter validation tests including fluid property, rock property, and operation schedule were conducted.

A new compositional numerical simulation model was built based on the experiment data proposed by Li and Sheng (2016). Dynamic gridding (amalgamation) was applied to the simulation model and helps to save computing time during a simulation by reducing the number of grid blocks used in the model. For all the simulation in this study, the initial grid starts with fine grid blocks with the same grid size as the laboratory model. The dynamic gridding procedure is applied during the run processes. Fine grid blocks were used in the zones with large property variations, while zones with small property gradients are amalgamated in blocks of 10 or 100 times coarsening.

Assuming that the fluid & rock properties and the well constraints are the same for both lab and field scales, all different scales can reach the same oil recovery if they have enough huff-n-puff time. After converting the operation time to dimensionless time, the oil recovery results of all the scales follow one single curve which can be called the type curve for gas huff-n-puff in shale oil reservoir production as shown in Fig.6.2.

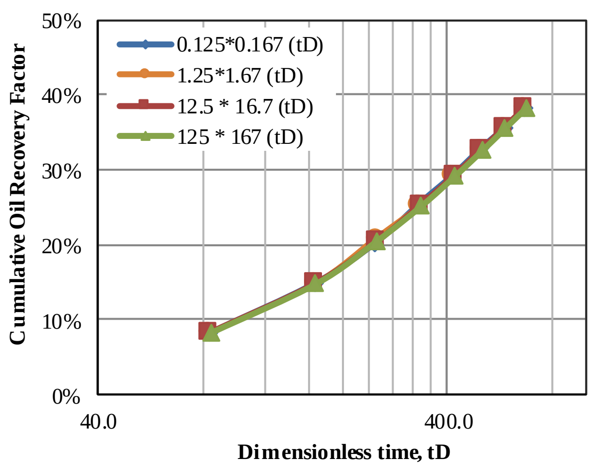

Fig. 6.2 – Oil R.F. vs. dimensionless time of different scales.

The fluid & rock properties including permeability, porosity, viscosity and perforation height are changed to validate the type curve.

Permeability. Take the case of a diameter of 12.5 ft and length of 16.7 ft as the base case. The permeability changed from 25 Nano-Darcy to 25,000 Nano-Darcy. The results show that as the permeability increases, the oil recovery factor increases, and the dimensionless pressure also increases. This confirms that the dimensionless pressure can be represented for the huff-n-puff effect. It also shows that, when the permeability is small, the dimensionless time is small, resulting in a low oil recovery, then the results follow on the type curve and located on the early stage. All the results follow on almost the same type curve as presented in Fig. 6.3, which confirms the concepts of dimensionless pressure and dimensionless time.

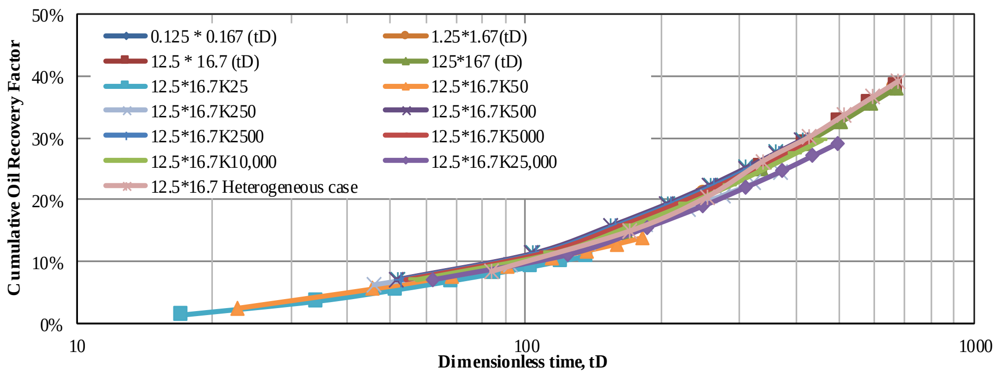

Fig.6.3 – Oil R.F. vs. dimensionless time for modified permeability validation test and heterogeneous test.

The validation tests for other parameters such as porosity, viscosity and perforation height were also investigated. The results indicate that all the results follow on almost the same type curve. This proves that the type curve can be used to predict the oil recovery for different scales with different parameter values. Also, from the example of high permeability cases, the operation condition can be modified based on the comparison of the calculated results with the type curve. If the result curve is located at the right side of the curve, the huff-n-puff time should be decreased. If the result curve located on the left side of the curve, the huff-n-puff time may need to be increased to get a higher oil recovery.

In all of the above discussions, the well constraints are the same with the one in lab scale which is also not realistic in the field production. the operation conditions were changed to more practical ones and confirmed the validity of this upscale theory.

For more details, read this paper:

13 Li, L. and Sheng, J. J. (2017). Upscale methodology for gas huff-n-puff process in shale oil reservoirs. Journal of Petroleum Science and Engineering, 153, 36-46.

14 Li, L., Sheng, J.J., and Sheng, J. 2016. Optimization of Huff-n-Puff Gas Injection to Enhance Oil Recovery in Shale Reservoirs, paper SPE 180219 presented at the SPE Low Perm Symposium held in Denver, Colorado, USA, 5–6 May.

15 Li, L., Sheng, J.J., Watson, M., Mody, F., and Barnes, W. 2015. Experimental and Numerical Upscale Study of Cyclic Methane Injection to Enhance Shale Oil Recovery, paper presented at the 2015 AIChE Annual Meeting, Salt Lake City, UT, 8-13 November.

Chapter 7 Asphaltene deposition in huff-n-puff gas injection

7.1 Introduction

Gas injection is believed to be more practical and efficient than other EOR methods in shale, huff-n-puff gas injection is more effective than gas flooding. Numerous studies on huff-n-puff gas injection EOR in shale have been done experimentally and numerically. The potential of huff-n-puff gas injection to enhance oil recovery in shale has been proved. One problem that comes with the gas injection EOR method is asphaltene deposition, which hasn't been considered in the previous studies on huff-n-puff gas injection EOR in shale. According to the studies in conventional reservoirs, the asphaltene deposition can cause severe permeability reduction and production loss during gas injection EOR. However, the effects of asphaltene deposition on the performance of huff-n-puff gas injection in shale oil reservoirs still remain unknown. Thus, this study to investigate asphaltene precipitation and deposition phenomenon during huff-n-puff gas injection in shale oil reservoirs, and their effects on formation damage and performance of huff-n-puff gas injection EOR method in shale oil reservoirs was performed. The following research activities were conducted in this study.

- Experimental study of asphaltene precipitation during CO2 and CH4 injection in shale oil
- Experimental study of asphaltene deposition induced formation damage during CO2 huff-n-puff injection in shale rock samples
- Simulation study of asphaltene deposition during CO2 huff-n-puff injection in shale rock samples
- Investigation of optimization strategy to reduce asphaltene deposition associated damage during CO2 huff-n-puff injection in shale

7.2 Experimental study of asphaltene precipitation during CO2 and CH4 injection in shale oil

The particle size of asphaltene precipitation plays an important role in pore and throat plugging in porous media. It is generally agreed that particles with a size greater than 1/3 of the size of pores and throats would block the pores and throats. In this study, we used a nanofiltration technique to investigate the size of asphaltene aggregates precipitated during CO2 and CH4 injection in an oil sample from a Wolfcamp shale reservoir. Nano membranes of 200 nm, 100 nm and 30 nm were used to filtrate oil samples injected with different mole fractions of CO2 and CH4 gas. The distribution of the particle size of asphaltene aggregates at different injected CO_2 and CH_4 concentrations were obtained and compared with the pore size distribution of shale cores. By comparing the particle size of asphaltene precipitation with pore-and-throat size of shale rock samples, the potential of pore plugging induced formation damage in shale during huff-n-puff gas injection can be evaluated.

The experiments were designed to study the amount and particle size of asphaltene precipitation during CO_2 and CH_4 injection into the shale oil sample as a function of injected gas concentration. The tests were conducted by isobarically and isothermally (at 69°F) filtering about 200 ml of the shale oil sample mixed with injected gas at different concentrations using 30 nm, 100 nm, and 200 nm membranes using the setup shown in Fig. 7.1. The total amount of asphaltene precipitation and the particle size distribution of the asphaltene precipitation at different injected gas concentrations were measured. The pore size distribution of core samples from a Wolfcamp shale oil reservoir, an Eagle Ford shale oil reservoir, and Mancos shale reservoir outcrop were measured using a mercury intrusion porosimeter.

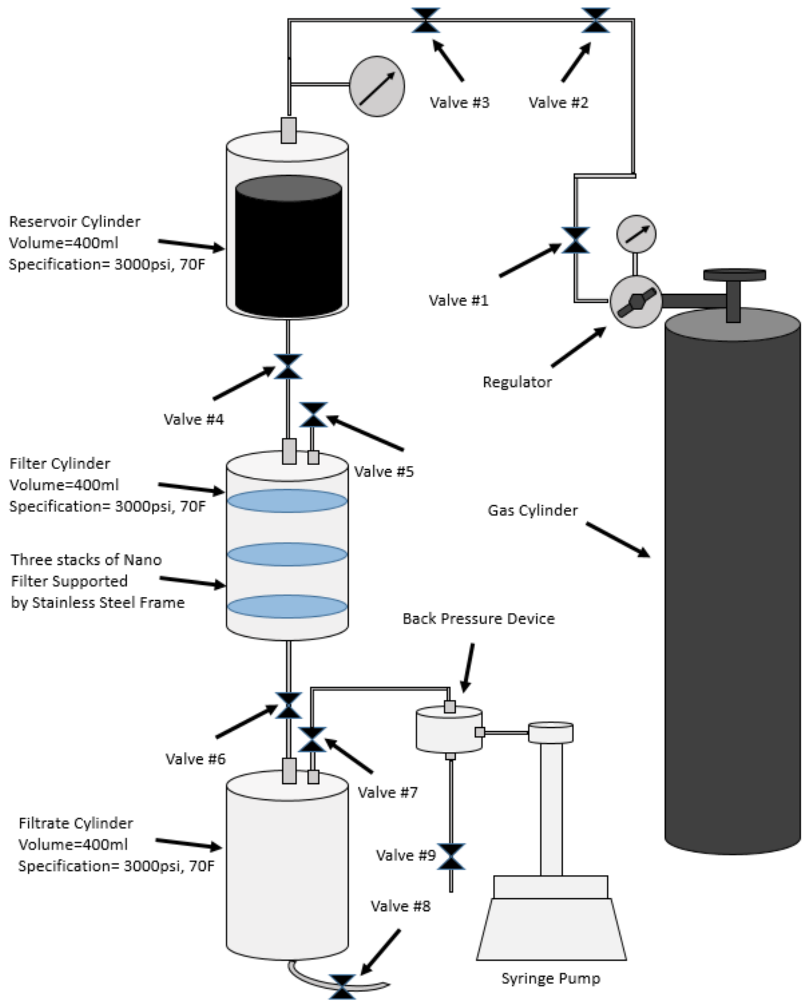

Fig. 7.1. Schematic of asphaltene precipitation particle size measurement apparatus

It was observed that incrementals of injected gas concentration of both CO2 and CH4 resulted in more asphaltene precipitation and greater amount of larger size asphaltene aggregates. CO2 had stronger effect on generating asphaltene precipitation and growth of asphaltene particle size than CH4. Significant amount of asphaltene precipitation generated during CO2 and CH4 injection had particle size larger than 100 nm. According to the pore size distribution results, the majority of the pore diameter lies in the range of 3 nm~50 nm in the three tested shale core samples. It can be seen that the particle size of the asphaltene precipitation generated during CO2 and CH4 injection in the shale oil sample was large enough to cause pore plugging in the three tested core samples.

For more details, read the following paper:

16 Shen, Z. and Sheng, J. J., 2016. Experimental Study of Asphaltene Aggregation during CO2 and CH4 Injection in Shale Oil Reservoirs. Paper SPE 179675 presented at the SPE Improved Oil Recovery Conference, 11-13 April, Tulsa, Oklahoma, USA.

7.3 Experimental study of asphaltene deposition induced formation damage during CO2 huff-n-puff injection in shale rock samples

In previous section, the potential of pore plugging caused by asphaltene precipitation during gas injection in shale was investigated. In this section, CO2 huff-n-puff injection was performed in outcrop core samples from an Eagle Ford shale reservoir to investigate formation damage caused by asphaltene deposition. The asphaltene deposition induced pore size reduction and permeability reduction in shale core samples were measured experimentally. The permeability reduction due to asphaltene deposition by mechanical plugging and adsorption mechanisms were also determined using the n-Heptane and toluene reverse flooding, respectively.

The shale core samples were firstly saturated with a dead oil sample from a Wolfcamp shale oil reservoir using the experimental setup shown in Fig. 7.2. This setup consists mainly of a pressure vessel, an accumulator, a vacuum pump, pressure gauges, and a Quizix QX6000 pump. The saturating process was designed to last for 120 hours at 4000 psi to make sure the core samples were fully saturated. The CO2 huff-n-puff injection was performed in the experimental setup shown in Fig. 7.3. This setup mainly consists of a syringe pump, a pressure vessel, and pressure gauges. The huff injection pressure, huff injection time and puff producing time can be controlled depending on the required testing scenarios. The pore size distribution of core samples before and after CO2 huff-n-puff injection were measured using mercury intrusion porosimeters to determine the pore size distribution change caused by asphaltene deposition. The permeability of core samples before and after CO2 huff-n-puff injection were measured using Autolab-1000 system to determine permeability reduction caused by asphaltene deposition. After the CO2 huff-n-puff was finished, a piece of rock with thickness of 0.9 cm was cut from the core plug to perform the n-Heptane and toluene reverse flooding using experimental setup shown in Fig. 7.4. Because asphaltene is not soluble in n-Heptane, the only effect of reversal of the flow direction with n-Heptane is removal of asphaltene deposition due to mechanical plugging mechanism. In contrast, the toluene will react with remaining asphaltene deposition from the previous n-Heptane reverse flooding, thus the effect of reversal of the flow direction with toluene is to remove asphaltene deposition due to adsorption mechanism.

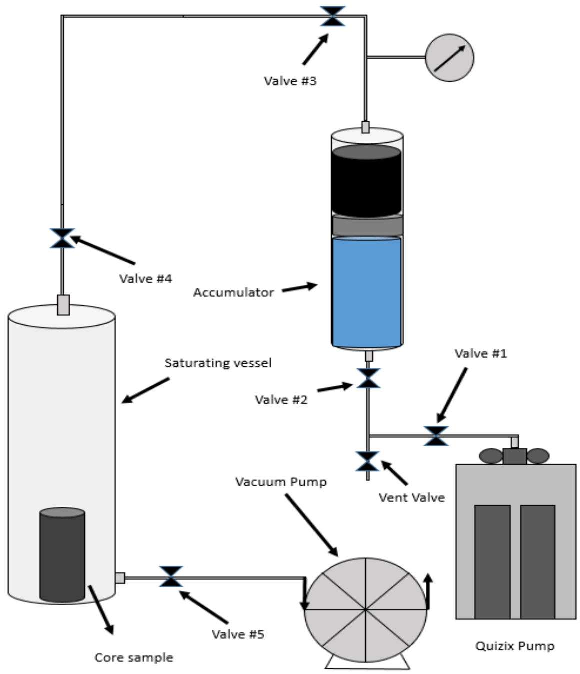

Fig. 7.2. Schematic of saturating setup.

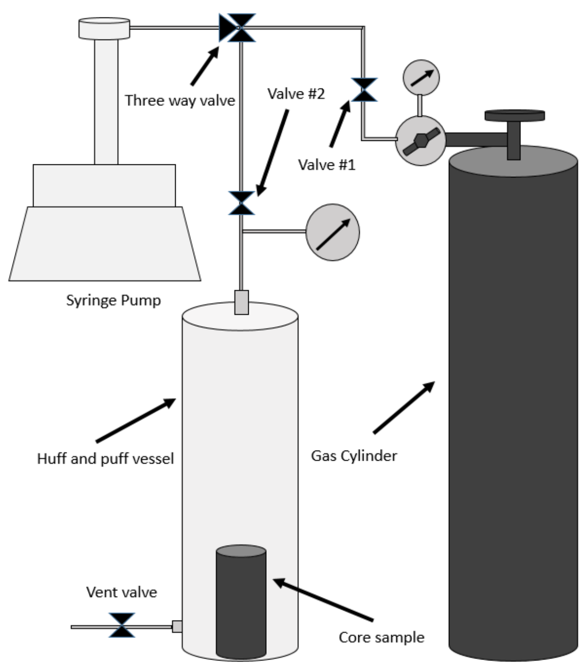

Fig. 7.3. Schematic of huff-n-puff setup.

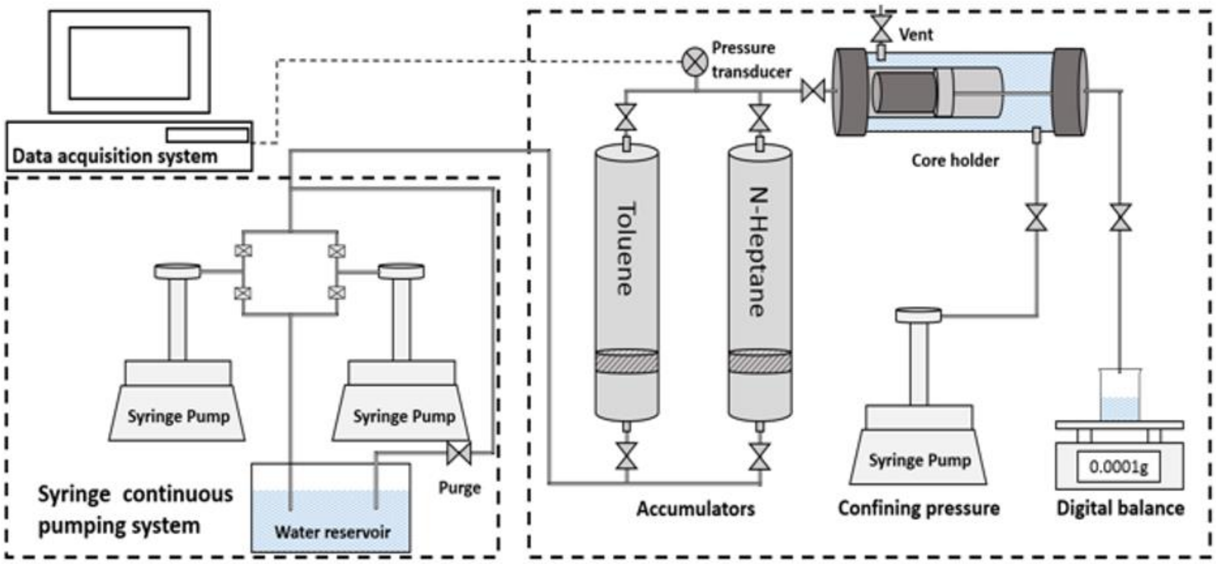

Fig. 7.4. Schematic of reverse flooding setup.

The results show that the permeability of one of the tested Eagle Ford shale outcrop core before CO_2 huff-n-puff injection was 126 nD, while the permeability of the same core after CO_2 huff-n-puff injection became 78.5 nD. Thus, a permeability reduction of 47.5 nD was caused by the asphaltene deposition generated during the CO_2 huff-n-puff injection. The comparison of pore size distribution of one of the tested Eagle Ford shale outcrop core before and after CO_2 huff-n-puff injection shows that the asphaltene deposition caused a reduction in the percentage of pores with larger size and an increase in the percentage of pores with smaller size as shown in Fig. 7.5. In the comparative experiments with Decane, no obvious decrease in permeability or percentage of pores with larger size was observed, which conformed that the permeability reduction and pore size distribution change were caused by asphaltene deposition. The results of n-Heptane and toluene reverse flooding showed that 83% of the total permeability reduction is due to asphaltene deposition by mechanical plugging mechanism, while 17% of the total permeability reduction is due to asphaltene deposition by adsorption mechanism. The critical interstitial velocity for entrainment of asphaltene deposition was around 0.0008 cm/sec.

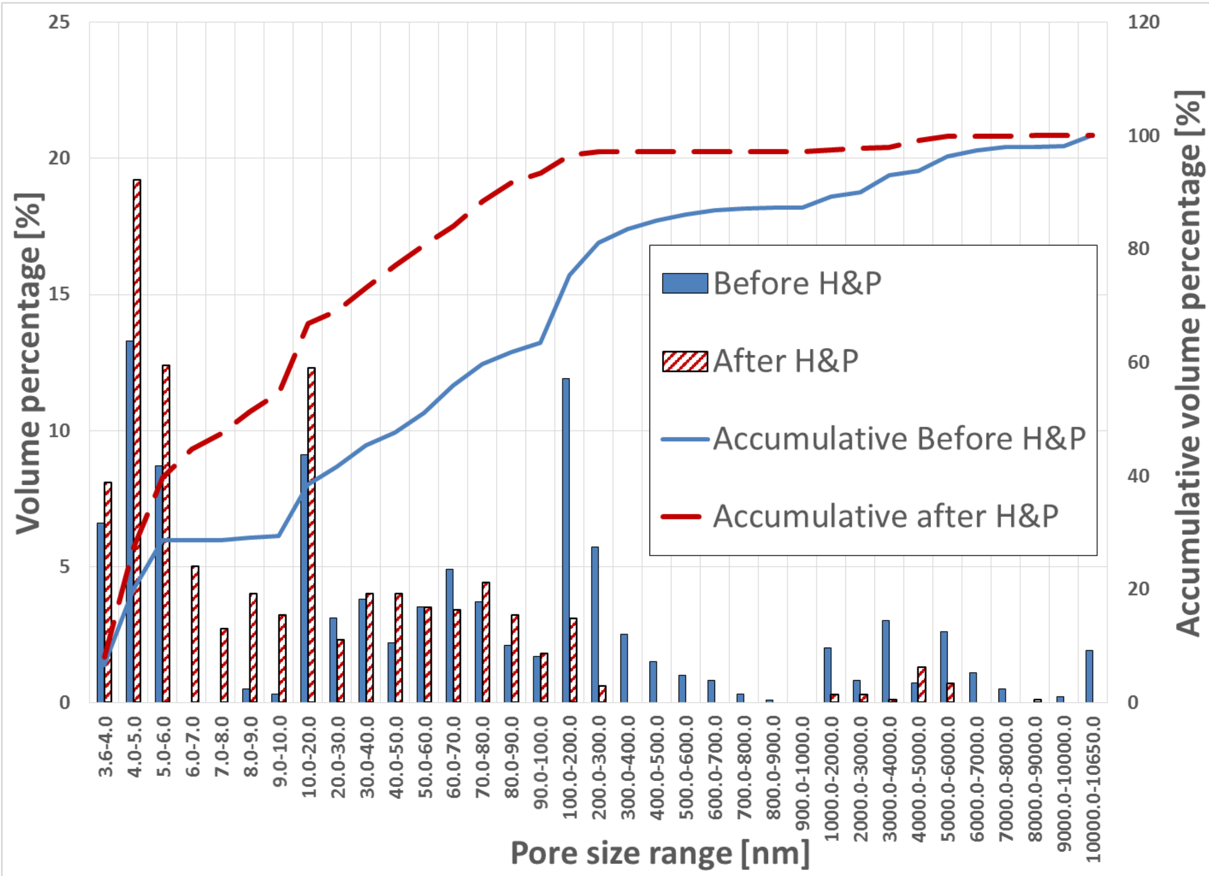

Fig. 7.5. Comparison of PSD in Eagle Ford shale outcrop before and after 6 cycles of CO2 huff-n-puff injection.

For more details, read this paper:

17 Shen, Z. and Sheng, J. J., 2017. Experimental study of permeability reduction and pore size distribution change due to asphaltene deposition during CO2 huff and puff injection in Eagle Ford shale, Asia-Pacific Journal of Chemical Engineering, 12(3), 381-390.

7.4 Simulation study of asphaltene deposition during CO2 huff-n-puff injection in shale rock samples

In this work, CO2 huff-n-puff injection experiments were conducted on Eagle Ford outcrop core plugs saturated with Wolfcamp shale crude oil. The oil recovery factor and permeability reduction were measured during the CO2 huff-n-puff injection after different cycles. Core scale simulation model was built using Winprop and GEM simulator in CMG software to mimic the CO2 huff-n-puff injection. The asphaltene precipitation and deposition processes were also simulated using the built-in asphaltene precipitation and deposition models in Winprop and GEM simulators. The core scale simulation model was tuned and adjusted to match the experimental oil recovery data and permeability reduction data. Parameters for asphaltene precipitation model and asphaltene deposition model in shale during the CO_2 huff-n-puff injection process were obtained which can be used for future simulation work.

Two Eagle Ford shale outcrop core plugs with similar initial permeability were selected to perform the CO_2 huff-n-puff injection. One of the core plugs was designed to have one cycle of CO_2 huff-n-puff injection, after which the core plug is saturated with Wolfcamp oil sample and the permeability of the core is measured again to calculate the permeability reduction caused by the first cycle of CO_2 huff-n-puff injection. The other core plug was designed to have six cycles of CO_2 huff-n-puff injection, after which the core plug is saturated with Wolfcamp oil sample and the permeability of the core is measured again to calculate the permeability reduction caused by the six cycles of CO_2 huff-n-puff injection. The oil recovery factors after each cycle of the huff-n-puff injection were determined by measuring the weight of the core plug after each cycle of the huff-n-puff injection. The experimental setups and procedures of core saturating and CO_2 huff-n-puff injection processes are similar to the ones used in section 7.3. In order to further investigate the asphaltene precipitation and deposition process during the CO_2 huff-n-puff injection, a numerical simulation method was applied to build up the asphaltene precipitation model and core scale model to match the experimental results. Compositional model of the Wolfcamp crude oil with asphaltene precipitation prediction was built using Winprop simulator in CMG software based on the oil compositions analyzed by GC. The core scale simulation model with asphaltene deposition was built using GEM simulator as shown in Fig. 7.6.

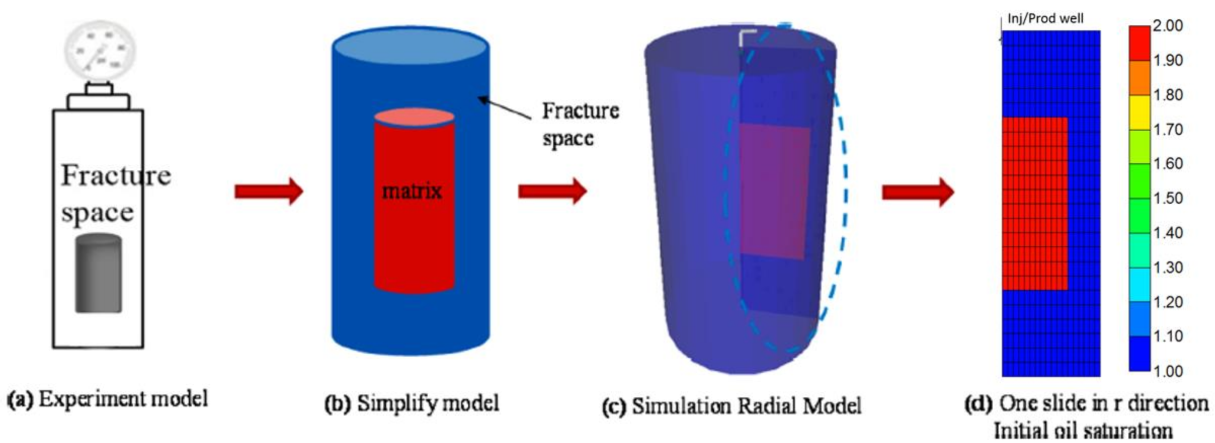

Fig. 7.6. Radial core experiment model buildup process.

The experimental results showed that the permeability reduction caused by asphaltene deposition after the first cycle of CO_2 huff-n-puff injection was 26.8%, and the permeability reduction caused by asphaltene deposition after sixth cycle of CO_2 huff-n-puff injection was 48.5%. In the core scale simulation model, the Peng-Robinson EOS fluid description of Wolfcamp crude oil, parameters of asphaltene deposition model in shale and relative permeability profile were tuned to match the experimental results, including both the oil recovery factor and permeability reduction factor as shown in Figs. 7.7 and 7.8. The tuned model gave a reasonable match.

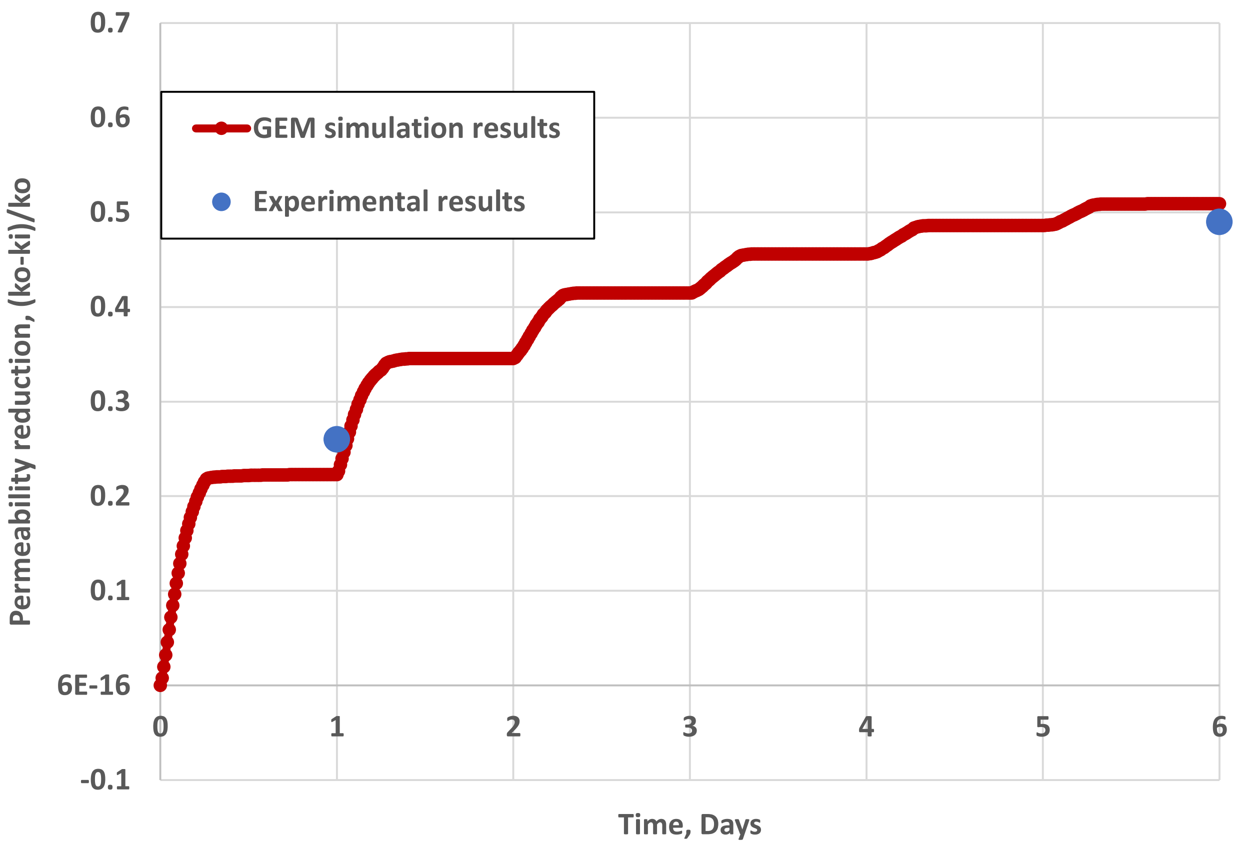

Fig. 7.7. Comparison of GEM simulator predicted permeability reduction data and experimental permeability reduction data.

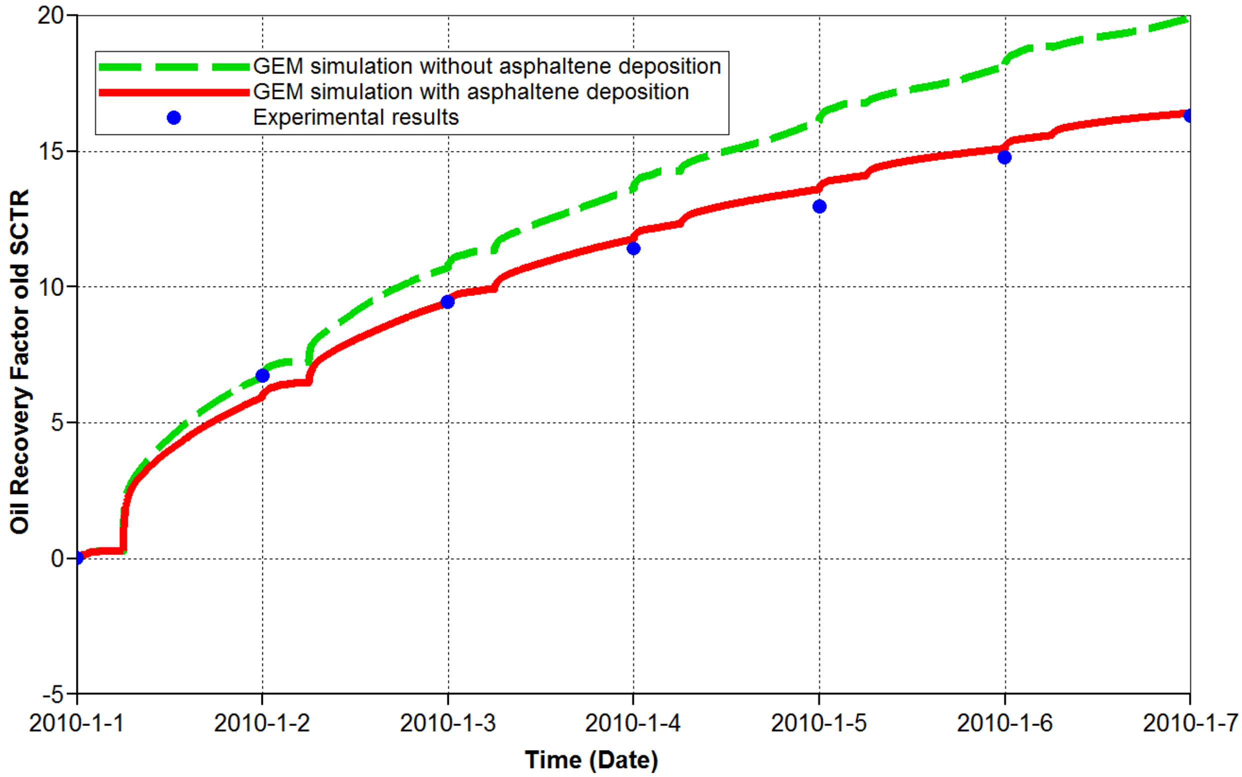

Fig. 7.8. Comparison of GEM simulator predicted oil recovery data and experimental oil recovery data.

Simulation results showed that the asphaltene precipitation and deposition during the CO2 huff-n-puff injection caused a 3.5% oil recovery factor reduction after 6 cycles as shown in Fig. 7.8. This oil recovery reduction started to show up right after the beginning of CO2 huff-n-puff injection and the effect of asphaltene deposition on oil recovery factor accumulated during the later cycles. Analysis of simulation results show that the asphaltene deposition was mainly formed in the near surface area of the core plug as shown in Fig. 7.9. It indicated that the CO2 penetration depth and concentration were the dominant factors in this process. Also, the CO2 concentration is quickly increased in the first cycle and more oil is near the rock surface in the first cycle, asphaltene precipitation and deposition were most significant during the huff period in the first cycle compared with the subsequent cycles. Simulation results also show that in the puff period of the first cycle, asphaltene precipitation is quickly decreased, as CO2 flow back. In addition, although oil in the inner blocks continuously flows to the outer blocks during the puff period, due to the extremely low permeability of the core plug, the amount of oil is small and this oil has already experienced the asphaltene precipitation process during the previous huff period, A very small amount of increase in the asphaltene deposition occurs during the subsequent puff periods.

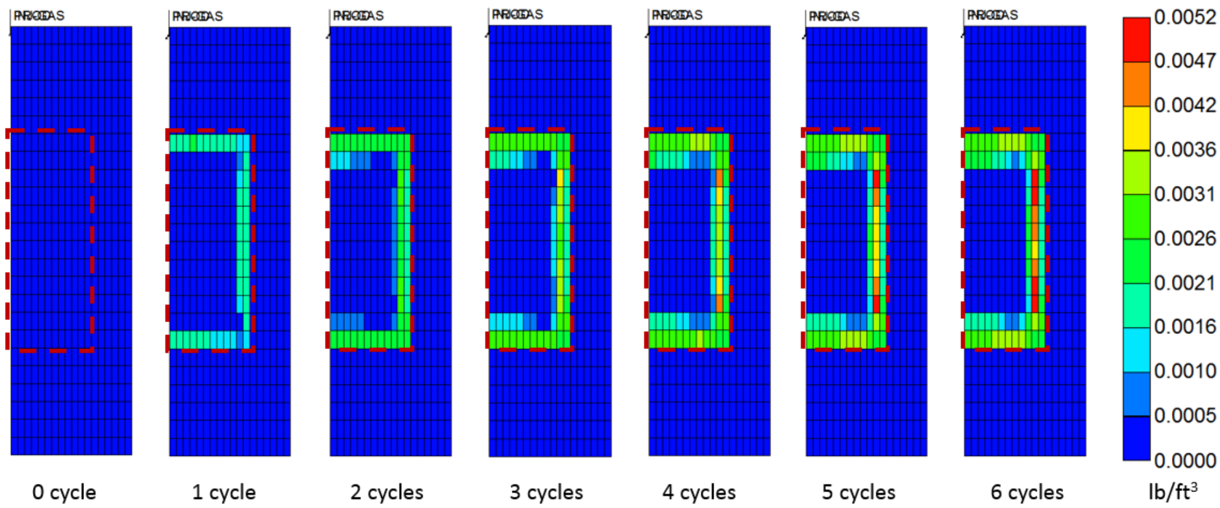

Fig. 7.9. Asphaltene deposition mass per bulk volume after different cycles of CO2 huff-n-puff injection.

For more details, read this paper:

18 Shen, Z. and Sheng, J. J., 2017. Experimental and numerical study of permeability reduction caused by asphaltene precipitation and deposition during CO2 huff and puff injection in Eagle Ford shale. Fuel 211, 432-445.

7.5 Investigation of optimization strategy to reduce asphaltene deposition associated damage during CO2 huff-n-puff injection in shale

In this study, numerical reservoir simulation method was used to model CO2 huff-n-puff injection process and CO2 gas associated asphaltene precipitation and deposition with typical reservoir and fracture properties from a hydraulic fractured shale oil reservoir. Effects of CO2 huff-n-puff injection operational scenarios including huff injection pressure, puff pressure, huff time, and puff time on asphaltene deposition and associated oil production loss were examined in detail. The numerical reservoir simulation modeling work provides a better understanding of the physical mechanisms and key parameters affecting the asphaltene deposition and the oil production loss during CO2 huff-n-puff injection in hydraulic fractured shale formation.

A numerical reservoir model was built of a half-fracture connected through a horizontal well assuming flow symmetry, using the compositional simulator, GEM, developed by Computer Modeling Group. The schematic of the half-fracture model is shown in Fig. 7.10. The simulation model includes two regions, namely the stimulated reservoir volume and un-stimulated reservoir volume. Different rock matrix and fracture network properties in the Non-SRV and SRV area in the half-fracture model to make the model close to realistic condition. Dual permeability model is used to simulate the natural fracture and hydraulic fracture network in the shale formation. The PVT and compositional data of a live oil sample from an Iranian oil reservoir published by Ashoori and Balavi (2014) was used in this study. In their experimental study, the amount of asphaltene precipitation during primary depletion and CO2 injection process were measured and reported. The Peng-Robinson EOS fluid description of the Iranian oil sample was tuned to match the asphaltene precipitation data from their experiments as shown in Fig. 7.11. The parameters of asphaltene deposition model in shale used in the simulation model were from the simulation work discussed in section 7.4. The relative permeability curves are from earlier simulation studies on Middle Bakken shale oil reservoir reported in the literature.

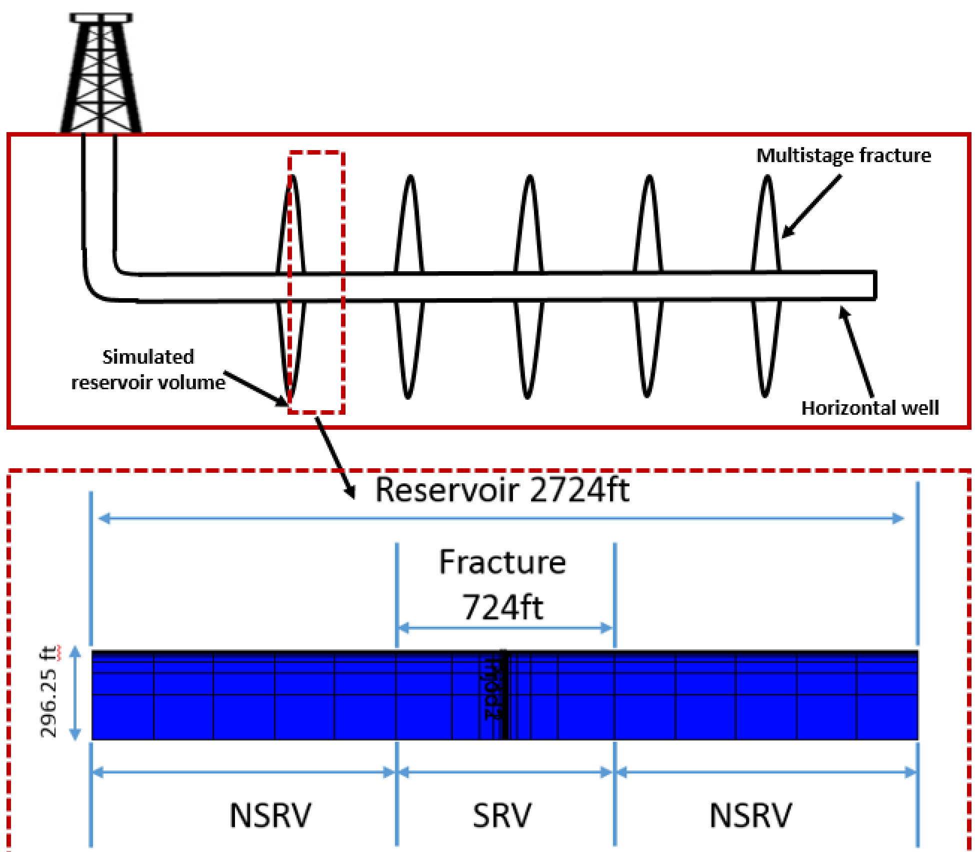

Fig. 7.10. Schematic of the half-fracture reservoir model.

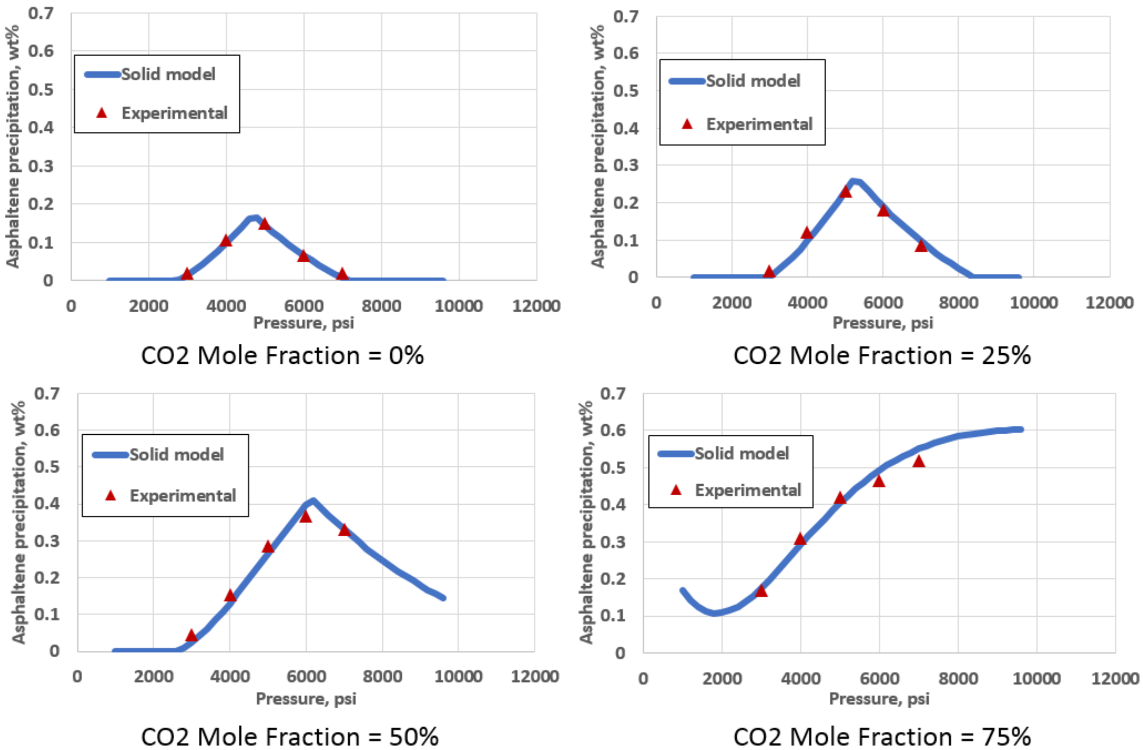

Fig. 7.11. Comparison of Winprop predicted asphaltene precipitation data with the experimental data by Ashoori and Balavi, 2014.

The simulation results showed that more severe oil recovery reduction caused by asphaltene deposition was observed in the CO2 huff-n-puff process than in the primary depletion, because more asphaltene precipitation and deposition is formed during the CO2 huff-n-puff process. The oil recovery factor reduction caused by asphaltene deposition gets accumulated as the cycles number increases during the CO2 huff-n-puff injection, and resulted in a totally 3.5% oil recovery factor reduction after 5600 days of CO2 huff and puff injection as shown in Fig. 7.12.

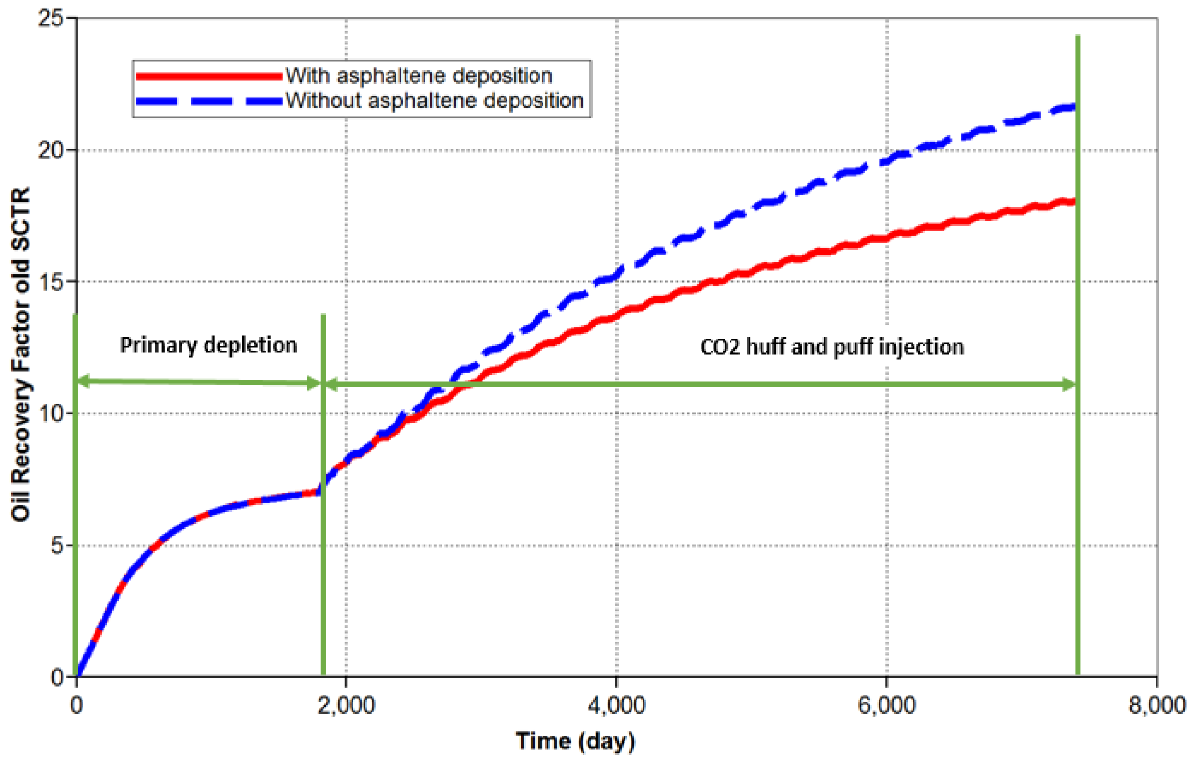

Fig. 7.12. Comparison of oil recovery factor in two cases with/without asphaltene deposition.

The asphaltene precipitation and deposition behaviors in the rock matrix and fracture network are different. In the fracture network, most of asphaltene precipitation and deposition is formed during the puff period, while in the rock matrix, the asphaltene precipitation and deposition is formed during both the huff period and puff period. It was observed that by reducing the huff period time or increasing the puff period time, the asphaltene deposition can be reduced significantly in the fracture system. It may be more favorable to adjust the huff time and puff time to control the asphaltene deposition. But huff period time should be long enough for the pressure near the wellbore to reach the set maximum injection pressure and the puff period time should be long enough for the pressure near the wellbore to reach the set minimum production pressure. The effect of puff pressure on asphaltene deposition reduction is not significant. Although by decreasing the huff injection pressure, he asphaltene deposition can be reduced, but meanwhile the oil production also suffers from significant decrease which leads to a significant reduction in the oil recovery.

Chapter 8 EOR potential of huff-n-puff gas injection in gas condensate reservoirs

8.1 Introduction

Condensate blockage is a serious problem in shale gas condensate reservoirs. As the pressure decreases lower than dew point pressure, condensate forms. This liquid dropout reduces gas relative permeability. As a consequence, gas production is decreased and liquid dropout-condensate, a valuable resource, remains in the reservoir. Thus, enhancing condensate recovery in shale gas condensate reservoir is an important issue. To study the efficiency and application of huff-n-puff gas injection to enhance condensate recovery in shale gas condensate reservoir, the following research was concluded:

- EOR potential of huff-n-puff gas injection in shale gas condensate reservoir.
- Comparison between huff-n-puff gas injection and gas flooding.
- Optimization of huff-n-puff gas injection.

8.2 EOR potential of huff-n-puff gas injection in shale gas condensate reservoir

This section examines the potential of huff-n-puff gas injection method to recover condensate in shale gas condensate reservoirs by conducting experiments on a shale core. Also, numerical models were developed to verify experiment results.

The Eagle Ford outcrop core used in the experiment was 1.5 inches in diameter and 4 inches in length, the porosity of the core was 6.8% and the permeability was 0.0001 mD. The gas condensate mixture used in the experiment was a synthetic gas condensate mixture: 85% methane and 15% n-butane. Fig. 8.1 shows the liquid dropout curve for the gas mixture at 68 °F. As seen from the figure, the methane and butane gas mixture had a wide condensate region at 68 °F. The dew point pressure of this gas condensate mixture at 68 °F was 1,860 psi. This gas mixture had very good gas condensate properties, which made it suitable for use in the experiment.

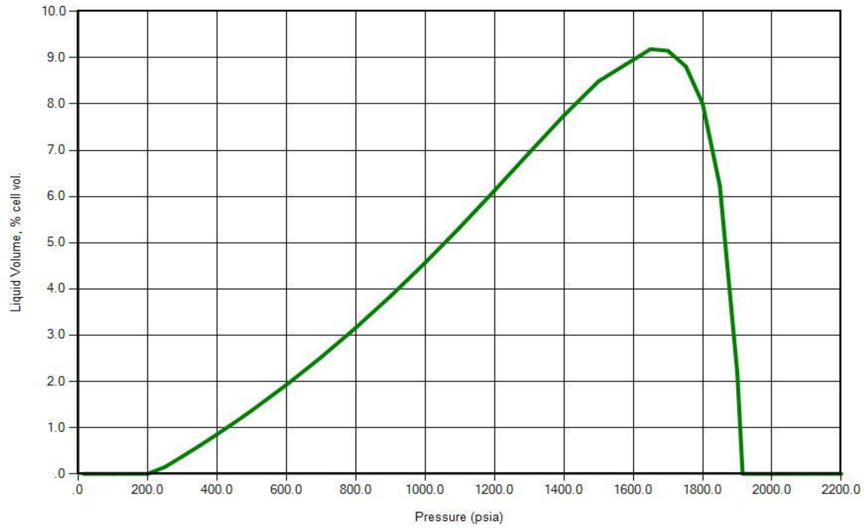

Fig. 8.1 Simulated liquid dropout curve for gas mixture at 68°F

The huff-n-puff process is shown in Fig. 8.2. The injection pressure was set to 1900 psi which was higher than the dew point pressure of the gas condensate mixture. The mixture of methane and n-butane was injected into the core holder from both of the two-end faces. The injection time was set to 30 minutes. After injection, the methane cylinder was disconnected and the pressure of the core holder was depleted to 1460 psi at a low-pressure depletion rate for 30 minutes. The condensate saturation was measured by using a CT scanner after every puff process. The experiment was run for 5 cycles of the huff-n-puff process. The condensate recovery was attained from the condensate saturation.

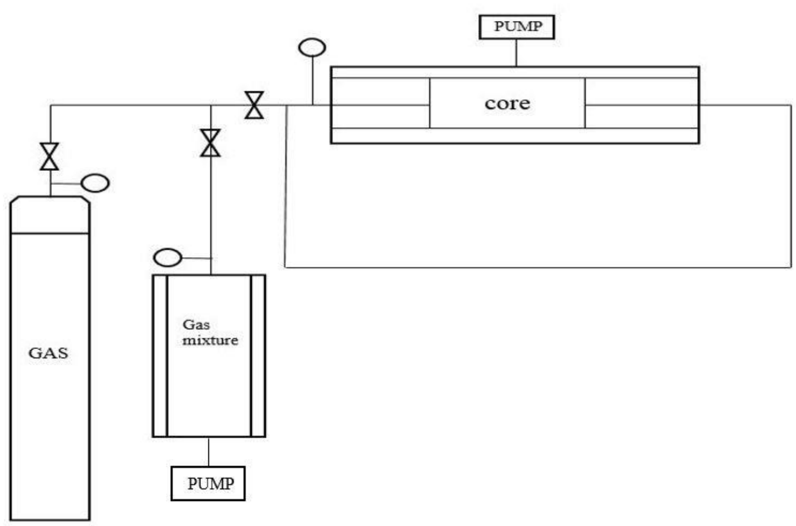

Fig. 8.2 Schematic of huff-n-puff gas injection apparatus

The simulation model was also built to simulate the experiment process. The model had the same size as the core used in the experiment. In the simulation work, the shape of the core was transferred to a rectangle, which had the same surface of the core that was used in the experiment. The permeability of the core sample was 0.0001 mD. Fig. 8.3 shows the huff-n-puff simulation model.

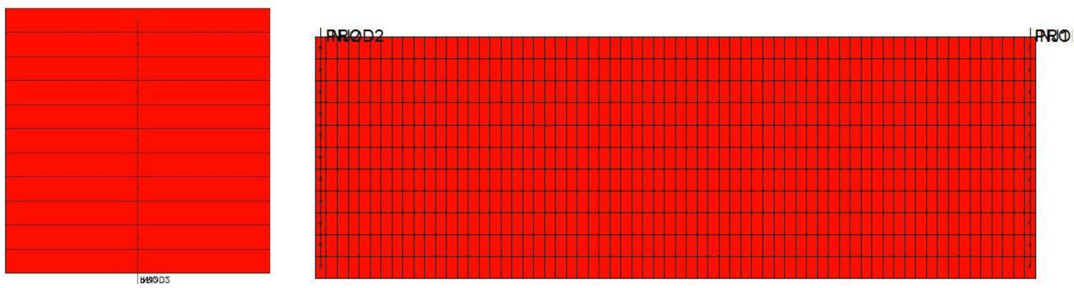

Fig. 8.3 Simulation model of huff-n-puff in JK view and IK view

As Fig. 8.4 shows, the condensate saturation after the primary depletion was 10%, and after the first cycle of huff-n-puff, at the end of puff process, the condensate saturation was decreased to 9.1%. From the variation of condensate saturation, the condensate recovery could be obtained. Fig. 8.5 shows the condensate recovery for five huff-n-puff cycles in the lab.

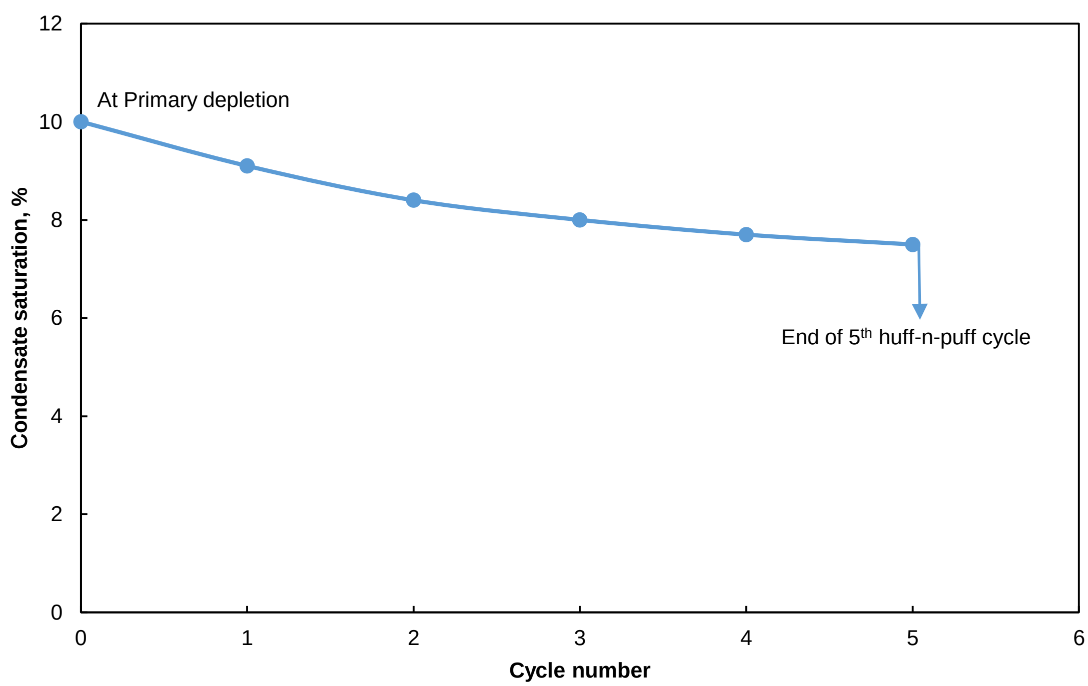

Fig. 8.4 Condensate saturations at the ends of different cycles

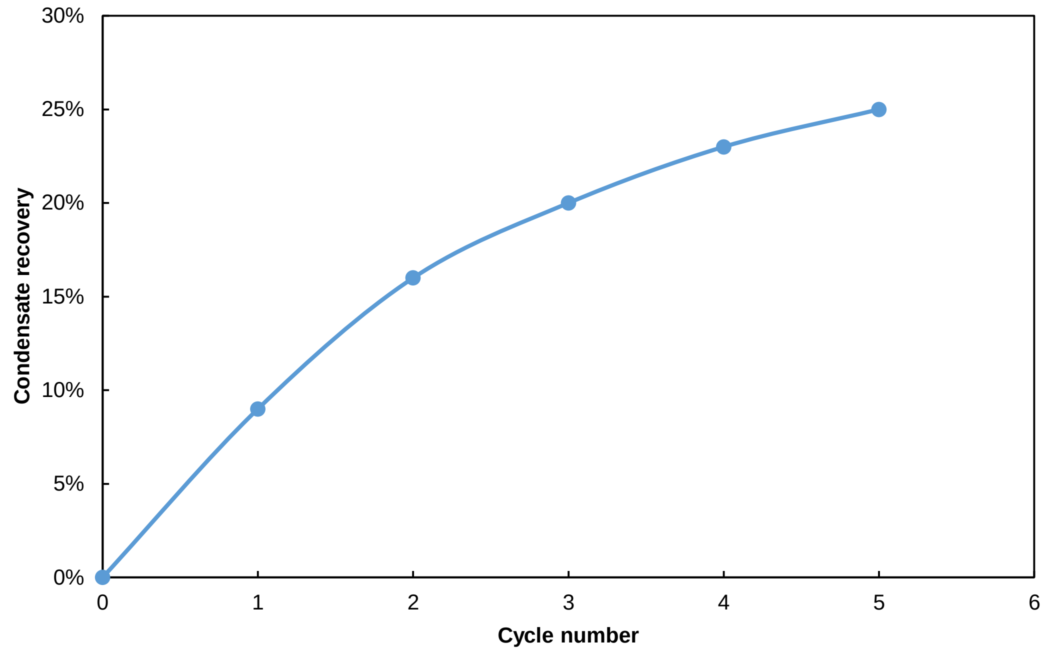

Fig. 8.5 Condensate recovery at the ends of different cycles

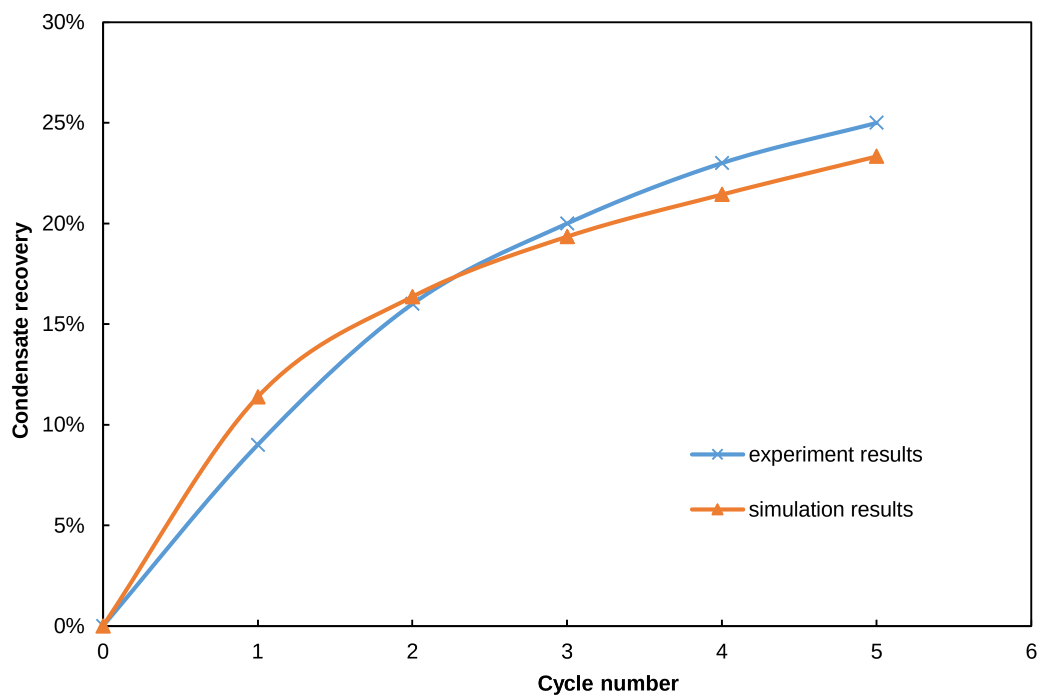

Fig. 8.6 Condensate recovery comparison of simulation results with experimental data for huff-n-puff

The experimental results show that the condensate recovery reached 25% by applying the huff-n-puff method, which validates the efficiency of the huff-n-puff method in shale core in the lab. Also, the simulation results were history-matched with the experiment results by adjusting relative permeability of simulation model, as shown in Fig. 8.6. It demonstrates a positive agreement between the condensate saturation measured by the CT and condensate recovery attained by simulation. Our simulation model verifies the experimental results. Both experimental and simulation results show a good potential of huff-n-puff gas injection to enhance condensate recovery.

8.3. Comparison between huff-n-puff gas injection and gas flooding

Although the experimental and simulation results illustrate the potential of the huff-n-puff method, it is necessary to compare the efficiency of huff-n-puff with that of gas flooding. Both of the methods can be applied to enhance condensate recovery by increasing the reservoir pressure and re-vaporizing the condensate. In order to investigate the efficiency of gas flooding method, both experimental and simulation works were conducted.

The core was same as in huff-n-puff gas injection experiment. Also, same gas condensate mixture was used. Fig. 8.7 shows the schematic of gas flooding. First, the pressure of the core was depleted to 1460 psi. Methane was then injected into the core from an inlet at a constant pressure of 1900 psi. A back-pressure regulator was used to maintain a constant production pressure of 1460 psi. A CT scanner was used to determine the condensate saturation every 30 minutes.

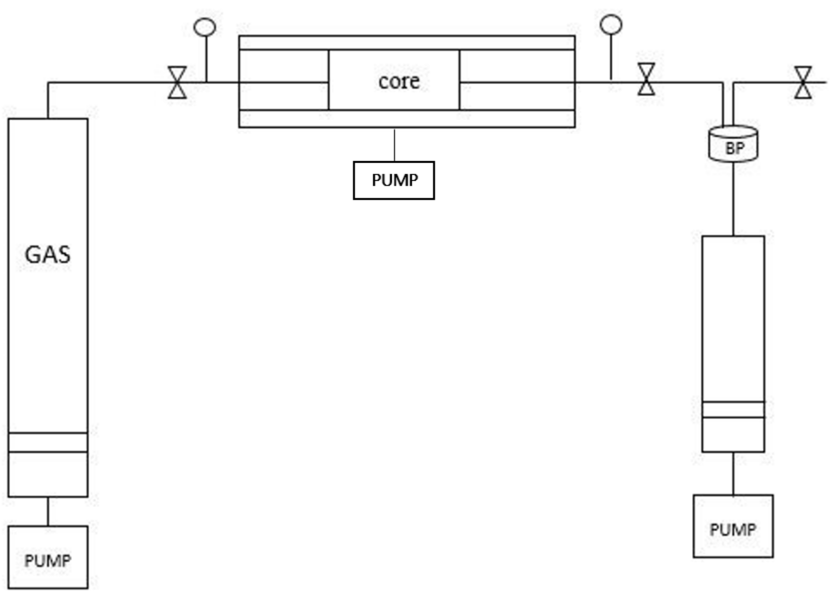

Fig. 8.7 Schematic of gas flooding experiment

The simulation model to simulate the gas flooding experiment process was similar to that of the huff-n-puff process, except that the injection well is at one end, while the production well is at the other end.

Fig. 8.8 shows the condensate recovery for gas flooding. At the end of same flooding whose time is the same as the time for five huff-n-puff cycles, the condensate recovery is 19%.

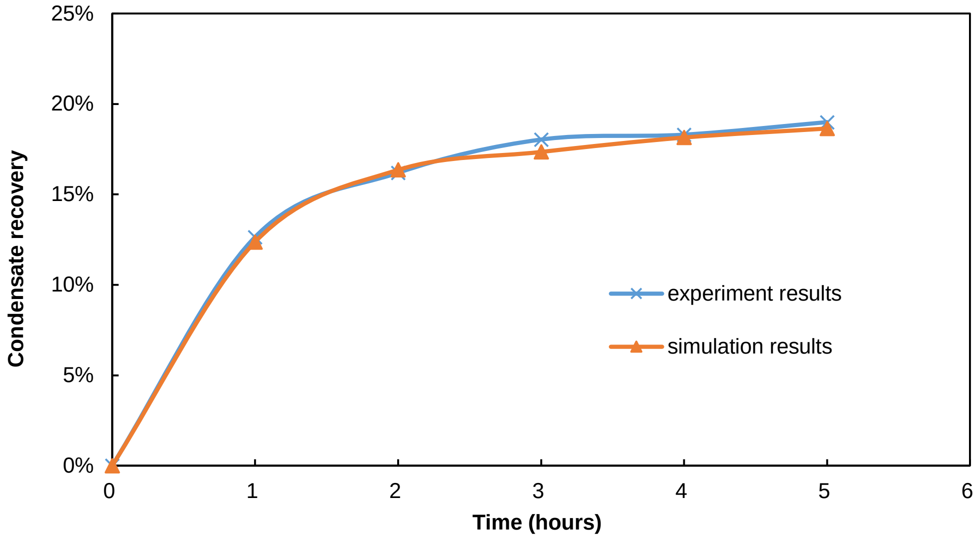

Fig. 8.8 Condensate recovery for gas flooding

For our experiments, one cycle took 30 minutes of injection time and 30 minutes of production time, totaling 1 hour. Five cycles took 5 hours. Therefore, the efficiency of huff-n-puff gas injection could be compared to the gas flooding as shown in Fig. 8.9.

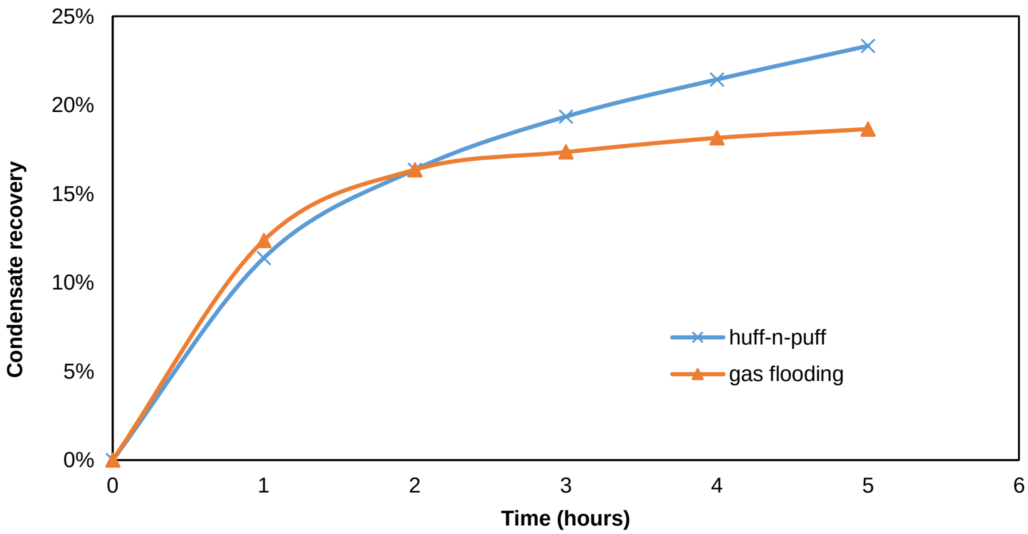

Fig. 8.9 Comparison between huff-n-puff and gas flooding

It can be seen that for the same period of time of 5 hours, the condensate recovery was increased to 23.3% by huff-n-puff gas injection. And the condensate recovery was enhanced to 18.6% by gas flooding. When the pressure near the production end fell below the dew point pressure, condensate accumulated near the production end. Thus, as the function of this end was changed into injecting gas, the pressure in condensate region increased very quickly because the condensate region was just near the injection end. Consequently, the condensate was re-vaporized and flowed out from the core during the puff process. Since the condensate region was near the production end, the pressure propagation time or pressure response time was much shorter and the efficiency was higher in the huff-n-puff method. Therefore, the huff-n-puff method was more effective than the gas flooding method.

For more details, read these papers:

19. Meng, X., Sheng, J. J., Yu, Y. 2017. Experimental and Numerical Study of Enhanced Condensate Recovery by Gas Injection in Shale Gas Condensate Reservoir. SPE Reservoir Evaluation & Engineering, 20(02), 471-477.
20. Meng, X. and Sheng, J.J. 2016. Experimental and Numerical Study of Huff-n-Puff Gas Injection to Revaporize Liquid Dropout in Shale Gas Condensate Reservoirs, J. of Natural Gas Science and Engineering, 35, 444-454.
21. Meng, X. and Sheng, J.J. 2016. Experimental Study on Revaporization Mechanism of Huff-n-Puff Gas Injection to Enhance Condensate Recovery in Shale Gas Condensate Reservoirs, paper SPE 179537 presented at the SPE Improved Oil Recovery Conference held in Tulsa, Oklahoma, USA, 11–13 April.
22. Meng, X., Yu, Y., Sheng, J.J., Watson, W., and Mody, F. 2015. An Experimental Study on Huff-n-Puff Gas Injection to Enhance Condensate Recovery in Shale Gas Reservoirs, paper URTeC 2153322 presented at the Unconventional Resources Technology Conference held in San Antonio, Texas, USA, 20-22 July.
23. Meng, X., Sheng, J.J., and Yu, Y. 2015. Evaluation of Enhanced Condensate Recovery Potential in Shale Plays by Huff-n-Puff Gas Injection, paper SPE 177283 presented at the SPE Eastern Regional Meeting held in Morgantown, West Virginia, USA, 13–15 October.
24. Meng, X., Sheng, J.J. 2015. Simulation of Huff-n-Puff Gas Injection to Enhance Condensate Recovery in Fractured Shale Gas Reservoirs, paper 425710 presented at the 2015 AIChE Annual Meeting, Salt Lake City, UT, 8-13 November.

25. Meng, X., Sheng, J.J., and Yu, Y. 2015. Study on huff-n-puff gas injection to enhance condensate recovery in shale gas reservoirs, poster presented at the SPE Liquid-Rich Basins Conference – North America, Midland, Texas, 2-3 September; Honourable Mention.

8.4. Optimization of huff-n-puff gas injection

Based on the laboratory study, huff-n-puff gas injection was proven as an effective method to enhance condensate recovery for Eagle Ford shale cores. The application of huff-n-puff gas injection in field scale is also important to be investigated. A numerical reservoir simulation study is conducted to optimize the application of huff-n-puff gas injection in an Eagle Ford shale gas condensate reservoir. Different parameters were investigated including injection time, soaking time, production time, and cycle numbers.

The reservoir simulation work for the application of huff-n-puff gas injection was performed by using the compositional simulator, GEM in Computer Modeling Group. The dimensions of the shale gas condensate reservoir were 592 ft wide in the I direction, 2724 ft in the J direction with 724 ft in the SRV area as shown in Fig. 8.10, and 50 ft in the K direction. In this reservoir model, the half fracture spacing was 296.25 ft in the I direction, the fracture length was 724 ft in the J direction, and the fracture height was 50 ft in the K direction. The half-hydraulic fracture width was 0.5 ft. Also, the reservoir rock properties used in this model were based on the published data in Eagle Ford shale. The properties of the reservoir are shown in Table 8.1. The producer was subjected to the minimum bottom-hole pressure constraint of 1500 psi, and the injection well was subjected to the maximum injection pressure constraint of 4000 psi. The injection and production times are discussed in a later section.

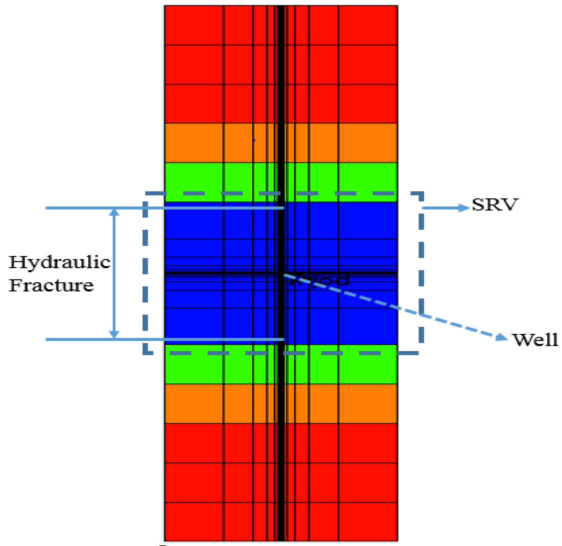

Fig. 8.10 Schematic of simulation model

Table 8.1: Reservoir properties

Parameters	value	unit
Initial reservoir pressure	5000	psi
Reservoir Temperature	200	°F
Thickness	50	ft
Matrix Permeability	0.0001	mD
Matrix Porosity	0.06	
Rock Compressibility	5.0E-06	
Hydraulic Fracture Permeability	100	mD
Permeability of Matrix	0.0001	mD

As it can be seen from Fig. 8.11, condensate starts to form when the pressure is lower than the dew point pressure 2750 psi. Then, the condensate volume continues to increase until the pressure reduces to 2500 psi when the maximum amount of condensate liquid is reached. After that, as the pressure continues to decrease, the liquid is revaporized and the condensate volume is reduced.

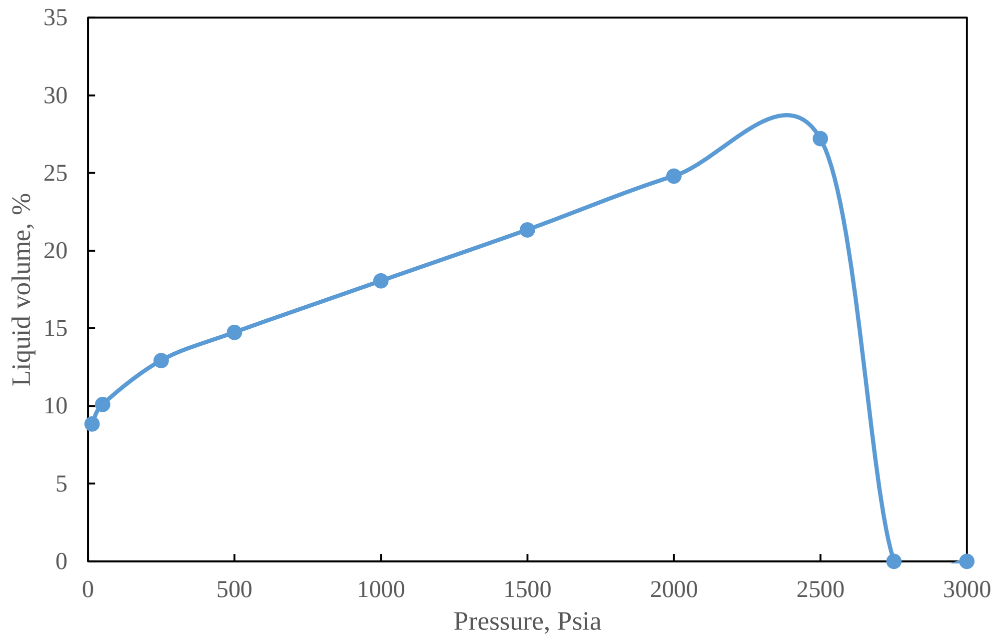

Fig. 8.11 The liquid dropout curve for CCE experiment at 200 ºF on the gas condensate mixture

Start of huff-n-puff. The beginning of huff-n-puff gas injection is an important time for the exploration of the shale gas condensate reservoir. One cycle of huff-n-puff gas injection was applied in the simulation model at different start times: 5 years, 10 years, and 15 years. The total production time in this work was 25 years. The results of different cases were compared with 25 years of primary depletion. For this single cycle the injection time was 200 days, and the rest time in 25 years was the production period. The results are shown in Fig. 8.12. Fig. 8.13 shows the gas production rate from the primary depletion period. As Fig. 8.13 indicates, the production decreased very fast in the first 5 years and in the following 20 years the production rate was very slow.

Combined with the gas production decline rate and the effect of the starting time of huff-n-puff, it can be seen that huff-n-puff gas injection is more effective when starting at the later period of primary depletion (when the production rate was decreased around 90% in this case). If the huff-n-puff is applied too early, the primary production rate is not that low and comparing the incremental recovery with the cost of injection process, it is unnecessary. When the huff-n-puff gas injection is applied in the later time, since the production rate is so low, the application of huff-n-puff gas injection can effectively enhance the recovery and increase profits.

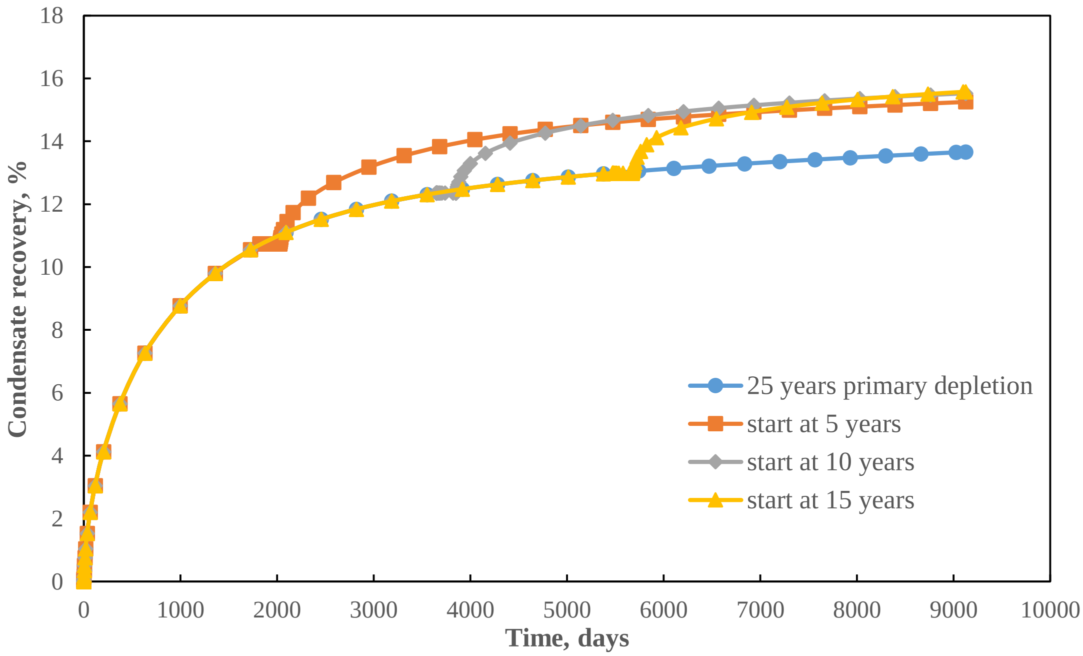

Fig. 8.12 Condensate recovery for different cases

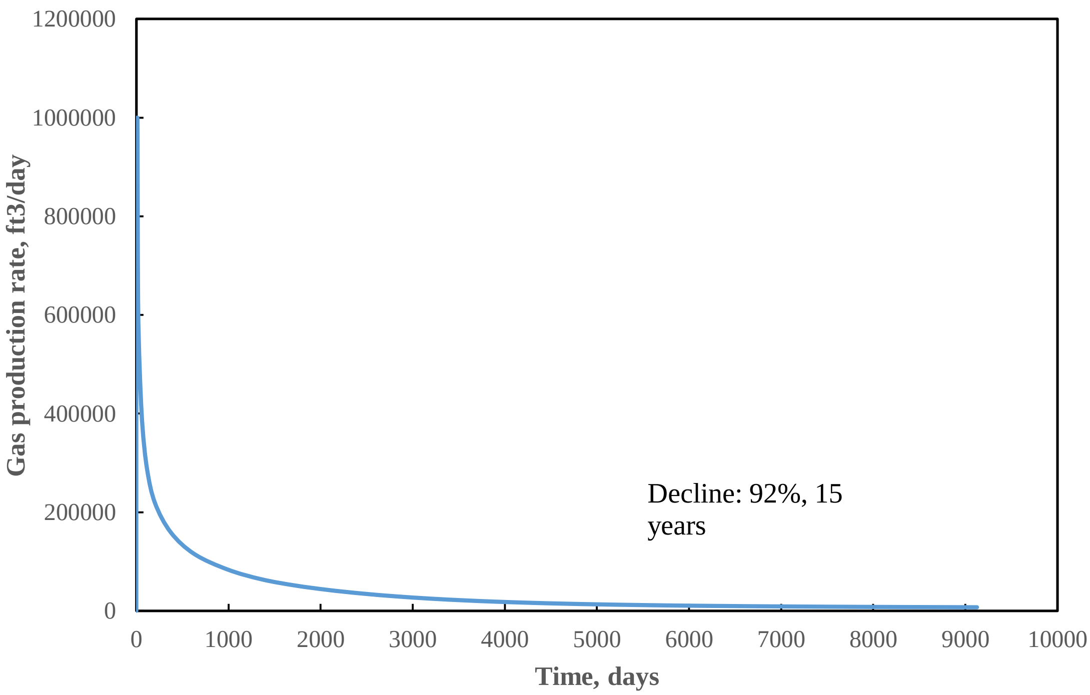

Fig. 8.13 Gas production rate for 25 years primary depletion

Injection Period. Though a longer injection has greater recovery, the longer injection time also indicates more gas needs to be injected into the reservoir. This means there can be more costs during the injection. If the costs of injection cannot achieve more profits, the application of huff-n-puff gas injection would fail. Three injection times were conducted in this study: 10 days, 50 days, and 100 days. Fig. 8.14 shows the condensate recovery for the different cases. The condensate recovery increased. It is obvious that when the injection time was increased, the increment of pressure in the reservoir increased. Thus, more condensate was recovered.

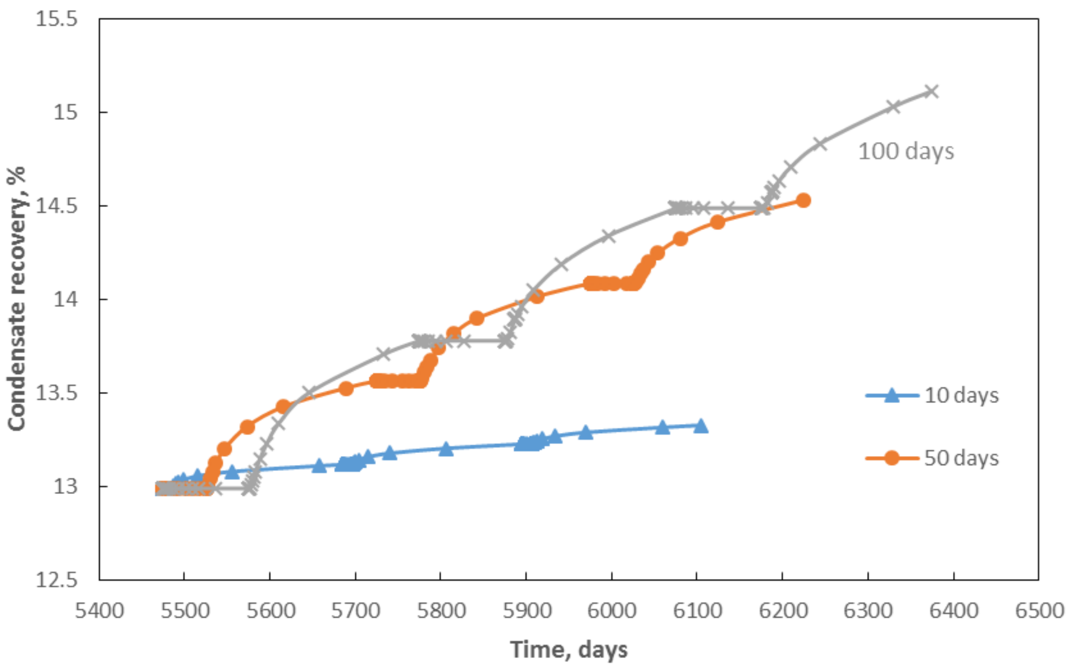

Fig. 8.14 Condensate recovery for different injection time cases

The profits of every case were investigated, excluding Taxes and OPEX. In this investigation of profits, we used a low oil price of 40 USD/bbl, and a gas price of 2 USD/Mscf. The purpose of profit analysis in this study is to compare the efficiency of different cases, so an optimized parameter such as injection time can be determined. As it can be seen from Table 8.2, the 100 day injection time case had the highest condensate recovery of 15.1%. However, the profits of 100 days injection time case were the lowest. Compared with the 10 day injection time case and the 50 day injection time case, the 100 day injection time case had a much larger volume of injected gas, and the cost of the injection period was much higher. Compared with the 10 day injection time case, the 50 day injection time case had a higher condensate recovery and the profit was also higher. By comparing the profit and condensate saturation after injection of three cases, it can be concluded that the optimized injection time is that during the injection time, the pressure of the main condensate region in the reservoir can be increased higher than dew point pressure. The condensate can be revaporized to gas phase, and both condensate production and gas production can be increased.

Table 8.2: Profits for different injection time cases

Injection time, days	Condensate RF,%	Produced oil, bbl	Injected gas, ft3	Produced gas, ft3	Profit, $USD
10	13.3	12933.2	30000000	315000000	1087328
50	14.5	14113.4	117000000	381000000	1092536
100	15.1	14678.5	164000000	407000000	1073140

Soaking time. A series of simulations was conducted using different soaking periods: 0, 50 days, and 100 days. In these three cases, two cycles were simulated: 100 days of injection and 200 days of production. It can been seen from Fig. 8.15 that all three cases had the similar condensate recovery, but the simulation without a soaking period had the largest condensate recovery (14.5%). The simulation with the longest soaking time (100 days) had the smallest recovery (14.23%).

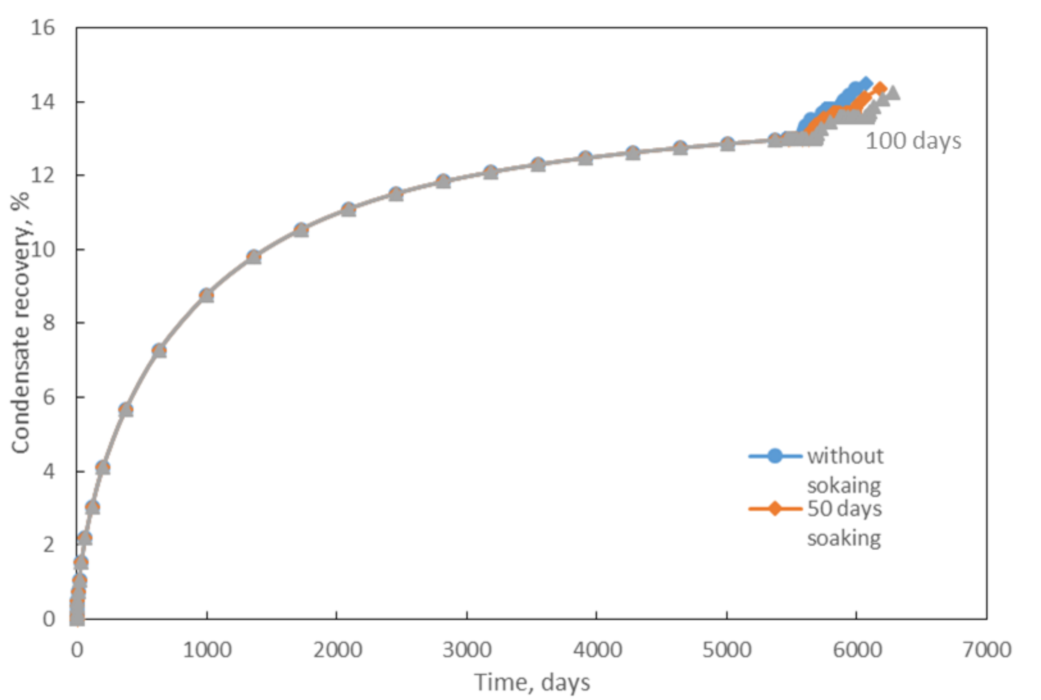

Fig. 8.15 Soaking time effect on condensate recovery

The reason why soaking time has a negative effect in this case is related to the gas condensate fluid property. In these three simulation cases, the injection pressure was already set to a high value: 4000 psi. When the gas was injected into the formation, the pressure of the region near the fracture increased rapidly. The pressure increased to higher than dew point pressure, the condensate was revaporized to gas phase, and the oil (condensate) saturation decreased. Though the injected gas could flow further into the reservoir and increase the further region pressure when the well was shut in and the soaking period was applied, the pressure of the region near the fracture decreased compared to the value when the well was just shut in. This is because the pressure in this near fracture region transferred to the further region in the reservoir. When the pressure decreased, the revaporized condensate could be formed into liquid again. This indicates that shorter or no soaking time is needed during a huff-n-puff operation in shale gas condensate reservoirs.

Number of huff-n-puff cycles. Huff-n-puff cycle number is also a very important parameter that needs to be seriously taken into account during the application of the huff-n-puff gas injection method in shale gas condensate reservoirs. In this simulation part, the injection time was the same as the previous one: 50 days, and based on the previous study, soaking time was also not taken into account. The production time was increased from 200 days to 400 days. The total exploration time of this case was same as the 11-cycles of huff-n-puff gas injection: 8825 days. Based on this different time, only 6 cycles were run in this new huff-n-puff gas injection project. Fig. 8.16 shows the condensate recovery comparison between 11-cycles of huff-n-puff and 6-cycles of huff-n-puff.

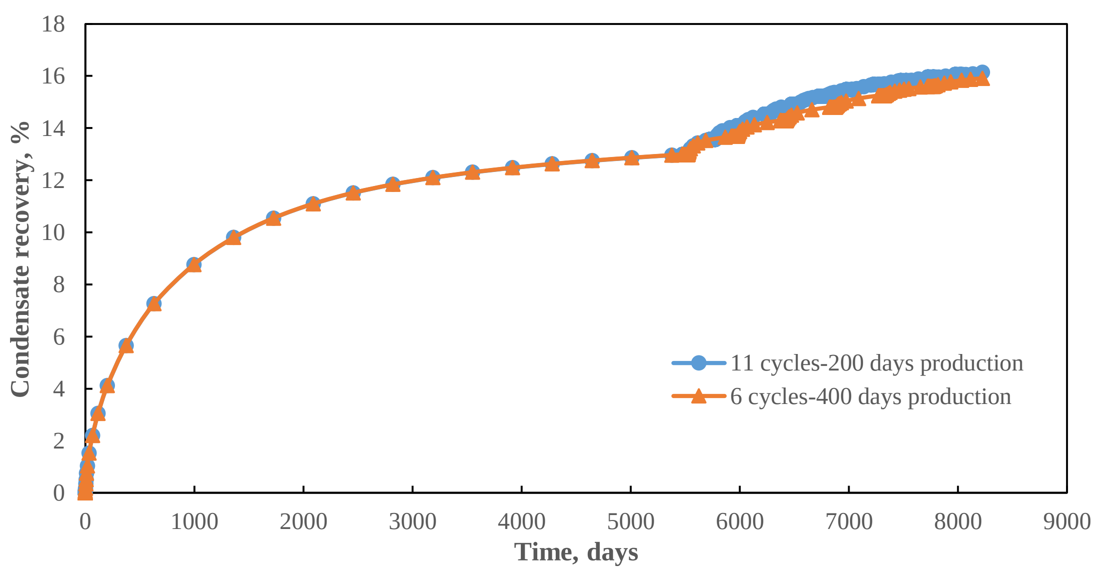

Fig. 8.16 Comparison between 11-cycles huff-n-puff and 6-cycles huff-n-puff

The condensate recovery was 16% in 6-cycles of huff-n-puff gas injection, and for 11-cycles of huff-n-puff gas injection, the condensate recovery was only 0.12% higher than that in 6-cycles of huff-n-puff. This indicates that the start of production time in huff-n-puff gas injection should follow the same optimization principle for the end time of primary depletion. By following this principle, fewer huff-n-puff cycles are needed to increase the condensate recovery. Also, fewer cycle numbers means less gas is needed to be injected into reservoir. This means lower costs for huff-n-puff gas injection projects. Table 8.3 shows the profits analysis for different cycle numbers of huff-n-puff gas injection and primary depletion. 6 cycles of huff-n-puff with 400 days production time had higher profits.

Table 8.3: Profits analysis for different cycle numbers of huff-n-puff gas injection and primary depletion.

	Condensate RF,%	Produced oil, bbl	Produced gas, ft^3	Injected gas, ft3	Cumulative Profits, \$USD	Profits incremental, \$USD
Primary	13.5	13136.2	300000000.0	N/A	1125448.0	N/A
11 cycles, 200 days production	16.1	15675.5	678226112.0	412651936.0	1158168.8	32720.8
6 cycles, 400 days production	16.0	15453.5	234300000.0	526000000.0	1201540.0	76092.0

From this field scale simulation work, it can be concluded that:

- Huff-n-puff gas injection is more effective when started at the later time. If huff-n-puff is applied too early, the production rate is not too low, and by comparing the profits of incremental recovery with the cost of injection process, it is not practical.
- An optimized injection time should be selected so that during this injection time, the pressure of the main condensate region in the reservoir can be increased higher than dew point pressure.
- There is no benefit to applying a long soaking time. For the application of huff-n-puff gas injection in the shale gas condensate reservoir, a short soaking time or even no soaking time would be better.
- The cycle number of huff-n-puff is combined with the injection time, soaking time, and production time. For a fixed time of exploitation, more cycles of huff-n-puff gas injection do not mean higher profits. The cycle number should depend on the optimized injection time and optimized production time.

For more details, read these papers:

26. Meng, X., Sheng, J. J. 2016. Optimization of Huff-n-Puff Gas Injection in A Shale Gas Condensate Reservoir. Journal of Unconventional Oil and Gas Resources, 16: 34-44.

27 Sheng, J., Sheng, J.J. 2015. Optimization of Huff-n-Puff Gas Injection in Shale Condensate Reservoirs to Improve Liquid Oil Production, paper 425368 presented at the 2015 AIChE Annual Meeting, Salt Lake City, UT, 8-13 November.

Chapter 9. Comparative Study of Gas Injection and Solvent Injection for Shale Gas Condensate Reservoirs

9.1 Introduction

A significant amount of condensate is left behind in gas condensate reservoirs as the reservoir pressure falls below the dew point pressure of the gas-condensate fluid. Gas injection for pressure maintenance and solvent injection for miscible condensate displacement are successful methods of recovering the lost condensate and restoring production in conventional reservoirs. Considering the low permeability of shale formations, investigating the feasibility of a huff-n-puff application is important with respect to recovery mechanisms, interaction with in-situ fluid and basic economic considerations. We used the reservoir simulation approach to study and compare gas and solvent huff-n-puff injection in the following setup:

- 1-D core model initiating EOR mechanism study for gas and solvent injection
- Field scale reservoir model to analyze the effect of reservoir and operating conditions

9.2 1-D core model initiating EOR mechanism study for gas and solvent injection

To remediate the condensate dropout, gases (methane and ethane) and solvents (methanol and isopropanol) were compared. The total huff-n-puff operation time is the same for all injection fluids allowing for long injection times and complete flowback of the fluid. Two reservoir fluid types are studied to investigate the effect of heavier components in the condensate fluid. Recovery factors are calculated to represent recovery of total barrel of oil equivalent (BOE) of the in place fluid at the end of primary depletion. This approach is unique to this comparative study.

The 1-D core model was developed and calibrated based on published experiments as in Al-Anazi, H.A., Experimental measurements of condensate blocking and treatments in low and high permeability cores, PhD dissertation, University of Texas at Austin, 2003. The permeability of the model is in the nanodarcy range representing the tightness of a shale core. Phase behavior model is regenerated as published in Bang, V., Pope, G.A., Sharma, M.M., 2010. Phase behavior study of hydrocarbon/methanol/water mixtures at reservoir conditions, SPE Journal, 15(4), 958-968. The reservoir fluid is a synthetic four component gas condensate mixture consisting of methane, butane, heptane and decane.

Ethane injection is an original idea for this work and demonstrates the highest recovery factor on three accounts – total operation time, total pore volume of injected fluid and total cost of the injected material. High recovery factor of ethane injection is attributed to re-vaporization of the condensate, dew point pressure reduction of the original gas-condensate fluid, reduced oil viscosity and enhanced mobility of the condensate in place. The difference in gas and solvent huff-n-puff recoveries is magnified for a richer composition of reservoir fluid with significantly higher recovery factors for methane and ethane. Solvents recover intermediate components really well and can be competitive with gas huff-n-puff for lean gas condensate fluids. Isopropanol is a better solvent than methanol for recovering heavier components, however, high costs may not justify application of isopropanol.

For more details, read the following paper:

28 Sharma, S. and Sheng, J.J. 2017. A comparative study of huff-n-puff gas and solvent injection in a shale gas condensate core, Journal of Natural Gas Science and Engineering, 38, 549-565.

9.3 Field scale reservoir model to analyze the effect of reservoir and operating conditions

This research study aims to validate results from the core model study to be applicable to reservoir scale. The work was further built upon by studying the effects of injection pressure, initial reservoir pressure, huff-n-puff cycle time, and reservoir fluid composition on the recovery efficiencies of the injection fluids. Condensate drop out is believed to be largely trapped around the stimulated rock volume (SRV) owing to the ultra-low permeability of a shale reservoir. The scope of this work is to highlight the differences in the recovery mechanisms of gases (methane and ethane) and solvents (methanol and isopropanol) in mitigating this problem in the SRV and non-SRV regions. It is found that, to optimize recovery benefits, gases require longer injection and production times whereas solvents exhibit an improved performance with a shorter injection time and a longer production time. Additionally, the effects of nanopore confinement on recovery performance of the injection fluids are analyzed.

The base reservoir model rock and grid properties were developed and calibrated as published in Sheng, J.J., Mody, F., Griffith, P.J., Barnes, W.N., 2016. Potential to increase condensate oil production by huff-n-puff gas injection in a shale condensate reservoir, Journal of Natural Gas Science and Engineering, 28, 46-51. The phase behaviour data for the reservoir and injection fluids is the same as in the 1-D core model. The phase behaviour data is modified for the nanopore confined fluid in the matrix gridlocks by applying the concept of shifting critical properties of the pure components in the nanopores as described in Zarragoicoechea, G.J., Kuz, V.A., 2004. Critical shift of a confined fluid in a nanopore, Fluid Phase Equilibria, 220, 7–9.

Fig. 9.1 demonstrates the superior performance of ethane in recovering the total hydrocarbon components in comparison to methane, methanol and isopropanol for a given injected reservoir pore volume. Ethane is capable of recovering a significant amount of the original methane in place in addition to the condensate components. This attribute can potentially help offset injection fluid costs to an extent. Although methane enhances the condensate component recovery significantly, it is not able to successfully recover the original methane in place and therefore it has the lowest total hydrocarbon recovery factor in Fig. 9.1.

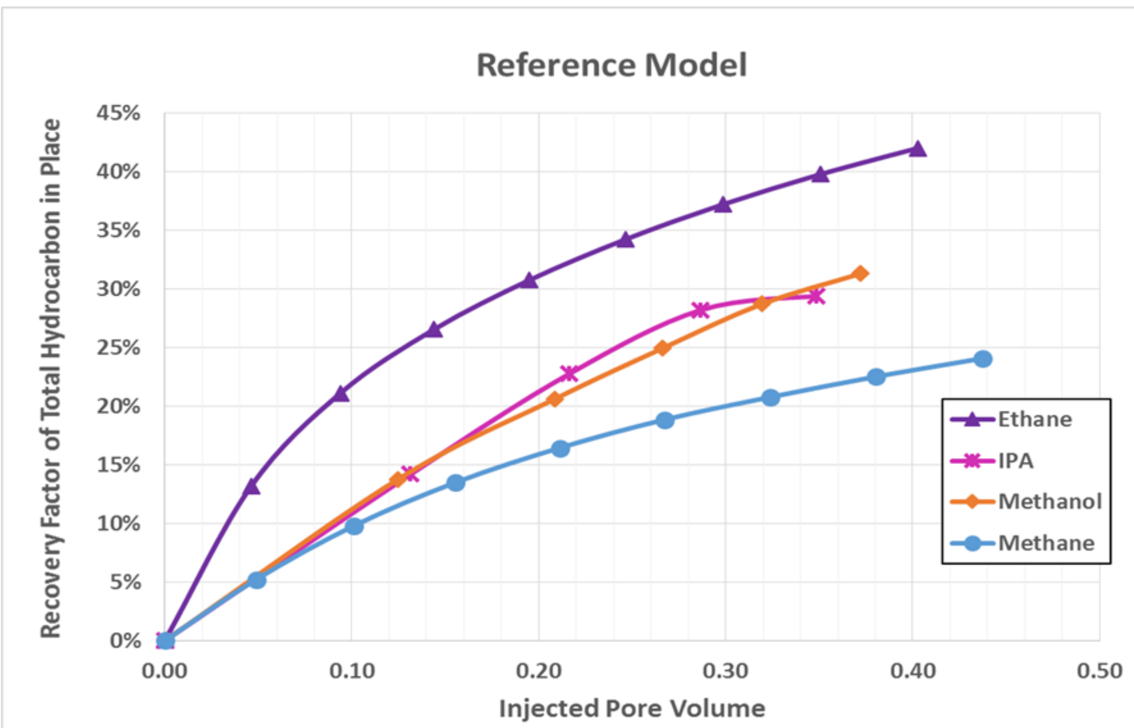

Fig. 9.1 – Total hydrocarbon recovery factor as a function of injected pore volume

Fig. 9.2 shows that ethane has a much higher effect in reducing the dew point pressure of the original reservoir fluid in comparison to methane. This proves to be important when the field has a low initial reservoir pressure close to the dew point pressure of the fluid resulting in greater liquid dropout in the reservoir within a short production time.

Although considering the nanopore confinement effect decreases the incremental recovery obtained from each injection fluid, it does not change the main conclusion from this work with respect to the relative performance of the injection fluids in enhancing the total hydrocarbon recovery from the reservoir.

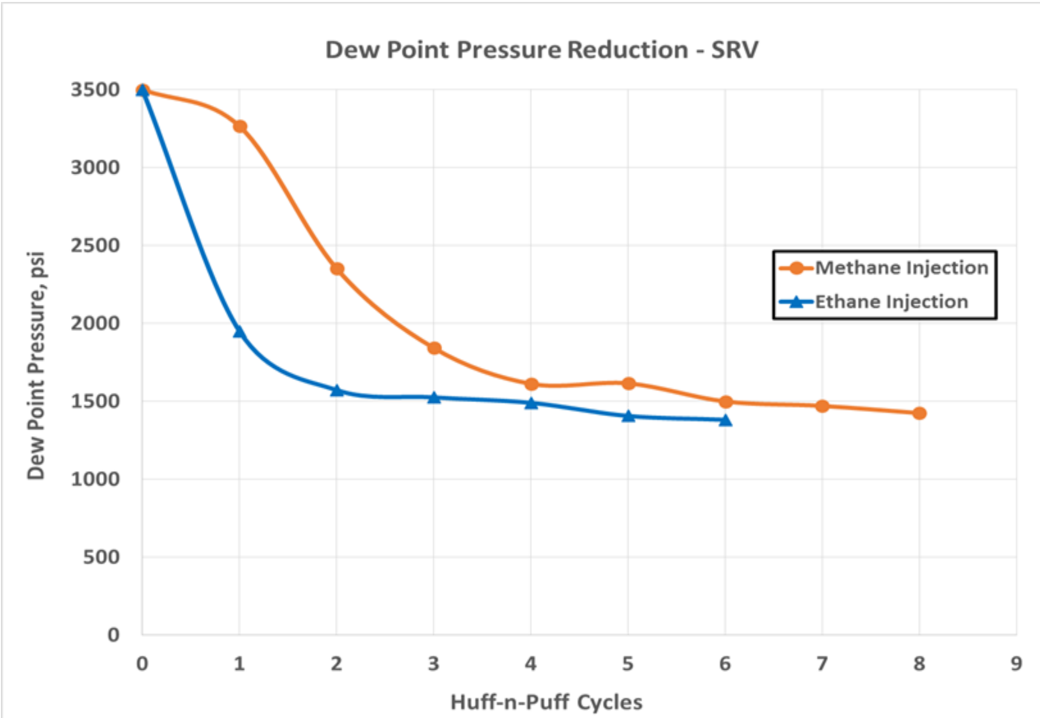

Fig. 9.2 – Dew point pressure reduction in the SRV block after each cycle of ethane & methane huff-n-puff

For further details on recovery mechanisms, read the following paper:

29 Sharma, S. and Sheng, J.J. 2017. A comparative study of huff-n-puff gas and solvent injection in a shale gas condensate reservoir, Journal of Natural Gas Science and Engineering, In Press.

Chapter 10 Design of Field Pilot Tests

10.1 Introduction

In terms of the field pilot test in a shale oil reservoir, Apache selected and cut core plugs. And the cores were sent to TTU lab for research. A sector model was built using the reservoir and fluid properties in the Wolfcamp formation in the Apache's Lin field. A typical production gas and oil rate histories and the well bottom-hole flowing pressure were reasonably matched. Facility injection capacity was considered in the design of a pilot test, such as compressor capacity, injection and production capacities. These capacities are included in the model prediction for a pilot test.

For the field test in a gas condensate reservoir, we also used the PVT data from an Apache gas condensate reservoir to conduct a simulation study to prepare for the field test. A paper has been published in Journal of Unconventional Oil and Gas Resources.

However, owing to the budget spending cut, Apache terminated the field tests of gas injection to enhance oil and liquid condensate recovery in their shale reservoirs.

Because proposed field tests were not executed, efforts were made to collect existing field project data. A review paper is published in Journal of Petroleum Science and Engineering (Sheng, 2017).

In this report, the design of field tests and collected field test results are reported.

10.2 Designed field tests

For the field test in a shale oil reservoir, a sector was built from a geological model and upscaled to a reservoir flow model, using the reservoir and fluid properties in the Wolfcamp formation in the Apache's Lin field. The performance at different scenarios are shown in Fig. 10.1. An optimization was performed. It appears that 3 month huff and 6 month production is an optimum scenario. The test design and performance prediction were completed. Operation conditions: $q_{gmax(prod)}$ = 5MMSCF/D, $q_{gmax(inj)}$ = 6MMSCF/D, P_{injmax} = 3000 psi < Pres.(3450 psi), $P_{prodmin}$ = 500 psi. 1 month injection and 3 month production for the first well. Move to the second well at the end of 4 months for gas injection. Then move to other wells for gas injection until all wells are injected.

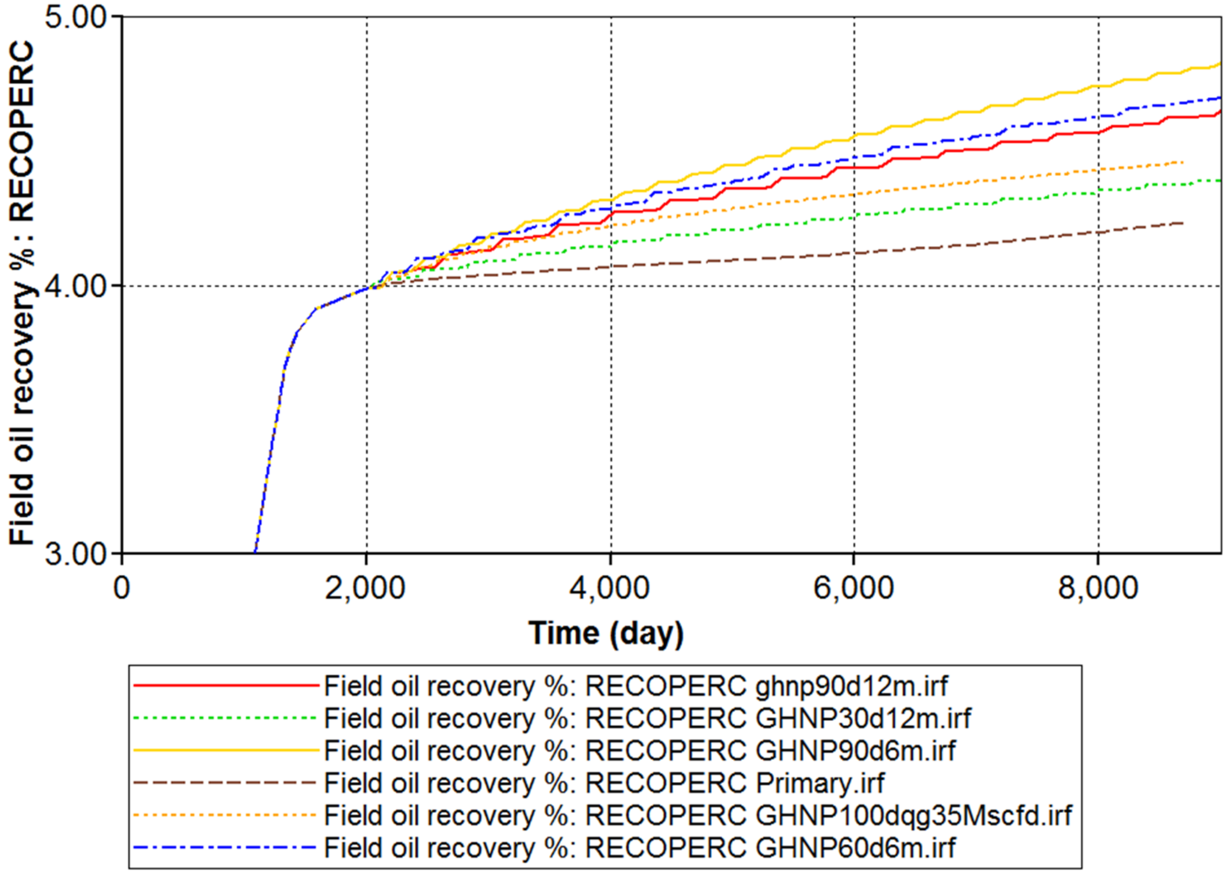

Fig. 10.1 Oil recovery factor at different scenarios of huff-n-puff gas injection.

For more details, read this paper:

30 Sheng, J.J., Mody, F., Griffith, P.J., and Barnes, W.N. 2016. Potential to increase condensate oil production by huff-n-puff gas injection in a shale condensate reservoir, J. of Natural Gas Science and Engineering, 28, 46-51.

10.3 Review of existing field test projects

Field tests of different methods were reviewed and analyzed. It was shown that water injection has been applied in large scale field projects in tight formations, and CO2 injection has been tested on many small scales in China. Gas injection and water injection have been tested in US and Canadian shale reservoirs. Water injection proves to be successful in Chinese tight formations, while results of water injection and gas injection in US and Canada are not reported in detail, with test benefits mixed. Although surfactants are added in fracturing fluids to improve oil recovery performance, the mechanisms have not been well understood.

The following are some of results from this review.

Summary of gas flooding performance

1. Three out of four projects demonstrated gas injection was successful with more oil produced.
2. The formation permeabilities were not less than 1 mD, not nano-Darcy level.
3. The oil viscosities were low.
4. Tests showed there was no gas injectivity issue. Some cases rather showed gas breakthrough issue.

Summary of gas huff-n-puff performance

1. Huff time is short, in the order of 10s days. The soaking time was not shorter than the huff time.
2. Surprisingly, gas breakthrough was observed in the three out of four projects. One intention of huff-n-puff is to avoid breakthrough.
3. Oil rate increase was observed in some projects, but not in others.
4. CO2 was injected in all the projects.

Summary of waterflooding performance

The three waterflooding projects reviewed were all conducted in Bakken formation. The low sweep efficiency was a problem. However, there are a number of other fields where direct water breakthrough channels occurred, but higher oil recovery factors reached.

Summary of water huff-n-puff performance

The three water huff-n-puff projects in US reviewed showed no oil production increase from any of them. But, the field cases in China showed that huff-n-puff water injection generally worked. The injection, soaking and production times were quite different from case to case.

For more details, read this paper:

31 Sheng, J.J. 2017. Critical Review of Field EOR Projects in Shale and Tight Reservoirs, Journal of Petroleum Science and Engineering, 159, 654-665.

Chapter 11 EOR potential of air injection

11.1 Introduction

It is much easier to inject gas in shale and tight reservoirs than to inject water or other liquids. In addition, air has immerse availability and free resources, and air injection may have heat effect. It is important to explore the feasibility and effects of air injection in shale and tight reservoirs. Considering that most of the oils in shale and tight reservoirs are light oils, this study focused on air injection in light oil reservoirs, which corresponds to low-temperature oxidation (LTO). To study the feasibility, mechanisms and EOR potential of air injection in shale and tight reservoirs, the following research was conducted:

- Discussion of the feasibility of air injection in shale oil reservoirs,
- Kinetic behavior of oxidation,
- Exothermicity of air injection,
- Simulation study of EOR potential of air injection in shale reservoirs.

11.2 Discussion of the feasibility of air injection in shale oil reservoirs

A comprehensive discussion on the feasibility and potential of air injection in shale oil reservoirs based on state-of-the-art literature review was initiated. Favorable and unfavorable effects of using air injection are discussed in an analogy analysis on geology, reservoir features, temperature, pressure, petrophysical, mineral and crude oil properties of shale oil reservoirs. The available data comparison of the historically successful air injection projects with typical shale oil reservoirs in the U.S. was summarized. Some operation methods to improve air injection performance are recommended.

Favorable conditions to implement air injection in shale oil reservoirs include the following. Shale oil reservoirs with high temperature and high pressure can accelerate light crude oil oxidation to release more heat. The clay-rich tight shale with a high specific surface area is favorable for performing catalytic oxidation, mitigating early gas breakthrough. In addition, the thermal effects generated in the air injection process have the potential to perform thermal induced microfractures in the reservoir to enhance air injectivity as well as improve fluid flow from the oil-saturated matrix into a fracture pathway. Crude oil oxidation process in air injection has the potential to extract more light hydrocarbons.

Unfavorable conditions could be that the excessive mature shale oil has a low content of unsaturates, mainly aromatics and asphaltenes. This is adverse for fuel loaded during the air injection process. The very thick zone needs a high amount of air injected to guarantee a stable oxidation reaction as well as a thermal front. The nano-Darcy matrix permeability and limited available fractures are the barriers for achieving high injection rate. The nano-meters diameter pore wall can have a drastic effect on the arrangement of molecules inside the pores. This confinement effect can significantly change the phase behavior in shale oil reservoirs, increasing the complexity to understand crude oil oxidation, evaporation, cracking, and combustion in the nanometer pores.

For more details, read the following paper:

32 Jia, H. and Sheng, J.J. 2017. Discussion of the feasibility of air injection for enhanced oil recovery in shale oil reservoirs, Petroleum, 3, 249-257.

11.3 Simulation study of EOR potential of air injection in shale reservoirs

A reservoir simulation approach was used to study the EOR mechanisms of air injection in a light oil reservoir. Effects of O_2 mole concentration, activation energy, intake air temperature, geological structure and development scheme on the well performance of air injection are examined. The driving mechanism of thermal effect is revealed through the observation of oil rate fluctuating and dynamic temperature distribution. Analysis of influence factors from this work indicates that the oil recovery factor is sensitive to O2 content in air and geological structure of the reservoir. The performance with gas injected up dip is better than that down dip. It is insensitive to intake air temperature or activation energy, if the reaction scheme favors the generation of more H_2O, insoluble CO and CH_4.

In the base simulation model, the reservoir and oil properties are based on the actual data in the North Sea oil field, the reaction schemes were same as those proposed in Tingas J., Numerical simulation of air injection processes in high pressure light & medium oil reservoirs, PhD dissertation, University of Bath, 2000. This model was further calibrated with the North Sea air injection performance.

Fig. 11.1 shows that the oil recovery factor is increased with the increase of O2 concentration, as was expected. This is because the prevalence of thermal effect plays an important role on production performance for high O2 content air injection in later stages.

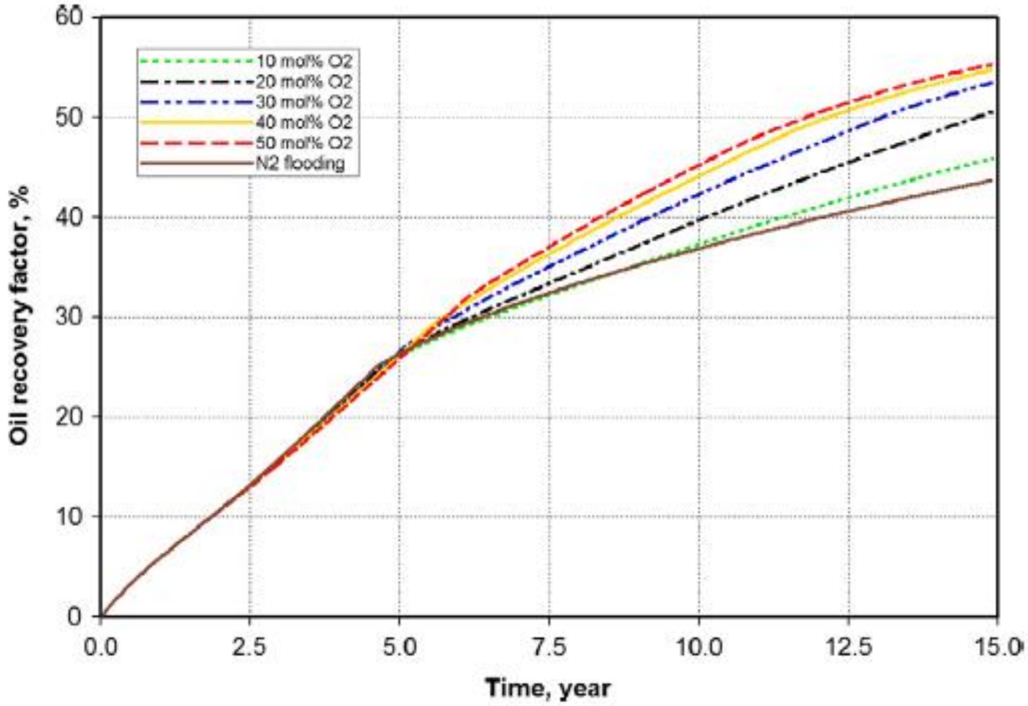

Fig. 11.1 – Effect of O2 concentration on oil recovery factor

Fig. 11.2 exhibits gas relative permeability in some grids initially increasing due to the decreasing of liquid saturation with gas flooding. It is then followed by a sudden decrease, showing the ‘‘pore blocking” mechanism caused by the rapid mobilization of oil into the downstream pores. The term "bulldozing effect or pore blocking" is used to describe this phenomenon. Temporary pore blocking can redirect gas flow, which can improve volumetric sweep efficiency. Moreover, it has the potential of delaying gas breakthrough due to this gas moving frontal ‘‘self-adjustment."

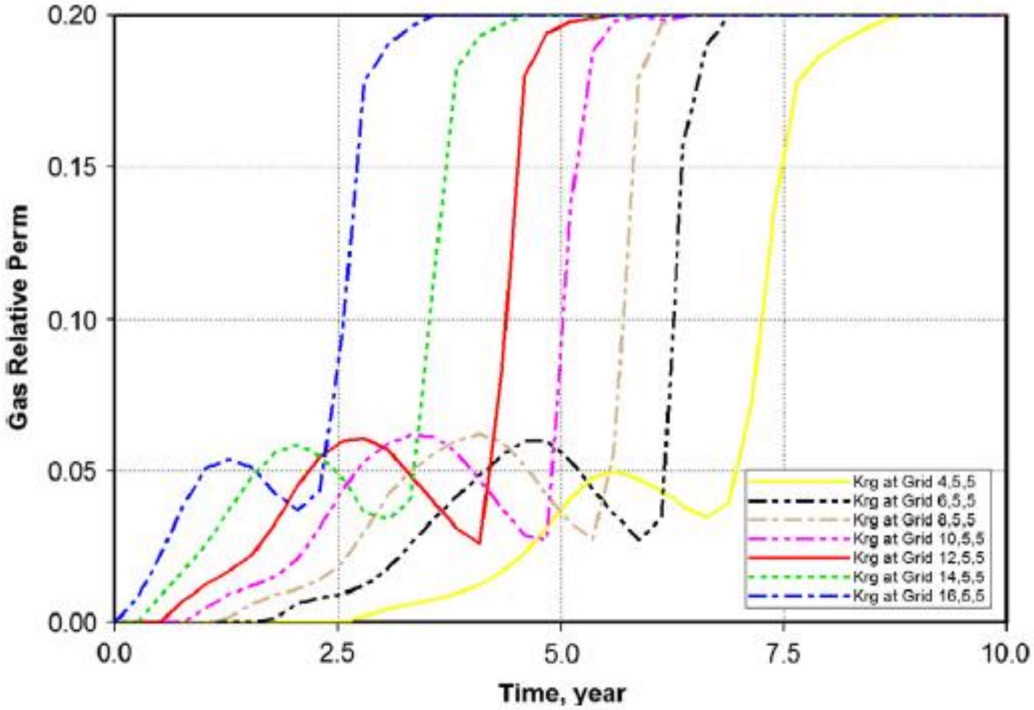

Fig. 11.2 – Changes of gas relative permeability at selected grid blocks

For more details, read this paper:

33 Jia, H. and Sheng, J.J. 2016. Numerical modeling on air injection in a light oil reservoir: Recovery mechanism and scheme optimization, Fuel, 172, 70-80.

11.4 Kinetic model development for air injection

The main difference between air injection and other gas injection processes is the complicated reactions among crude oil, rock and air. A kinetic model is often used to describe the reaction scheme which consists several reactions, and each reaction is characterized by corresponding kinetic parameters and enthalpy value. A well-defined kinetic model can be used to evaluate the feasibility and recovery performance of an air injection project.

The experimental methods applied to study the chemical reactions during an air injection process were discussed based on state-of-the-art literature review, and the shortcomings of obtaining kinetic data based on thermal experiments were revealed. An innovative method was proposed to build a comprehensive kinetic model by combing TGA (thermogravimetry analysis)/DSC (differential scanning calorimetry) experiments with numerical simulation. An application to a Wolfcamp shale oil was performed, and the corresponding kinetic model was developed which can be used in future study.

The workflow of developing the comprehensive kinetic model for air injection process is shown in Fig. 11.3. The schematic of TGA/DSC experiments is shown in Fig. 11.4.

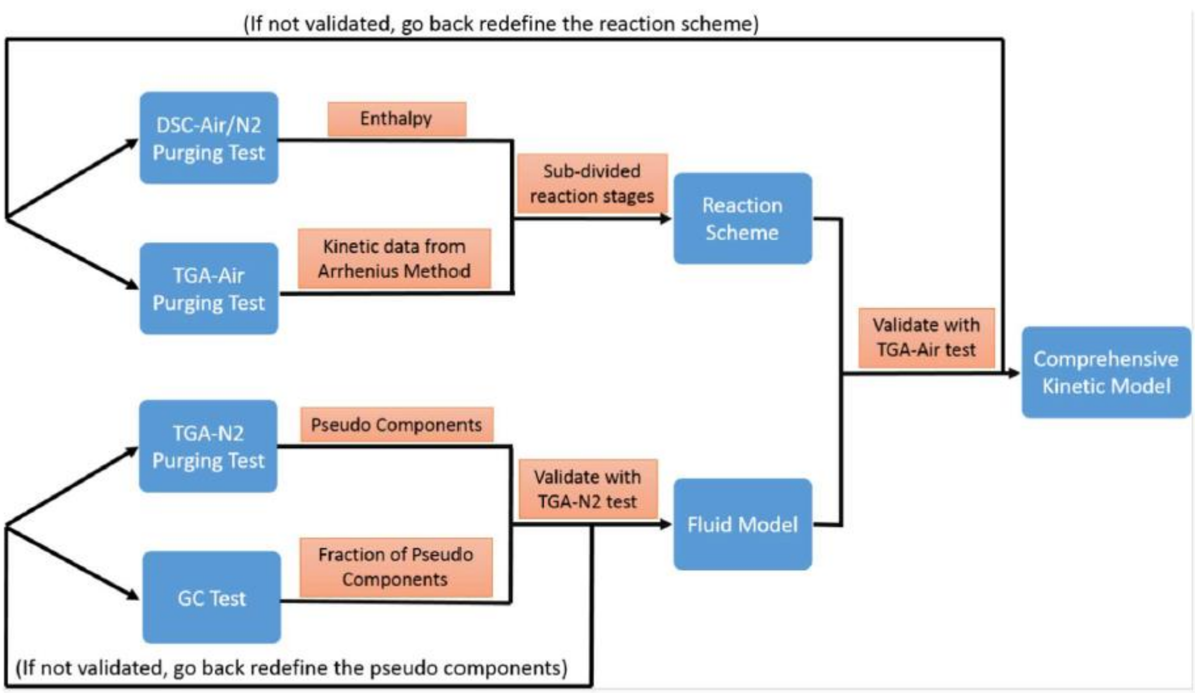

Fig. 11.3 Workflow of developing the comprehensive kinetic model for air injection process

Fig. 11.4. DSC (left) and TGA (right)

The main roles of the thermal experiments are to work as a low-cost method to pre-screen the candidate oils before conducting combustion tube tests and to estimate the relevant kinetic data and study the thermo-oxidative behavior of the crude oil. The API gravity of the crude oil has no relation to the reaction temperature regions and kinetic data of the crude oil. The general activation energy of crude oil in low temperature oxidation stage (20 – 70 kJ/mol) is lower than that in the high temperature oxidation stage (70 – 180 kJ/mol). A lower activation energy is more favorable for oil recovery, but the frequency factor may not.

Table 11.1 shows the kinetic model for the Wolfcamp oil. The kinetic model was defined by three reactions with combination of isomerization reactions and oxygen addition reactions, the negative temperature coefficient was associated with isomerization reaction with negative activation energy. The kinetic data was obtained from the Arrhenius method and further calibrated with the air purging TGA experiments. The enthalpy value of each reaction was obtained from the DSC experiments. This model can be used in future study.

Table 11.1 Air injection kinetic model for Wolfcamp oil

Stages	RTEM LOW, ºC	RTEM UPR, ºC	Activation Energy, KJ/min	Frequency factor, s^{-1}	Enthalpy, J/g	Reaction schemes
LTO1	215	272	18.93	2.40E-03	8.44E+02	C20-22 + O2 = C25+
LTO2	272	308	20.02	2.80E-03	1.21E+03	C23-25 + O2 = C25+
NTC	308	350	-10.63	3.40E-04	3.33E+03	C25+ + O2 = HP1 + HP2 + HP3 + CO2 + H2O + Coke

For more details, read the following papers:

34 Huang, S. and Sheng, J. J. 2017. An innovative method to build a comprehensive kinetic model for air injection using TGA/DSC experiments. Fuel, 210, 98-106.
35 Huang, S., and Sheng, J. J. 2017. A practical method to obtain kinetic data from TGA (thermogravimetric analysis) experiments to build an air injection model for enhanced oil recovery. Fuel, 206, 199-209.
36 Huang, S. and Sheng, J. J. 2017. Discussion of thermal experiments' capability to screen the feasibility of air injection. Fuel, 195, 151-164.
37 Huang, S., Jia, H., and Sheng, J. J. 2016. Effect of shale core on combustion reactions of tight oil from Wolfcamp reservoir. Petroleum Science and Technology, 34(13), 1172-1179.
38 Huang, S. Y., Jia, H., and Sheng, J.J. 2016. Exothermicity and oxidation behavior of tight oil with cuttings from the Wolfcamp shale reservoir. Petroleum Science and Technology, 34(21), 1735-1741.
39 Huang, S. Y., Jia, H., Sheng, J.J. 2016. Research on oxidation kinetics of tight oil from Wolfcamp field. Petroleum Science and Technology, 34(10), 903-910.

11.5 Discussion of kinetic behavior of oxidation

An oxidation kinetics study is important for the application of air injection. The chemical reactions associated with the oxygen and crude oil can be grouped into three classes: low temperature oxidation (LTO), intermediate temperature reactions (ITO) which are also known as cracking reactions, and high temperature oxidation (HTO). LTO is more feasible in light oil reservoirs. A small batch reactor (SBR) experiment was used to study the LTO of the Wolfcamp light oil. The reaction rates under different temperature conditions were measured. The reaction order, the activation energy and Arrhenius constant were calculated which could be used for a simulation study.

The setup of the small batch reactor is shown in Fig. 11.5. A known quantity of oil was loaded into the reactor in the experiments. The reactor was put into the oven and then the temperature was increased to a certain value. After the oil temperature increased to the designed temperature, the reactor was filled with air at the required pressure. At first, the system pressure would increase as the gas temperature increased. After the gas temperature increased to the designed temperature (the oven temperature), the system pressure would decrease due to the oxygen consumption. In order to find the pressure reduction caused by the oxygen consumption, the data was recorded after a steady decline in pressure. After several days, the gas from the reactor was collected and measured by a GC/MS.

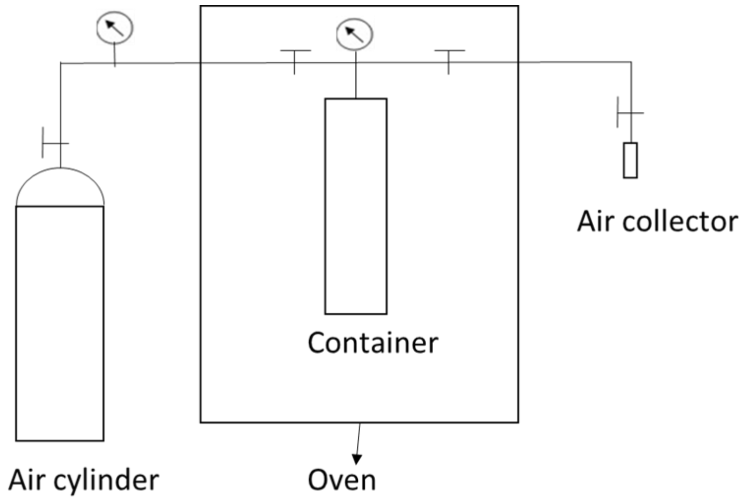

Fig. 11.5 – Schematic of the SBR experimental apparatus

The SBR experiment was conducted under different pressure and temperature conditions. Table. 11.2 and 11.3 show the results of the SBR at different pressures and temperatures. The oxygen consumption rate increased with the increase in the oxygen partial pressure and temperature. When the temperature reached 140℃, the oxygen concentration was decreased to a low level (5.7%) after 6 days. According to the Arrhenius equation, the activation energy and Arrhenius constant were 69894.97 J/mol and 0.0133 respectively.

Table. 11.2 – Results of the SBR at different pressures

No.	Reaction time	Temp	Initial pressure	Final pressure	Oxygen mole fraction	Initial oxygen partial pressure	Reaction rate
	hour	℃	psi	psi	%	psi	mol/hr/g(oil)
1	60.48	119	529	511	17.7085	111.1	9.41E-07
2	68.09	119	838	813	17.6378	176.0	1.33E-06
3	72.46	119	1280	1264	15.338	268.8	2.86E-06

Table. 11.3 – Results of the SBR at different temperature

Temp	Reaction time	System pressure	Oxygen volume fraction	Oxygen	Reaction rate	Oxygen partial pressure	Oxygen partial pressure
℃	hour	Psi	%	mole	mol/hr/g(oil)	psi	pa

116	9.92	1315	21	0.044187	1.66E-06	276.15	1903988
	49.13	1286	19.66999	0.040476	1.47E-06	252.956	1744071
	119.59	1256	17.2115	0.034591	1.33E-06	216.1764	1490484.4
	142.58	1242	16.52823	0.032847		205.2807	1415361
124	9.3	1308	21	0.04273	2.31E-06	274.68	1893852.7
	44.42	1275	19.2132	0.038108	1.98E-06	244.9683	1688997.9
	91.24	1225	17.22226	0.03282	1.82E-06	210.9727	1454606
	113.7	1213	16.15769	0.030489		195.9928	1351323.4
140	9.79	1294	21	0.04113	5.71E-06	271.74	1873582.1
	44.3	1218	16.20742	0.029879	4.64E-06	197.4064	1361069.6
	92.06	1181	9.642971	0.017237	2.53E-06	113.8835	785199.35
	122.35	1170	7.268199	0.012871	2.27E-06	85.03792	586316.07
	143.96	1165	5.709667	0.010068		66.51762	458623.03

For more details, read the following paper:

40 Zhang, Y and Sheng, J.J. 2016. Oxidation kinetics of Wolfcamp light oil, Petroleum Science and Technology, 34, 1180-1186.

41 Zhang, Y and Sheng, J.J. 2017. The mechanism of the oxidation of light oil, Petroleum Science and Technology, 35(12), 1224-1233.

Chapter 12 Non-Darcy flow mechanisms in shale and tight formations

12.1 Introduction

Generally, the fluid flow mechanisms in shale and tight formations are believed to be different from the conventional reservoirs. Due to the dominated nanoscaled pores in shale and tight formations, the solid-fluid interaction is significant enough to deviate the fluid flow mechanisms away from the classical Darcy equation in conventional reservoirs. In shale and tight formations, there are proposed non-Darcy flow mechanisms: gas non-Darcy flow and liquid low velocity non-Darcy flow. To study the mechanisms and significances of non-Darcy flows in shale and tight reservoirs, the corresponding research was conducted separately.

- Liquid low velocity non-Darcy flow
- Gas non-Darcy flow

12.2 Liquid low velocity non-Darcy flow

The studies related with liquid low velocity non-Darcy flow were carefully analyzed and discussed the existence of Threshold Pressure Gradient (TPG) which needs to be overcome before liquid flow happens. We concluded that the low-velocity non-Darcy flow consists of a nonlinear flow regime and a linear flow regime and that the nonlinear flow regime starts from the zero pressure gradient instead of TPG. A low velocity non-Darcy model was introduced and the corresponding parameter correlations were developed by fitting the experimental data. Both the vertical well model and horizontal well model with multi-fractures were used to study the production performance of shale or tight reservoirs.

For a vertical well, the production rate of non-Darcy flow is much smaller than that of Darcy flow, and the ultimate oil recovery of non-Darcy flow is approximately 48% of the Darcy flow. The production rate of a multi-fractured horizontal well if non-Darcy flow is considered is smaller in the beginning but greater than the corresponding Darcy flow rate after some time (in our example model, 2700 days). The ultimate recovery factor of non-Darcy flow is 80% of the Darcy flow, which indicates that multi-fractured wells are less affected by the low-velocity non-Darcy phenomenon compared with the vertical wells. Multi-fractured horizontal wells exhibit a significant advantage in developing shale and tight reservoirs, and low velocity non-Darcy flow plays a significant impact on the well production performance in tight and shale reservoirs.

For more details, please read the following papers:

42 Wang, X. and Sheng, J.J. 2017. Effect of low-velocity non-Darcy flow on well production performance in shale and tight oil reservoirs. Fuel, 190, 41-46.

43 Wang, X. and Sheng, J. J. 2017. Discussion of liquid threshold pressure gradient. Petroleum, 3(2), 232-236.

12.3 Gas non-Darcy flow

Gas sorption and non-Darcy flow are two important issues for shale gas reservoirs and both effects are closely related with each other. The sorption consists of dissolution and adsorption. In this study, the Langmuir equation was used to describe adsorption and Henry's law was used to describe dissolution. The apparent permeability model was established by combining the free gas flow and surface diffusion of adsorbed gas. For free gas, the weighted slip flow and Knudsen flow were combined together. For the surface diffusion of adsorbed gas, the surface diffusion coefficient was suggested to be of the same scale as the gas self-diffusion coefficient, and the corresponding effective permeability was derived. The essential sensitivity analyses were conducted for this established gas apparent permeability model.

In this work, only using the Langmuir equation without considering dissolution can lead to a significant underestimation of the amount of sorbed gas in shale reservoirs. For gas non-Darcy flow, when $\frac{1}{p}$ increases, $\frac{k_{app}}{k_D}$ increases, but the relationship is not linear as Klinkenberg effect suggested. The effect of adsorption on the gas flow is significant at small pores ($r \leq 2\ nm$). Adsorption increases gas apparent permeability in shales at low pressure and decreases at high pressure.

For more details, please read these papers:

44 Wang, X. and Sheng, J. 2017. Gas sorption and non-Darcy flow in shale reservoirs. Petroleum Science, 1-9. https://doi.org/10.1007/s12182-017-0180-3.

45 Wang, X. and Sheng, J.J. 2017. Understanding Oil and Gas Flow Mechanisms in Shale Reservoirs Using SLD–PR Transport Model, Transport in Porous Media, 119, 337-350. DOI 10.1007/s11242-017-0884-2

Chapter 13. Gas injection pore-scale experiments and simulation

13.1 Introduction

The work described in this section was led by Los Alamos National Lab (LANL) and was primarily an experimental effort to directly measure and observe hydrocarbon displacement processes in fabricated fracture networks. The work also involved simulation of pore-scale processes controlling the mobility and displacement of oil in shale using lattice Boltzmann modeling. The primary aim of this work was to quantify through direct observations the effectiveness of cyclic gas injection processes in light-oil recovery from fractured rock.

The experimental approach utilized a microfluidic system that is optimized for observing pore-scale fluid displacement and mobilization. The LANL experimental system is unique in that the experiments can be done at elevated temperature and pressure characteristic of reservoirs and can be done on micromodels made of actual rock. In the experiments, fracture networks are etched into shale thin sections to better represent fracture-matrix interactions and to capture the physicochemical fluid-rock interactions (e.g., wettability, pore-scale reactions) that occur in subsurface formations. Experiments at reservoir conditions are extremely important for energized fluids (compressed gas) such as carbon dioxide and nitrogen, for which the fluid properties and flow processes are highly dependent on the specific pressure and temperature conditions within a given rock formation. A schematic of the experimental system is provided in Fig. 13.1. The system is specifically designed to work with brine, oil (e.g., n-Decane, soltrol), and gas (e.g., CO_2, N_2). The maximum working pressure and temperature is 10.34 MPa (1500 psi) and 80 °C (176 °F), respectively, and the pressure vessel is heated with a custom-fit heating jacket (HTS/Amptek).

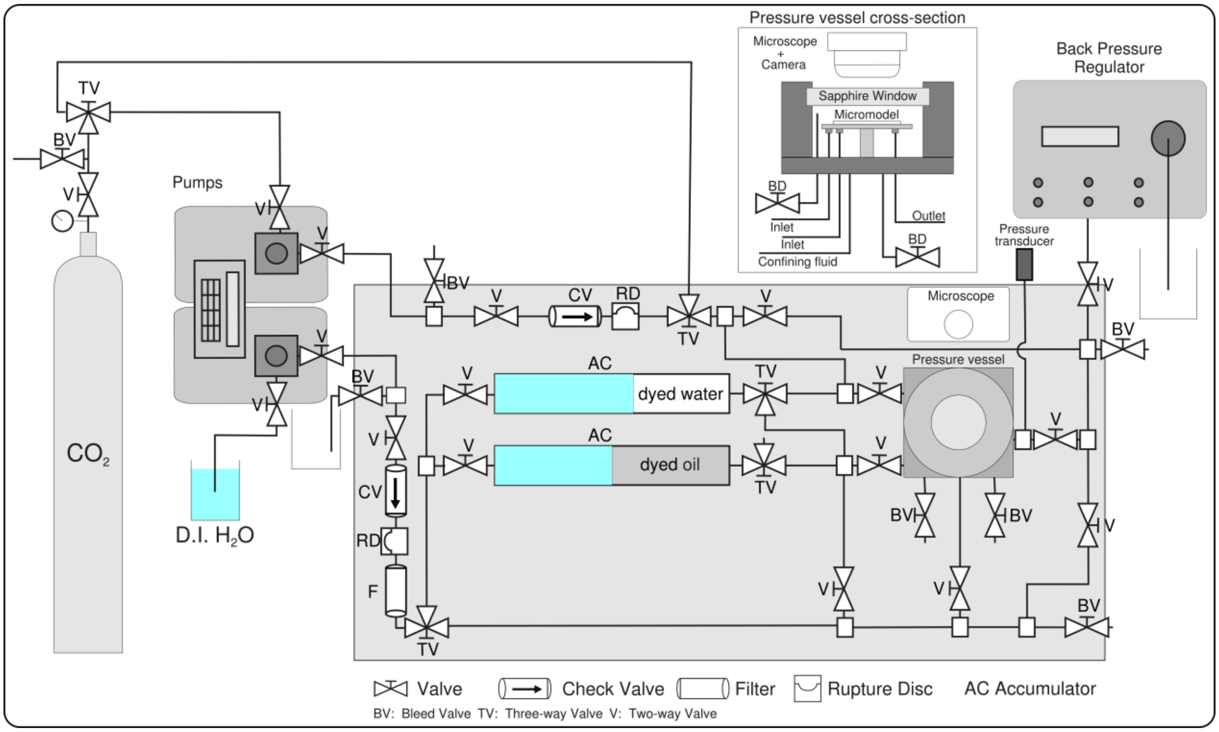

Fig. 13.1 Schematic of the high pressure and temperature microfluidics experimental system. A microscope peers into a high-pressure cell as fluids are injected through a fracture network etched into a 2-dimensional micromodel composed of rock, glass, silicon, cement, etc. The injected fluids include water, oil and gas (CO_2 or N_2) at pressures up to 1500 psi through the use of confining pressure within the cell. The pressure vessel is jacketed with a thermal mantle to allow elevated temperature measurements.

The following project results are described in more detail below.

- Simple fracture systems and three-phase fluid dynamics (section 13.2)
- Complex fracture systems and three-phase fluid dynamics (section 13.3)
- Cyclic gas injection in connected and dead-end fracture networks (section 13.4)

Additional details on the experiments and microfluidics experimental system are given in:

46 Porter, M. L., Jiménez-Martínez, J., Martinez, R., McCulloch, Q., Carey, J. W., and Viswanathan, H. 2015. Geo-material microfluidics at reservoir conditions for subsurface energy resource applications. Lab on a Chip, 15:4044–4053.

13.2 Simple fracture systems and three-phase fluid dynamics

In the first phase of the work, activities focused on simple fracture patterns etched in glass micromodels in order to conduct proof of concept experiments for cyclic gas injection. The fracture pattern consisted of a pore doublet with a primary fracture that branches into two alternative pathways of larger and smaller dimensions (Fig. 13.2). The working fluids were CO_2 and n-decane. CO_2 was chosen to work with due to its relatively high miscibility with n-decane (75% at 8.6 MPa and 45 °C) at working pressure and temperature (P_{max} = 10.3 MPa, T_{max} = 80 °C). The experimental procedure consisted of first saturating the micromodel with n-decane and then pressurizing both the confining pressure and the CO_2 injection pressure to 2 MPa (Fig. 13.3). The system was allowed to equilibrate for 210 minutes time to allow the oil to become energized due to diffusion of CO_2 into the oil, corresponding to a simulated injection phase of cyclic gas injection. Production was simulated by then decreasing system pressure at a rate of 200 kPa/min. It was observed that CO_2 exsolved from the oil forming bubbles that displaced the oil from the micromodel in a process that one could directly observe and image (Fig. 13.2). In Fig. 13.2, the first row of images corresponds to ~ 2 min into the depressurization and CO_2 gas bubbles are observed to form close to the inlet channel. The second row corresponds to ~ 7 min into the depressurization (i.e., lower pressures) and CO_2 bubbles are observed to form in the smaller channels further into the micromodel. Another key observation, is that the CO_2 bubbles preferred the larger (upper) fracture in the experiment showing that fracture geometry controls displacement behavior.

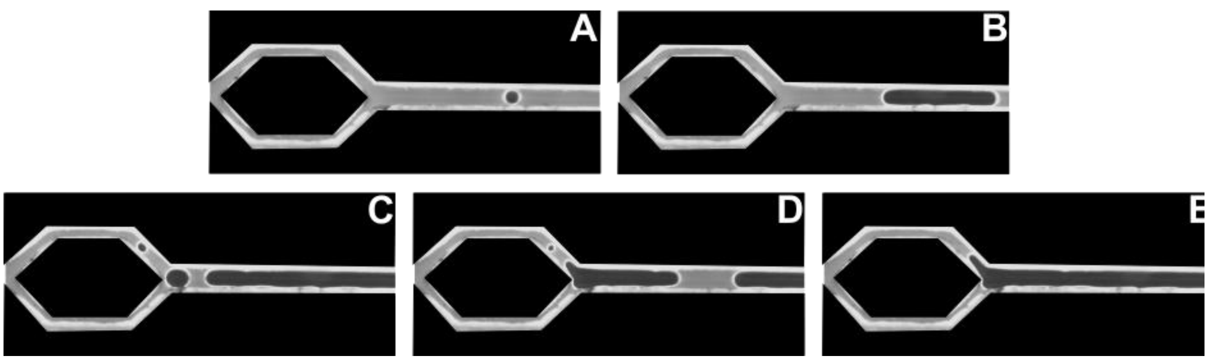

Fig. 13.2 Time series of CO_2 gas bubbles (dark grey) exsolving from n-Decane (light grey) during depressurization of the system. The top and bottom rows correspond to approximately 2 and 7 minutes, respectively, into the depressurization stage. The white boundary is likely caused by light diffraction due to residual adhesive.

These results illustrate the important consequences of miscibility of gas with oil. In this experiment, CO_2 is partially miscible with n-Decane. Depressurization results in exsolution of the CO_2 dissolved in the oil. Expansion of the CO_2 gas displaces oil from the micromodel in a process representing enhanced oil recovery. As pressure decreases, more oil is displaced, however it appears unlikely that this experiment would result in complete removal/recovery of the oil.

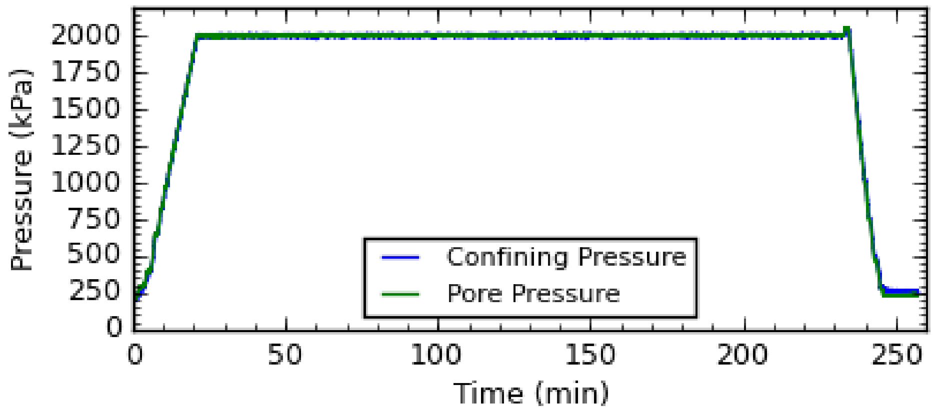

Fig. 13.3 Confining and pore pressure profiles during the gas injection experiment shown in Fig. X.2.

In addition to these experiments, LANL has begun developing LBM simulations aimed at modeling the diffusion of CO_2 into oil as pressure increases. This will require considerable effort to match times scales of diffusion and known values of solubility at a given pressure. The initial simulations focused on single the channel experiments in order to simplify the system and provide an opportunity to compare with existing theory.

In addition to the experiments described above, LANL developed three-phase lattice-Boltzmann (LB) simulations to represent oil recovery in the system gas (N_2 or CO_2)-brine-oil. These were developed with LANL's open source software package Taxila LBM (website). These simulations are challenging due to the presence of interfaces separating each fluid phase and the existence of moving three-phase contact lines. Care was taken to reduce spurious currents at these locations, which are known to cause stability and accuracy issues within LB methods for two-phase flow. Fig. 13.4 shows images of two static immiscible bubble configurations within straight channels. In both cases the bubbles were initiated as squares and allowed to relax to equilibrium conditions. The simulations were run for 25,000 iterations ensuring that the results were stable. Fig. 13.5 shows the movement of two immiscible bubbles within a straight channel, simulating dynamic three-phase flow in simple geometries. These results benchmarked LANL's ability to represent 3-phase processes.

LANL next turned to a simulation of the pore-doublet experiment shown in Fig. 13.2. A blob of oil (red) trapped in the upper branch of the pore-doublet was simulated and its interaction with miscible CO_2 (green) within the context of a brine (blue)-filled channel system was studied. The simulations show that the CO_2 diffuses through the brine into the oil. The oil expands and is pushed out of the doublet-trap. The simulation captures the miscibility of CO_2 and oil and the displacement of oil from the system.

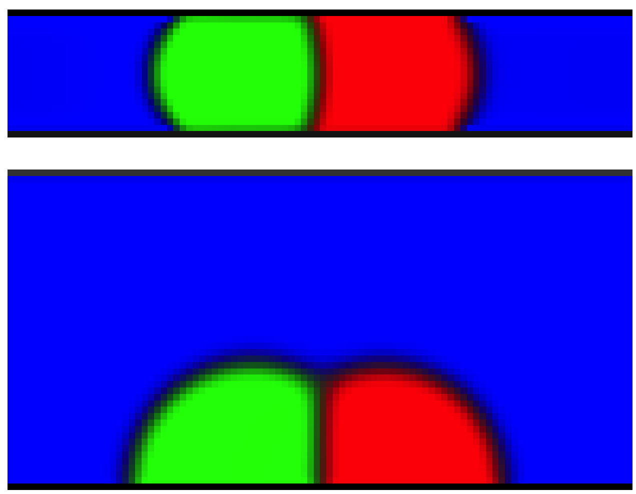

Fig. 13.4 Three-phase simulations of static bubbles in straight channels. The green and red bubbles are non-wetting (i.e., oil and gas), whereas blue represents the wetting phase (i.e., brine). The bubbles were placed as squares and were calculated to correctly relax to the expected curvature.

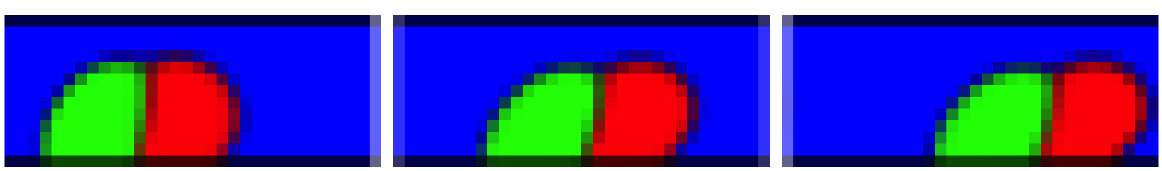

Fig. 13.5 Three-phase flow simulation of moving, immiscible bubbles (representing gas and oil) in a straight channel filled with brine. The green and red bubbles are non-wetting, whereas blue represents the wetting phase.

Some of these results in addition to other studies of microfluidics in geomaterials were published in the following:

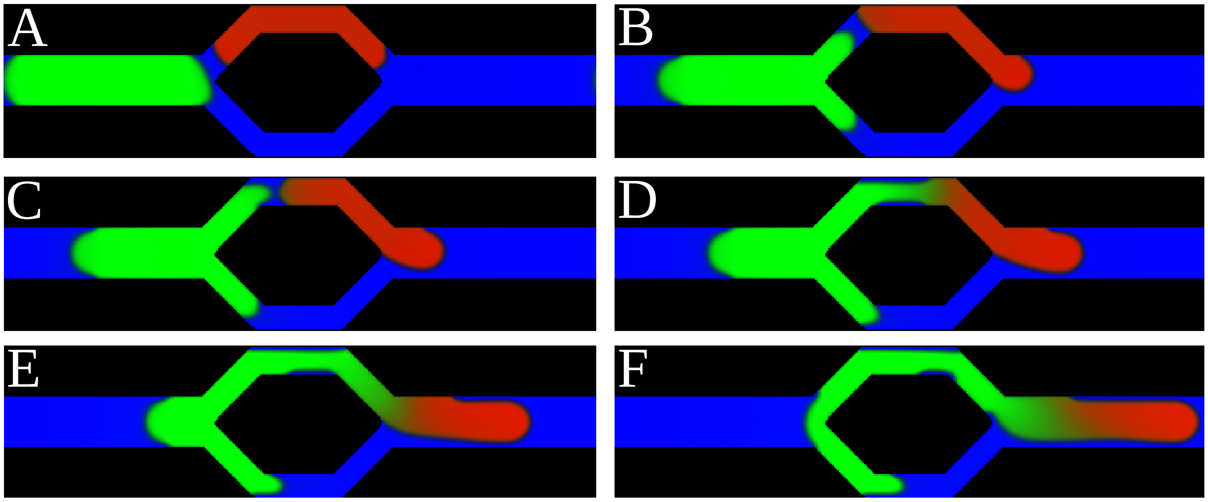

Fig. 13.6 Partially miscible three-phase flow simulations in a pore doublet. Red, blue, and green represent oil, water, and gas, respectively. The gas (CO_2) diffuses into the oil and displaces it from the pore-doublet.

46 Porter, M. L., Jiménez-Martínez, J., Martinez, R., McCulloch, Q., Carey, J. W., and Viswanathan, H. 2015. Geo-material microfluidics at reservoir conditions for subsurface energy resource applications. Lab on a Chip, 15:4044–4053.

13.3 Complex fracture systems and three-phase fluid dynamics

In this phase of the project, LANL examined the impact of complex fracture geometries on the effectiveness of cyclic gas injection on enhanced oil recovery. For this work, LANL etched a realistic fracture pattern (derived from actual fracture patterns in shale) into a glass micromodels (Fig. 13.7). Cyclic gas experiments involving the displacement of oil by either N_2 or CO_2 were conducted. The glass system was expected to behave differently than a shale micromodel system since the glass in impermeable outside of the etched regions whereas a porous matrix exists outside the etched region in the shale. In a second set of experiments, a shale micromodel was used where the porous matrix in the shale allows for additional diffusion of both N_2 and CO_2.

Fig. 13.7 shows the pressure profile used in the experiment and four stages of depressurization (A-D) for an experiment using N_2. In these experiments, the maximum pressure was 1.25 MPa and the temperature was 35 °C. At these conditions N_2 and n-decane have limited miscibility. The fracture network was initially saturated with oil and then a disconnected finger of N_2 was injected into the micromodel. In previous experiments in simpler fracture geometries (Section 13.2), it was observed that no oil was produced when the fractures were fully saturated with oil. This is expected since the oil is incompressible and N_2 is essentially immiscible with the oil on these time scales. The existence of a disconnected finger of N_2 allows for the finger to compress during depressurization and leads to oil displacement as the finger decompresses during depressurization. Moreover, capillary forces cause the fluids to move within the fractures during depressurization. The system was pressurized with N_2 at the inlet/outlet port located middle-left of the images in Fig. 13.7. The N_2 was allowed to soak for approximately 20 min and then depressurized in approximately 5 min. During depressurization oil was produced until the N_2 finger reaches the inlet/outlet port (Fig. 1C). Once the N_2 finger reaches the inlet/outlet the phase configuration does not noticeably change (Fig. 1C and 1D). In the second cycle shown in the pressure profile of Fig. 13.7, little to no oil was produced since the N_2 finger was attached to inlet/outlet port.

These experiments were repeated at the same pressures and temperatures using CO_2 and following a similar time evolution of pressure. Although CO_2 is partially miscible with n-decane at these pressures and temperatures, the soak time did not allow for significant dissolution of CO_2 into the oil. Thus, the system behaved similar to the N_2 experiments and no oil was produced when the CO_2 finger became attached to the inlet/outlet port.

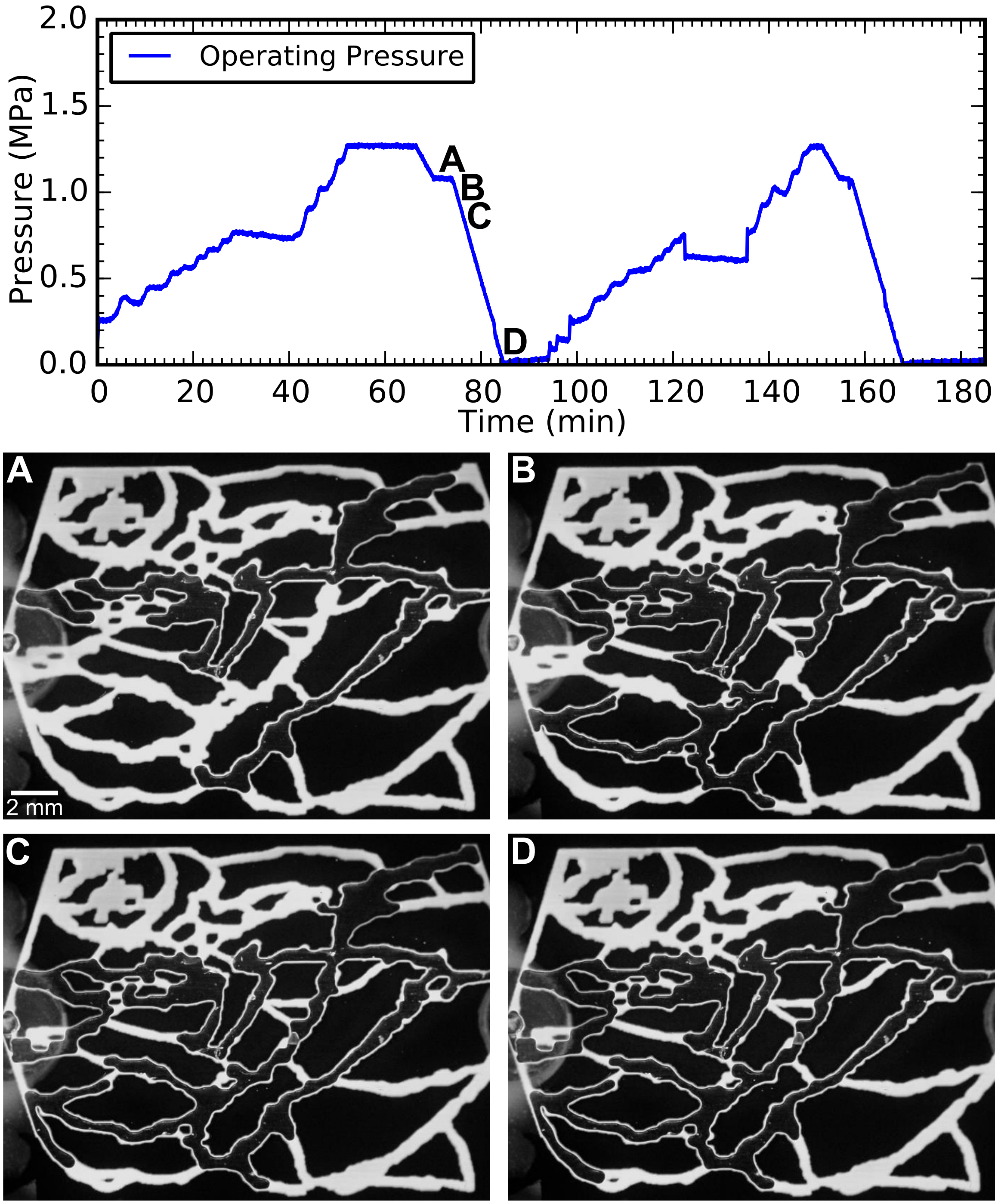

Fig. 13.7 Pressure profile and images of a complex fracture network filled with oil during depressurization of N_2. In the images, the oil is white and the N_2 is black. At the start of the experiment (A), nitrogen fills part of the fracture system. Oil is displaced as pressure is dropped. However, oil production ceases when the N_2 reaches the inlet/outlet port.

LANL next conducted an experiment with CO_2 at an operating pressure and temperature of 8.25 MPa and 35 °C, respectively. In this case the CO_2 is supercritical above 7.1 MPa and near the minimal miscibility pressure with n-decane. Thus, the CO_2 is partially miscible with n-decane with a solubility of approximately 75%. Fig. 13.8 shows the pressure profile along with six images of the phase configurations during depressurization. Figs. 13.8A – 13.8C shows CO_2 dissolving into the upper left corner of the fracture network (the oil in this region is slightly darker gray than the oil in other regions of the fracture network). In addition, a finger of CO_2 is observed entering the fracture network from the inlet/outlet in Fig. 13.8C. Fig. 13.8D shows a significant amount of CO_2 exsolves from the oil in the upper left corner of the fracture network. This occurs just below the transition of supercritical CO_2 to gas. Thus, the thermodynamics are complex at this stage in the depressurization. Figs. 13.8E and 13.8F show that the exsolved CO_2 continues to expand and displace oil as the pressure continues to decrease.

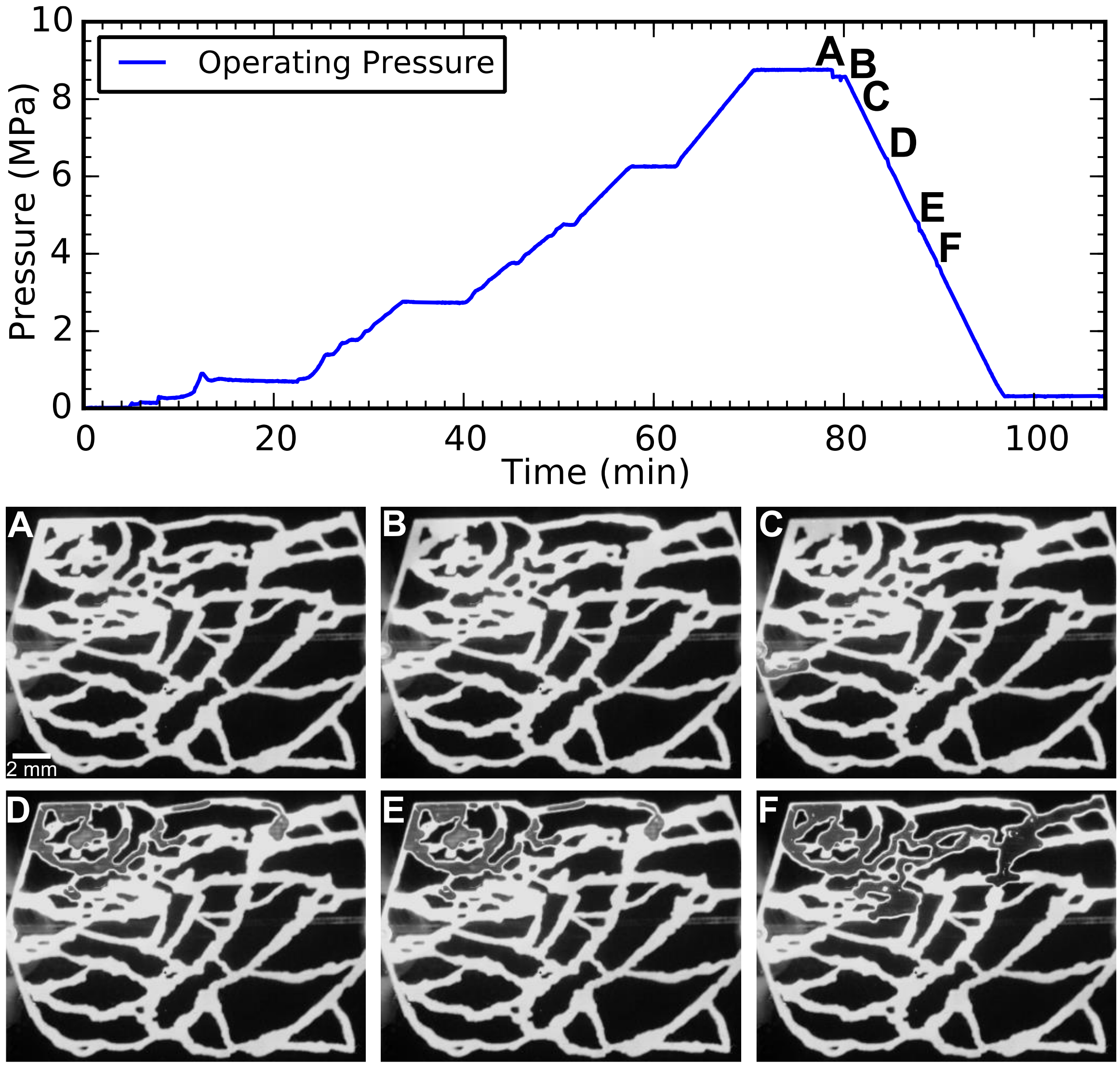

Fig. 13.8 Pressure profile and phase configuration images during depressurization of CO_2. In the images, the oil is white and the CO_2 is black.

A final set of experiments was done with the same complex fracture system but etched into a shale substrate. These experiments involved a three-phase displacement process involving brine, supercritical CO_2 ($scCO_2$) and oil in which the gas phase is partially miscible with the oil phase. The shale gas injection experiments were conducted at 8.4 MPa and 45 °C. The fracture network system was initially saturated with oil and then water was injected to reach residual oil saturation prior to gas injection. At this pressure and temperature, the solubility of $scCO_2$ into water is approximately 5%, whereas the solubility of $scCO_2$ into oil is approximately 75%. Snapshots of gas injection as a function of time are shown in Fig. 13.9. The images show first diffusion of CO_2

into water that separates the inlet from oil (light blue). With time, the CO_2 spreads through the system and diffuses into the oil (pink). As the oil expands with CO_2 it is pushed out of the system in an enhanced oil recovery mechanism. Note that water is not displaced by the CO_2. The results show that CO_2 can enhance oil recovery even in water-rich environments by diffusion through water barriers.

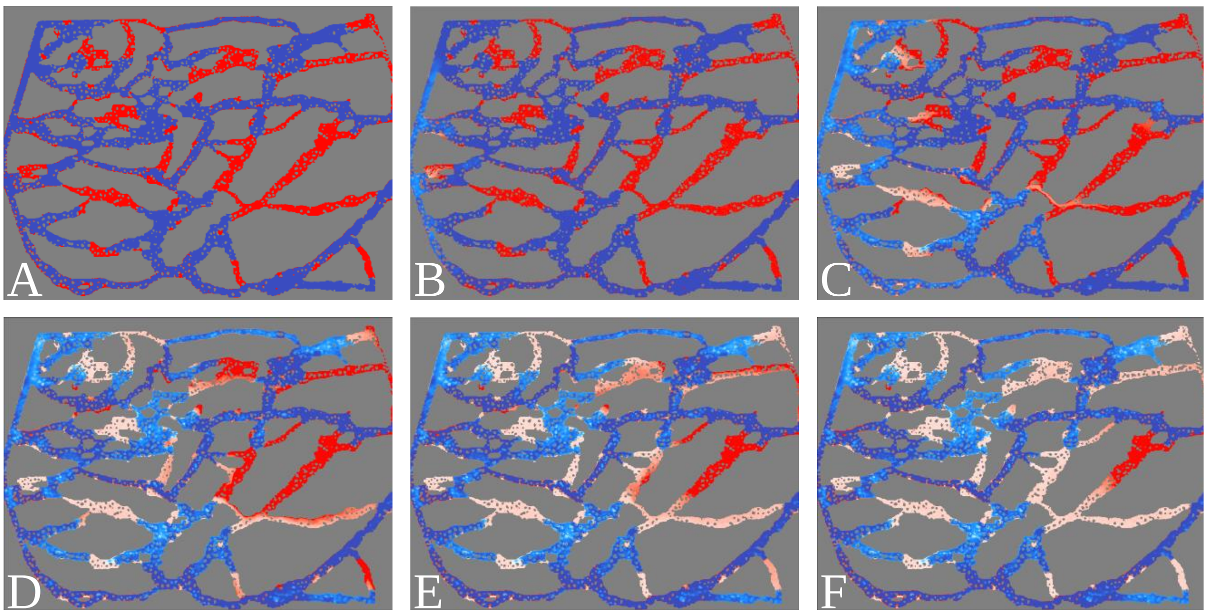

Fig. 13.9 Snapshots of supercritical CO_2 (white) diffusing into water (blue) and n-decane (red). The $scCO_2$ displaces very little water but mobilizes the trapped oil. The light blue and pink colors represent the concentration of scCO2 dissolved into water (5% maximum) and oil (75% maximum), respectively.

LANL developed a statistical model of the depressurization and gas solution drive observed in our experiments. The model is designed to estimate the oil saturation, S_o, as a function of system pressure. In this way, the model can be used as a constitutive relationship for reservoir models. Briefly, LANL's model assumes that quasi-equilibrium interfaces are formed between the two phases, which enables the use of the Young-Laplace equation. As a first approximation, a set of pores is considered filled with CO_2 when the pressure difference between two disconnected n-decane liquid phases is approximately 30 Pa as estimated from the exsolution experiments (Fig. 13.2). In order to perform statistical analysis, a cumulative pore-diameter distribution is generated through image analysis of the experiments and fit to a Weibull cumulative distribution function. Pore diameters that match the cumulative distribution from the experiment are then extracted by choosing a random number between 0 and 1. In addition, it is necessary to determine the probability that a pore with a given diameter will be adjacent to a pore of another diameter. This has been determined by averaging the pore diameters around a pore and then determining the cumulative distribution of these averages. This distribution has also been fit to a Weibull cumulative distribution function. Pore diameters of adjacent pores can now be obtained with reasonable probability by choosing a random number between 0 and 1. To calculate the probability of pores filled with exsolved CO_2, a pore diameter is randomly selected and then the probability of this pore being adjacent to another pore is calculated. Next a radius of curvature is determined from these two pore diameters for a given system pressure. If this radius of curvature is within the propagation of error of the predicted radius of curvature using 30 Pa as the estimated pressure drop, then the pore is considered filled with CO_2. For a given system pressure, the percentage of filled pores for 500 different pore combinations is calculated. Note that a pore combination consists only of the two different pore diameters. This simulation process is repeated 20 times and the average and standard error of all 20 experiments is obtained. This results in the prediction of the percentage of pores that are expected to be filled at a given pressure

Two comparisons between model and experiment are shown in Fig. 13.10. For the experiment with a depressurization time of 15 minutes (Fig. 13.10, left) the onset of CO_2 gas exsolution was captured by the statistical model. However, the model does not capture the CO_2 gas saturation trends below 2.5 MPa. In the 30-minute depressurization experiment (Fig. 13.10, right), the model predicts the onset of CO_2 gas exsolution at 5 MPa, whereas the onset of gas exsolution does not occur until 3 MPa in the experiments. Additional, experiment and model comparisons indicate similar discrepancies. This model captures some key features of the exsolution process but shows that it does not capture all of the relevant processes. To make further progress on this front, it was necessary to examine a complex fracture system but with simple geometric relationships as discussed in section 13.3.

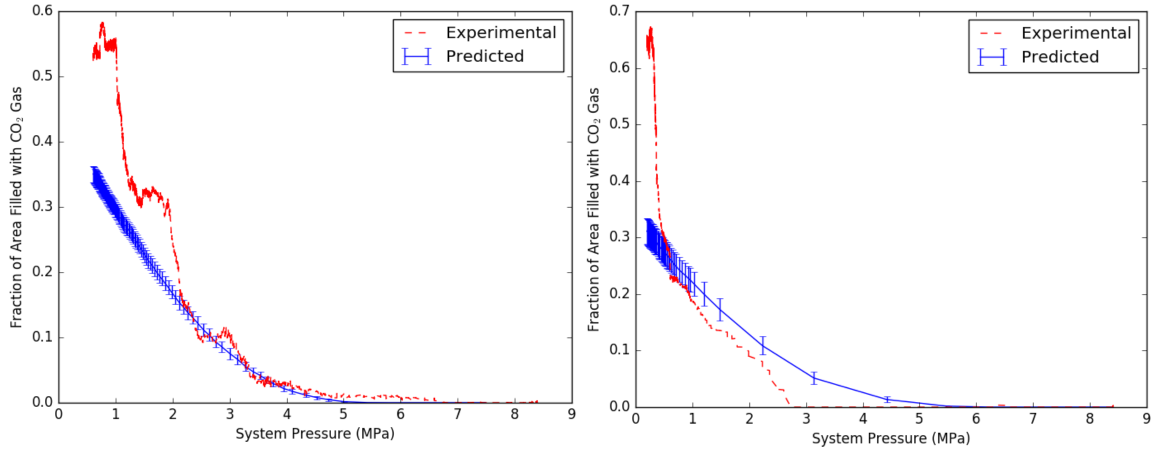

Fig. 13.10 Comparison between experimental observations of CO2 exsolution in experiments similar to Fig. X.8 and a statistical model of oil saturation. Depressurization times were 15 (left) and 30 (right) minutes.

13.4 Cyclic gas injection in connected and dead-end fracture networks

Introduction. In order to facilitate quantitative analysis, LANL developed new fracture designs that more clearly and reproducibly characterize oil recovery during cyclic gas injection. A system was designed that allowed establishment of both a through-going path of injected gas (as would be found in an EOR operation) and one that allowed recovery of oil through the inlet port (simulating a huff-and-puff operation). The new system allows precise control of pressurization and depressurization cycles. This effort has produced good oil recovery data and insights into mechanisms governing oil recovery during cyclic gas injection into fracture networks.

Two new fracture patterns were used to investigate recovery rate: a closed-end network and a connected network as shown in Fig. 13.11. The experiments were conducted by first filling the network with oil from the inlet end. Then low-pressure fluid (N_2, CO_2 or H_2O) is injected through the inlet, simulating the initial displacement of oil during the injection portion of a huff-and-puff operation. This process displaces oil out the outlet and fills only the largest connected channel with displacing fluid. The oil in the dead-end and in the connected fractures remains unmodified. The filling port is then closed. The fracture network is then pressurized with injection fluid from 100 kPa to 10 MPa. The system is kept at a constant temperature of 50 ºC. The system is soaked at 10 MPa for about 2 hours until no changes in fluorescence signal intensity is observable indicating equilibration of the fluid-oil system. The system is then depressurized from 10 MPa to 0.1 MPa. Images were recorded at a frame rate of 1 fps with corresponding pressure recording. The experiments were performed using LANL's unique chip fabrication, assembly method and manifold along with high pressure and temperature connections through an intricate confining pressure system. Images were taken using fluorescence microscope. An illustrative schematic of the experimental setup is shown in Fig. 13.12.

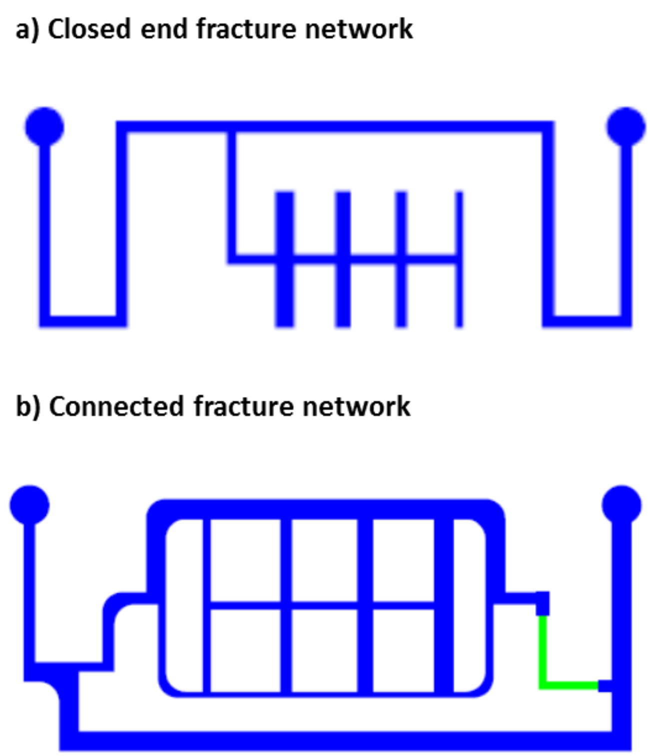

Fig. 13.11 Fracture network patterns etched into geomaterials (glass); a) a dead-end pore-network; b) a connected network. Inlet was on the left; outlet on the right.

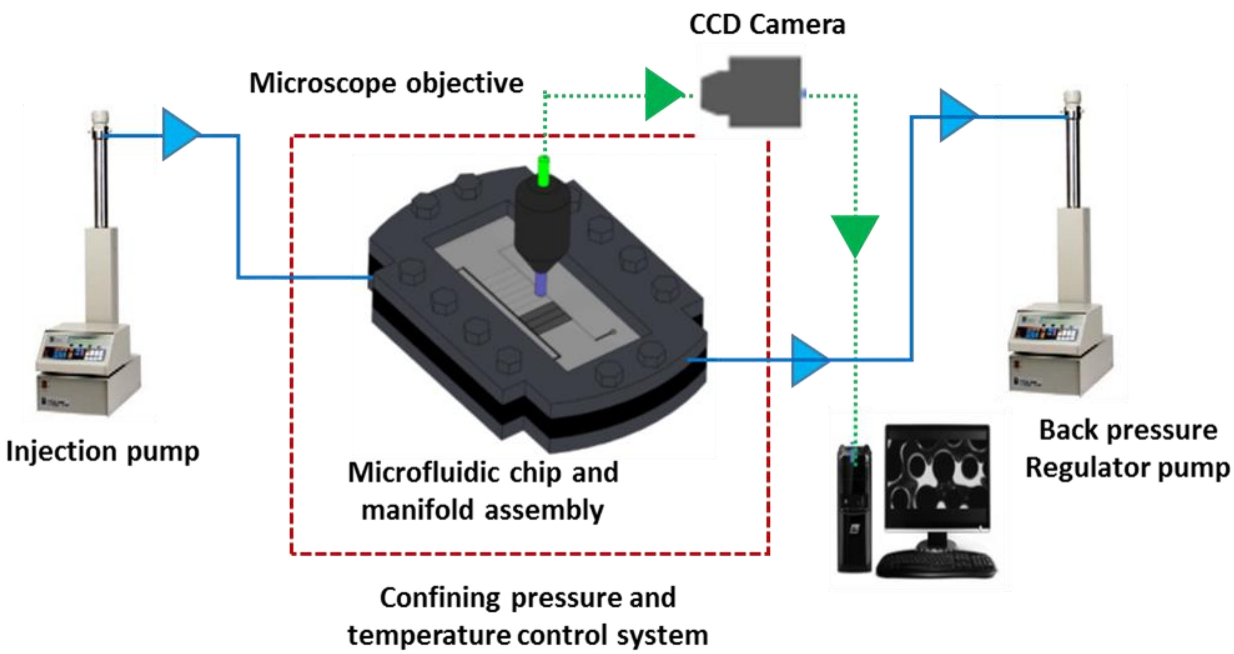

Fig. 13.12 Schematic of the high pressure and temperature microfluidic chip assembly and manifold and the confining pressure system experimental setup.

Each CO_2 or N_2 cyclic injection was conducted in 3 stages: pressurization, soaking, and depressurization. Oil recovery was calculated during depressurization cycle from 10 MPa to 0.1 MPa. Images were taken every second during the depressurization cycle. The images were segmented based on fluorescence intensity, binarized, and used for calculating oil saturations. Four repeated experiments were conducted to evaluate the efficiency of both supercritical CO_2 ($scCO_2$) and N_2 injection in the displacement of oil from the connected and closed-end fracture networks. In addition, a single experiment was conducted using water as the displacing fluid in the two different fracture networks.

CO_2 injection in connected fracture network: Fig. 13.13 shows images of oil saturation and the corresponding oil recovery at different stages of depressurization. Oil saturation is 100% as shown in Fig. 13.13a at the beginning of depressurization. Fluorescent dye was added to the oil phase making it show as green. As pressure is decreased CO_2 nucleation occurs and coalesces in many places of the fracture network. CO_2 bubbles grow and displace oil out of the fracture network. The plot of oil saturation vs. CO_2 pressure is shown in Fig. 13.14. The initial oil recovery rate is limited

to about 8 MPa recovery and is then driven by depressurized volume expansion of the supercritical CO_2 and oil mixture. Fast oil recovery rate occurs at pressures between 8-6 MPa which corresponds to the phase change of supercritical CO_2 to gas. During this pressure range, CO_2 nucleation appears in multiple places in the network. These small bubbles expand quickly and push oil out of the network at a faster rate down to about 6 MPa. The recovery rate is slower at pressures below 6 MPa, while the gas bubbles continue to coalesce and expand to push more oil out. Oil saturation continues to decrease down to below 10% as pressure is decreased to below 1 MPa, resulting in nearly complete oil recovery.

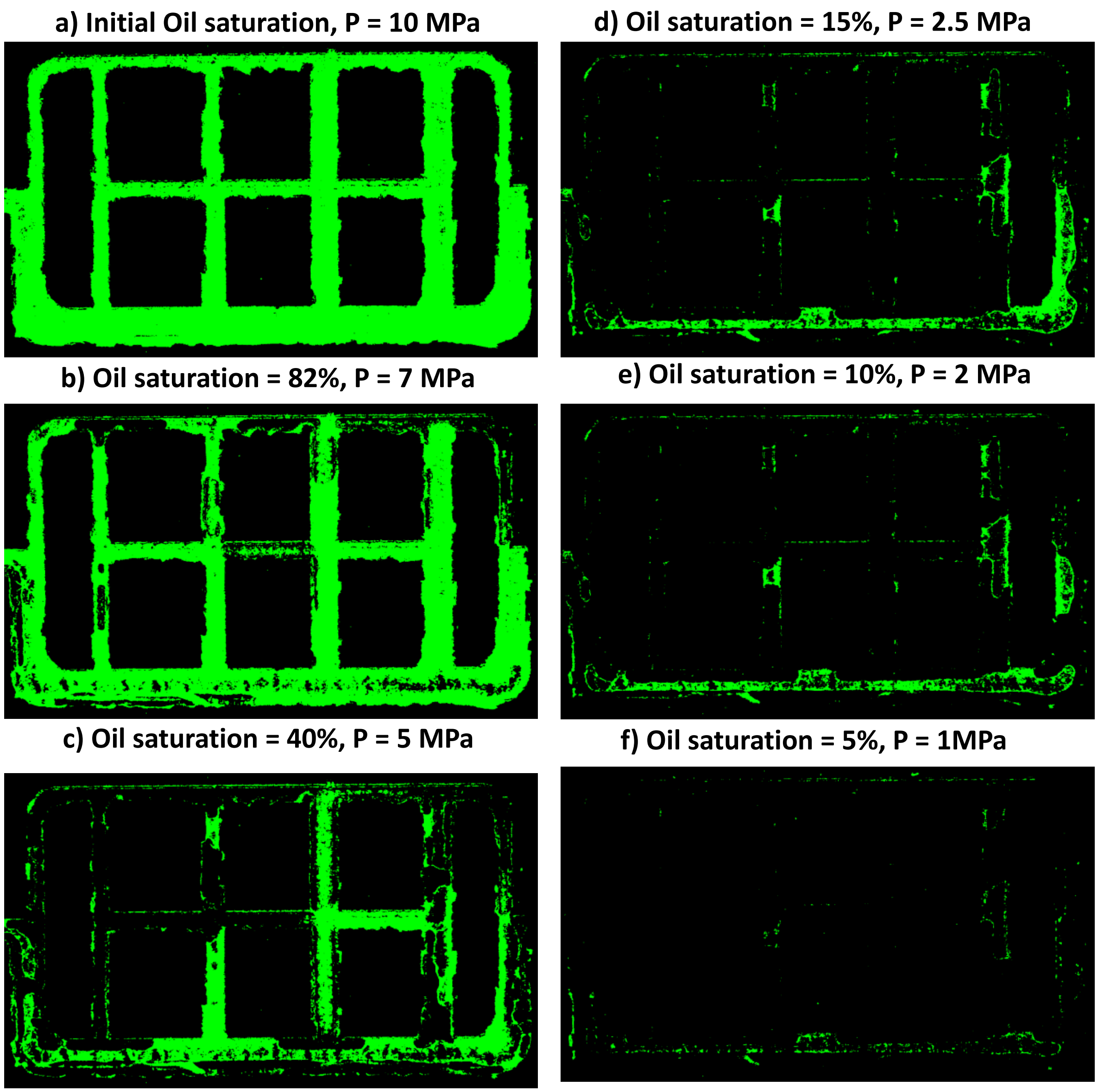

Fig. 13.13 Images of oil saturation at different pressures during depressurization cycle of a CO2-injection experiment within the connected fracture network. Oil is green, CO_2 and rock matrix are black.

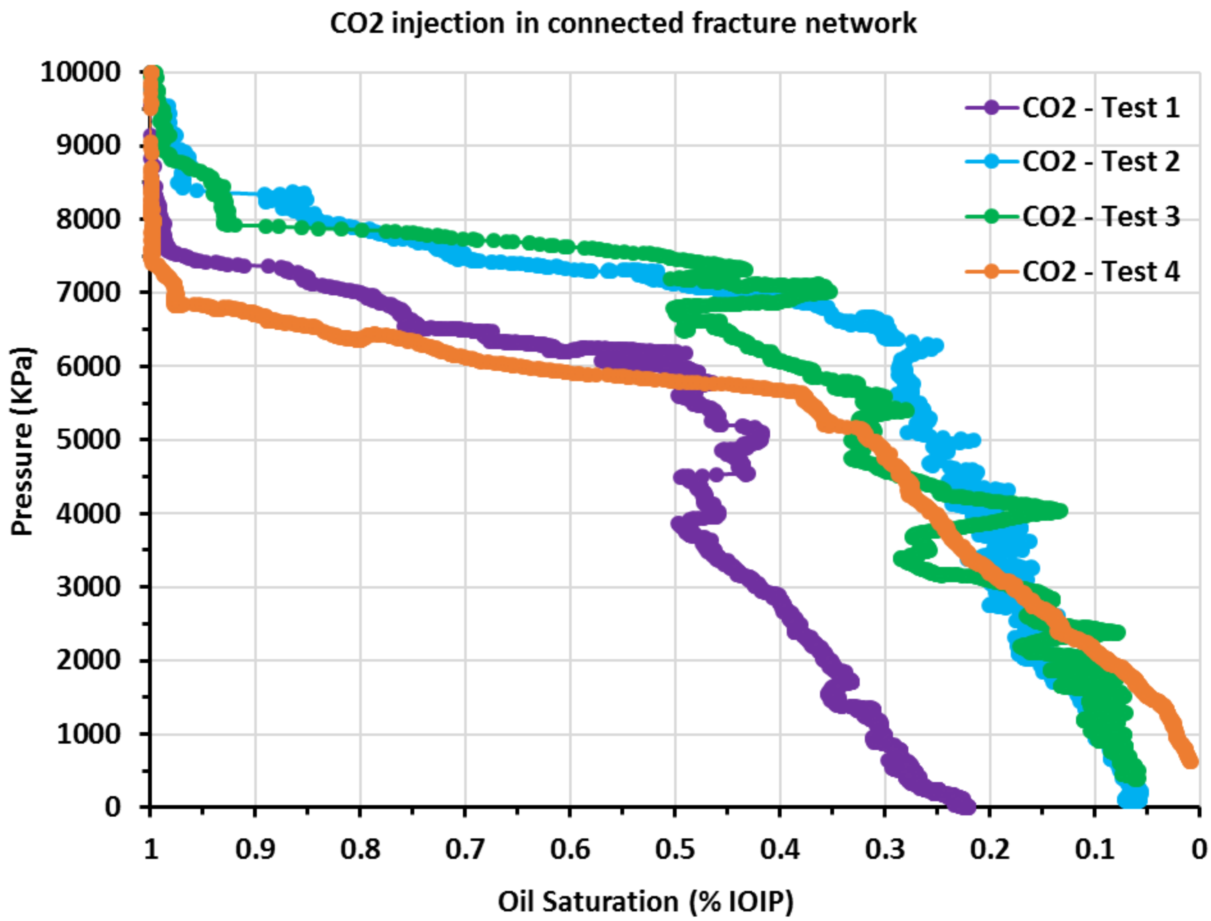

Fig. 13.14 Oil saturation for four experiments during depressurization of CO_2 in the connected fracture network.

N_2 injection in connected fracture network: Figs. 13.15 and 13.16 show the oil displacement images and plots of oil saturation in the connected fracture network. The same experimental procedures were followed as with CO_2. The oil recovery rate is significant but is more limited in comparison with the CO_2 injection. The final oil saturation is also higher (i.e., more oil left in the reservoir compared with CO_2).

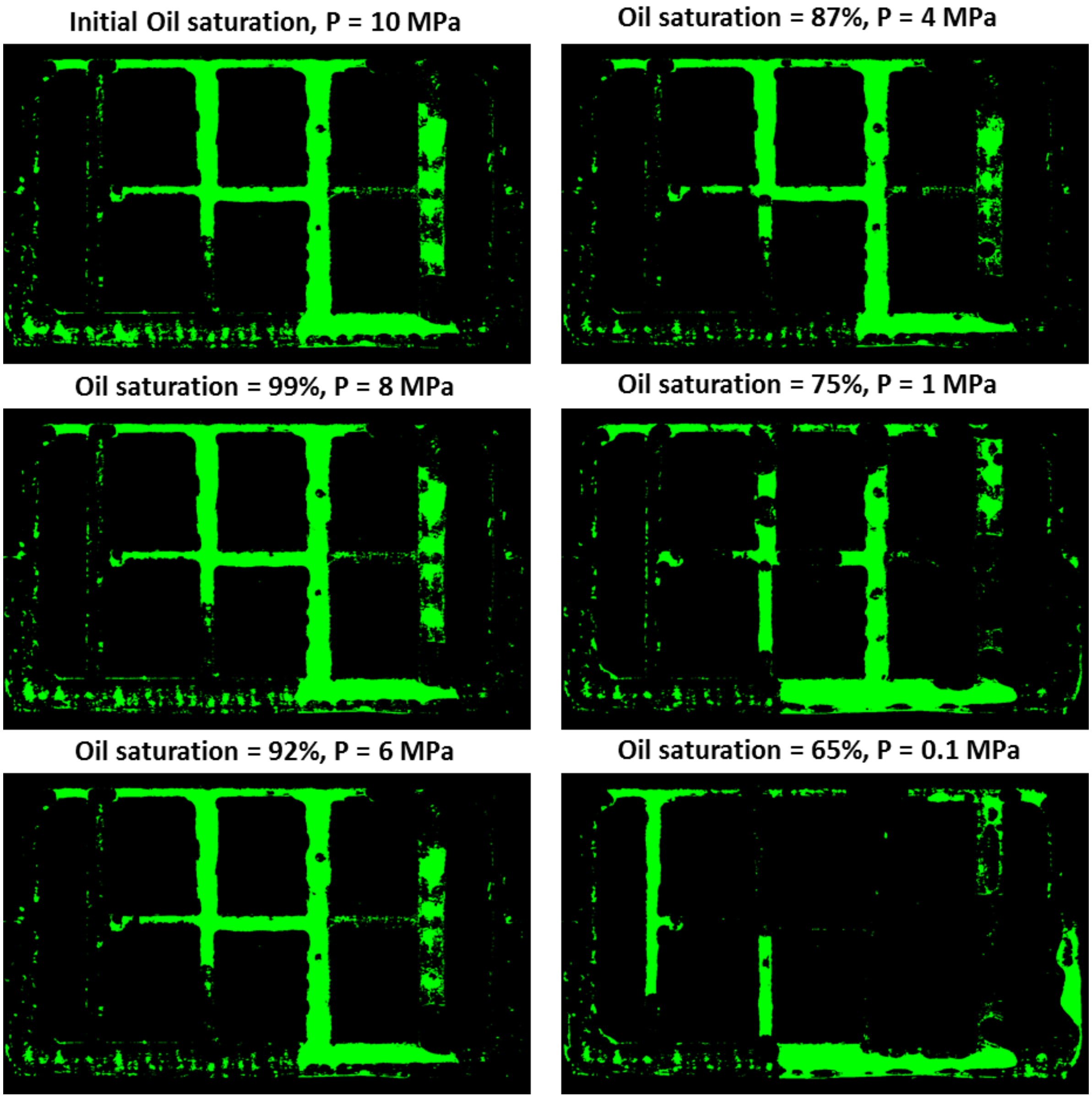

Fig. 13.15 N_2 injection into the connected fracture network. Images of oil saturation at different pressures during depressurization. Oil is green, N_2 and rock matrix are black.

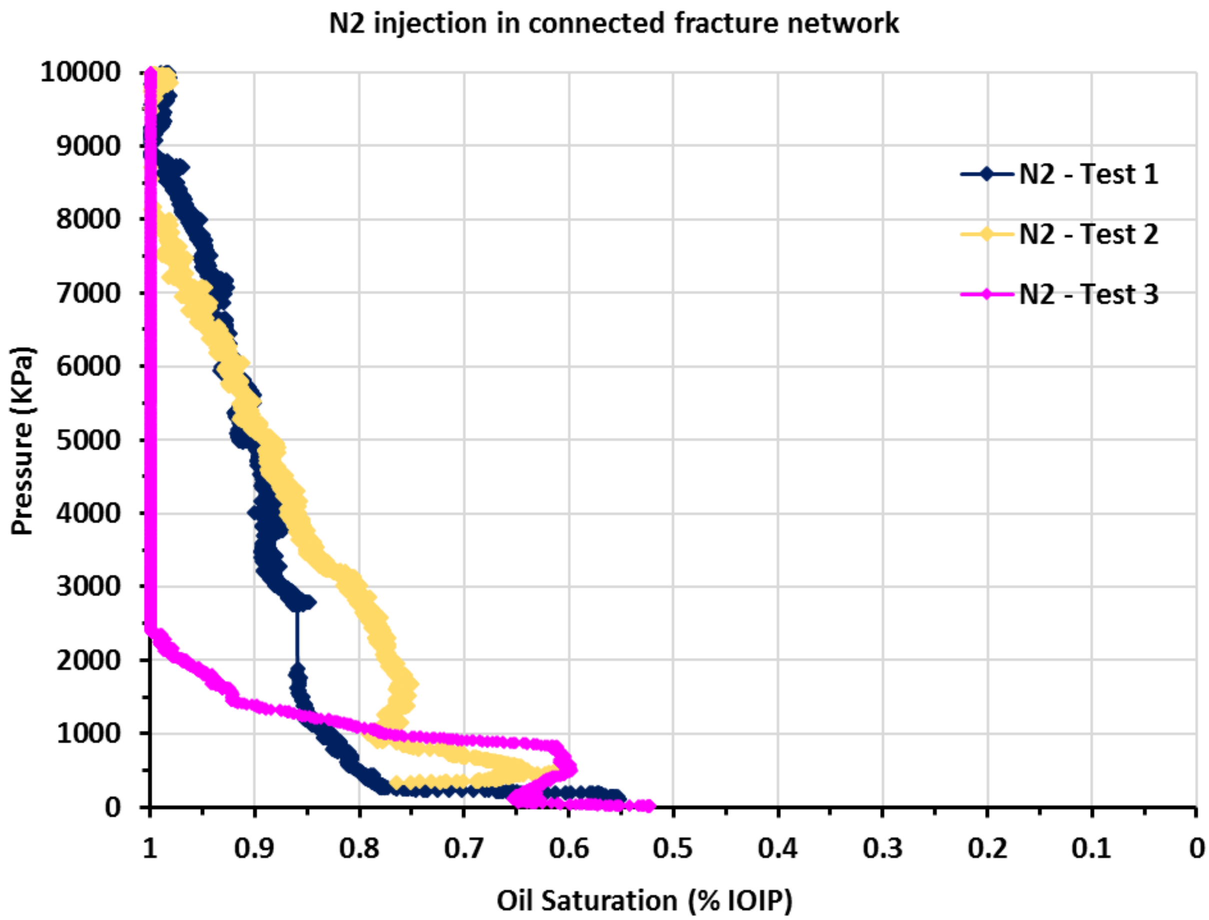

Fig. 13.16 Oil saturation for three experiments during depressurization of N_2 in the connected fracture network.

Fig. 13.17 shows a comparison between CO_2, N_2 and water injection in the connected fracture network. CO_2 has much higher solubility in oil than N_2, which allows for more bubble nucleation to occur during depressurization. The bubbles grow and push the oil out as the main recovery mechanism and energy that drives oil recovery. As a result of higher solubility and more bubble nucleation, the recovery rate for CO_2 is significantly higher than N_2. However, N_2 recovers a significant fraction of the oil (about 40%) but also requires a greater pressure drop to accomplish this. Water has almost no effect on oil recovery. It has no solubility in oil and with its very low compressibility has limited capacity to expand and remove oil during depressurization.

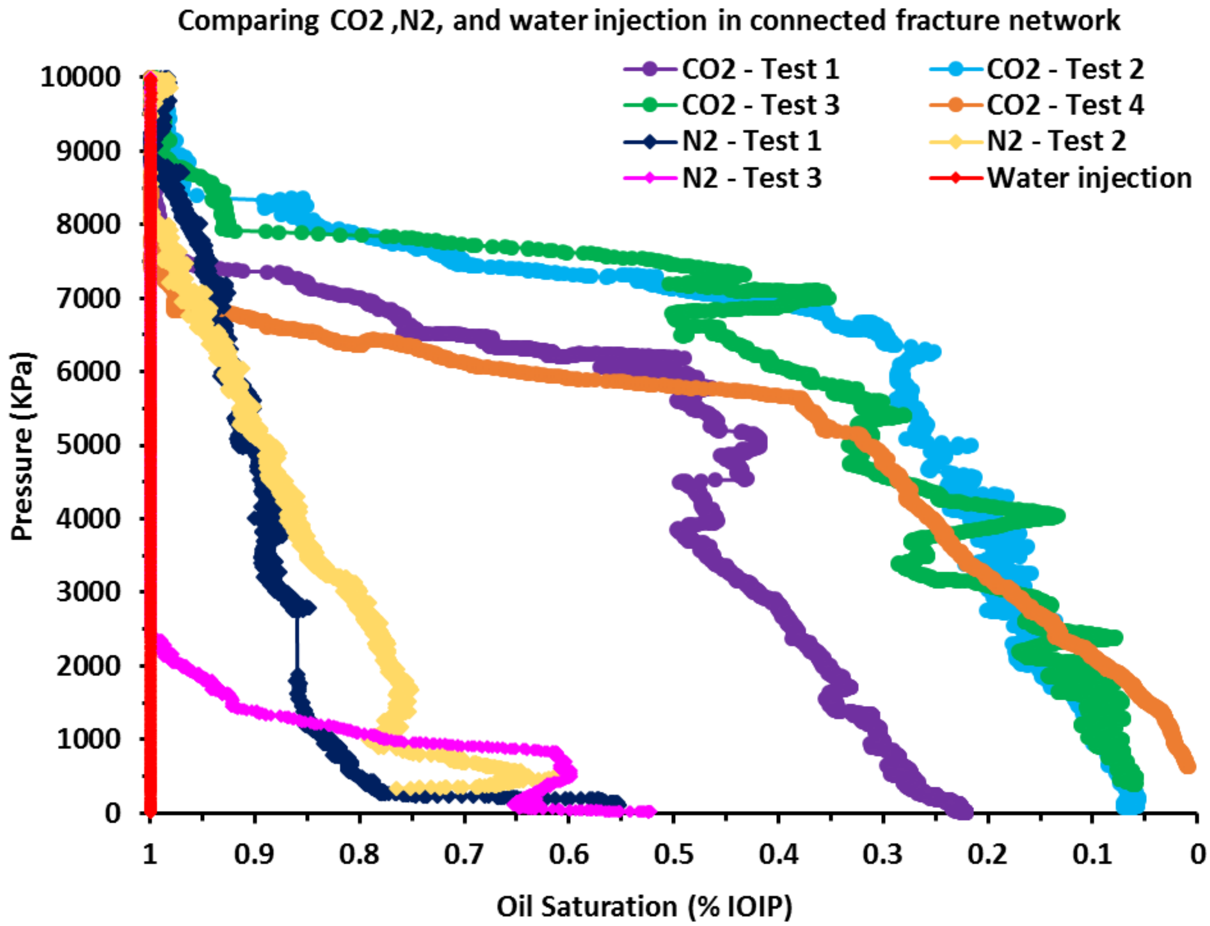

Fig. 13.17 Oil saturation during depressurization of CO_2, N_2 and water in the connected fracture network.

CO_2 injection in closed end fracture network: CO_2 injection into a dead-end fracture network also showed good oil recovery, despite the one-way access of CO_2 to oil. However the recovery rate is lower than the connected fracture network. This is consistent with less CO_2 diffusing into the oil since the oil/CO_2 interface is at one location at the neck of the network off the main fracture channel with limited contact surface area. Thus in order to be effective, the CO_2 had to dissolve into a much longer fracture channel. The displacement process is shown in Fig. 13.18 which shows that while CO_2 appears in the entire network, its expansion is unable to drive all of the oil out of the dead-end fracture. The recovery rate is shown in Fig. 13.19.

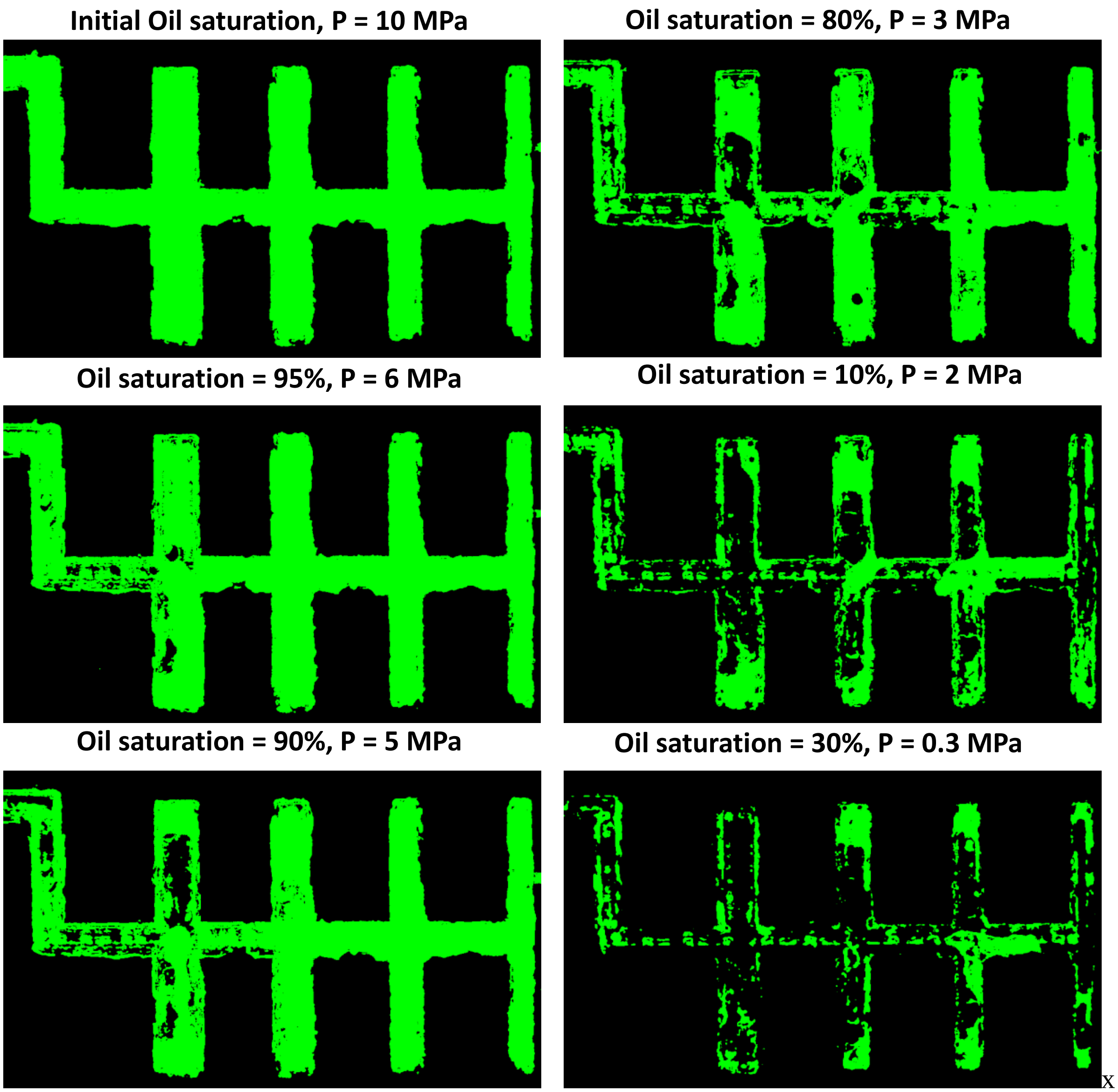

Fig. 13.18 CO_2 injection and depressurization in the dead-end fracture network. Images of oil saturation at different pressures during depressurization. Oil is green, CO_2 and rock matrix are black.

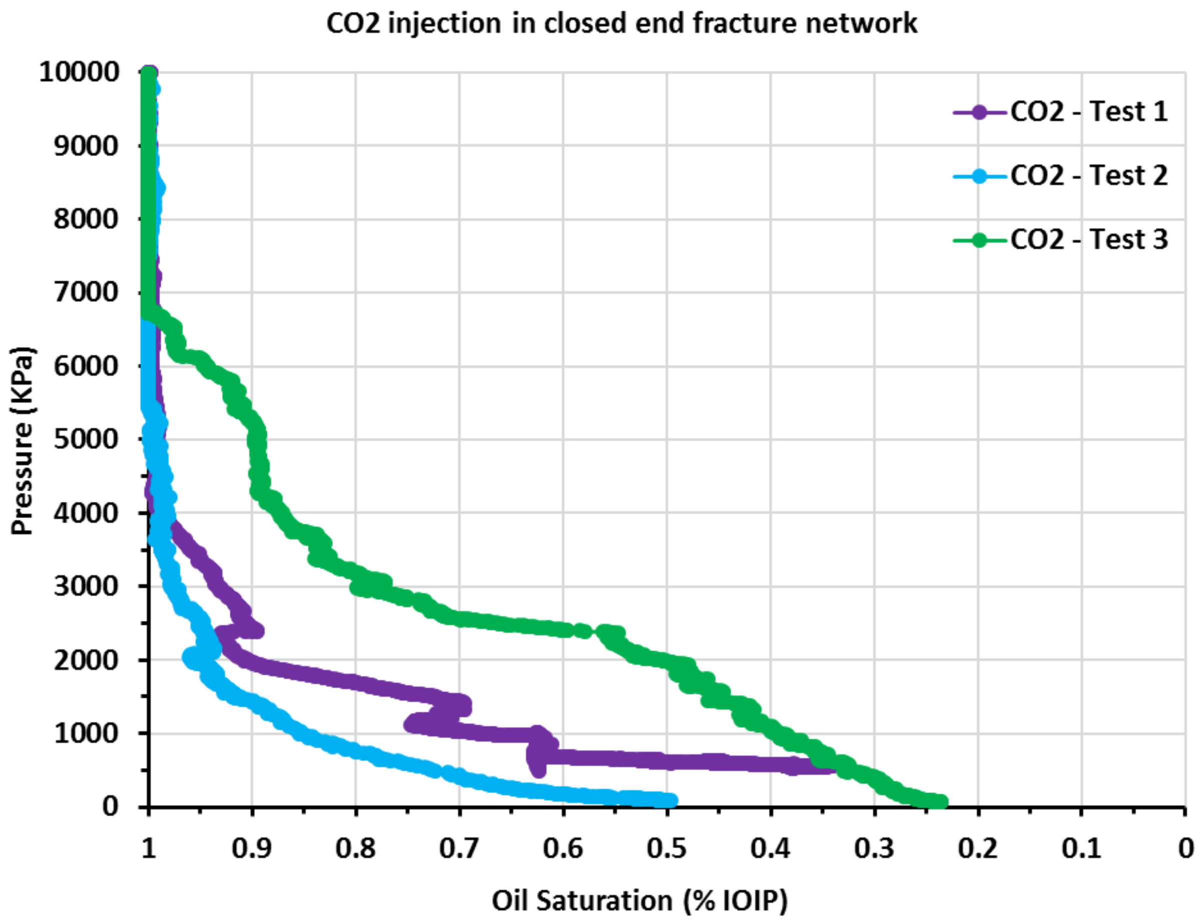

Fig. 13.19 Oil saturation during depressurization of CO_2 in the closed-end fracture network. Compare with Fig. 13.18.

N_2 injection in closed end fracture network: N_2 injection into closed end fracture network has low to moderate oil recovery rate since N_2 has low solubility in oil and the N_2/oil interface is localized to one location. This results in few bubble nucleation events of N_2 and very low recovery in one experiment and moderate recovery in a second experiment (Figs. 13.20 and 13.21).

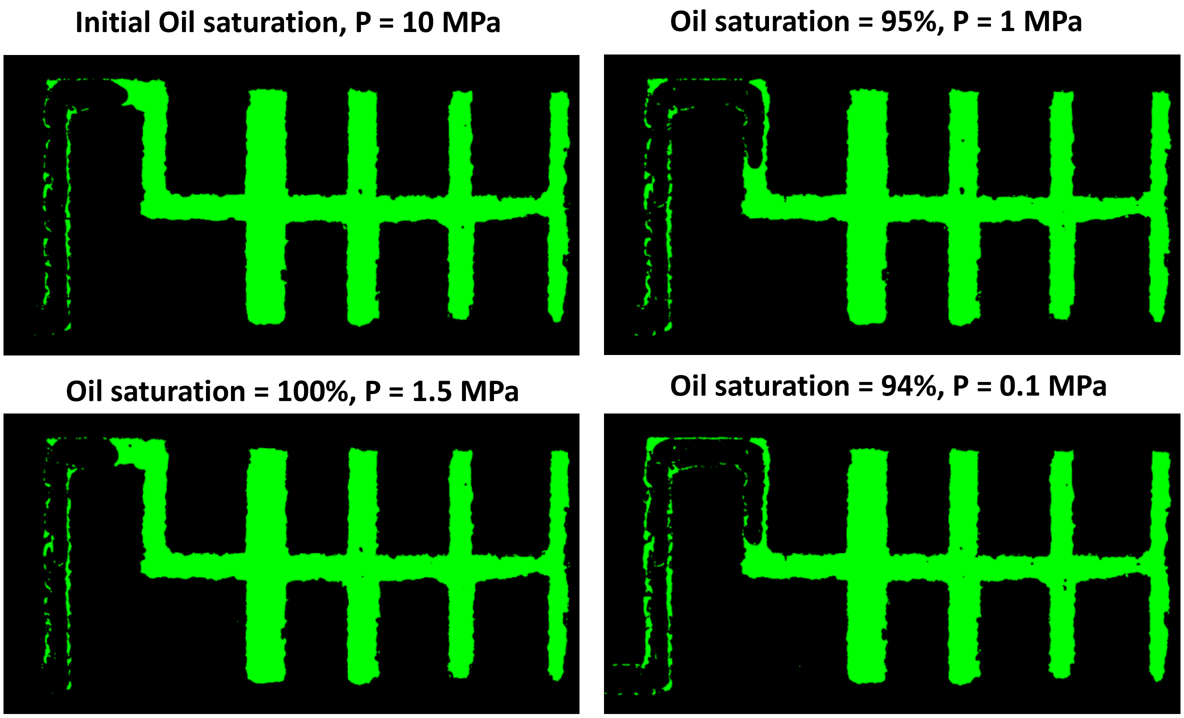

Fig. 13.20 N_2 injection in closed end fracture network. Images of oil saturation at different pressures during depressurization.

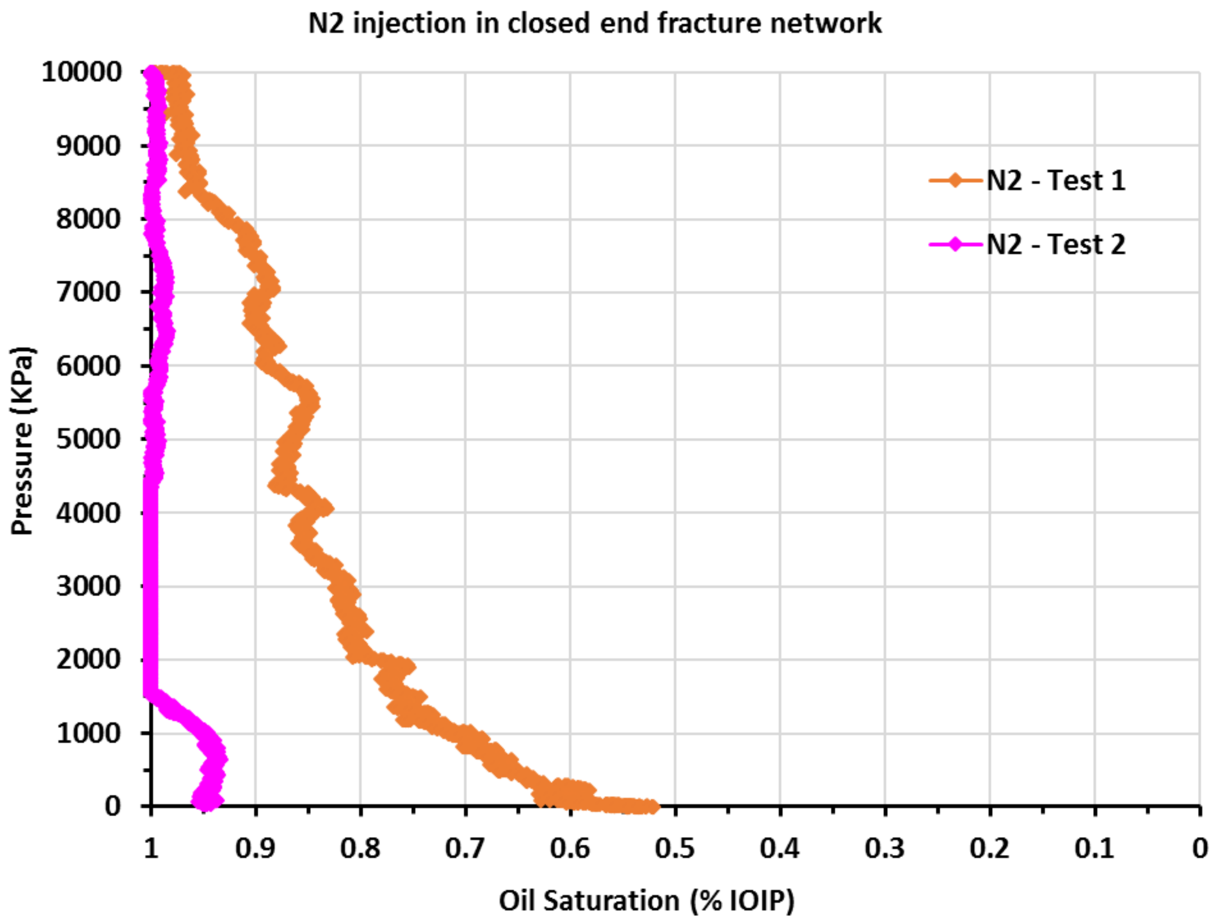

Fig. 13.21 Oil saturation during depressurization of N_2 in closed end fracture network.

As with the connected fracture network, Fig. 13.22 shows that CO_2 performs better than N_2 enhanced oil recovery in the closed-end fracture network. The oil recovery for CO_2 is better due to its higher solubility, which allows greater exsolution and bubble nucleation during depressurization. The recovery in closed end fracture is not as effective as connected fracture network due to multiple gas/oil interfaces that allow for more gas to be dissolved in the oil in the connected fracture case.

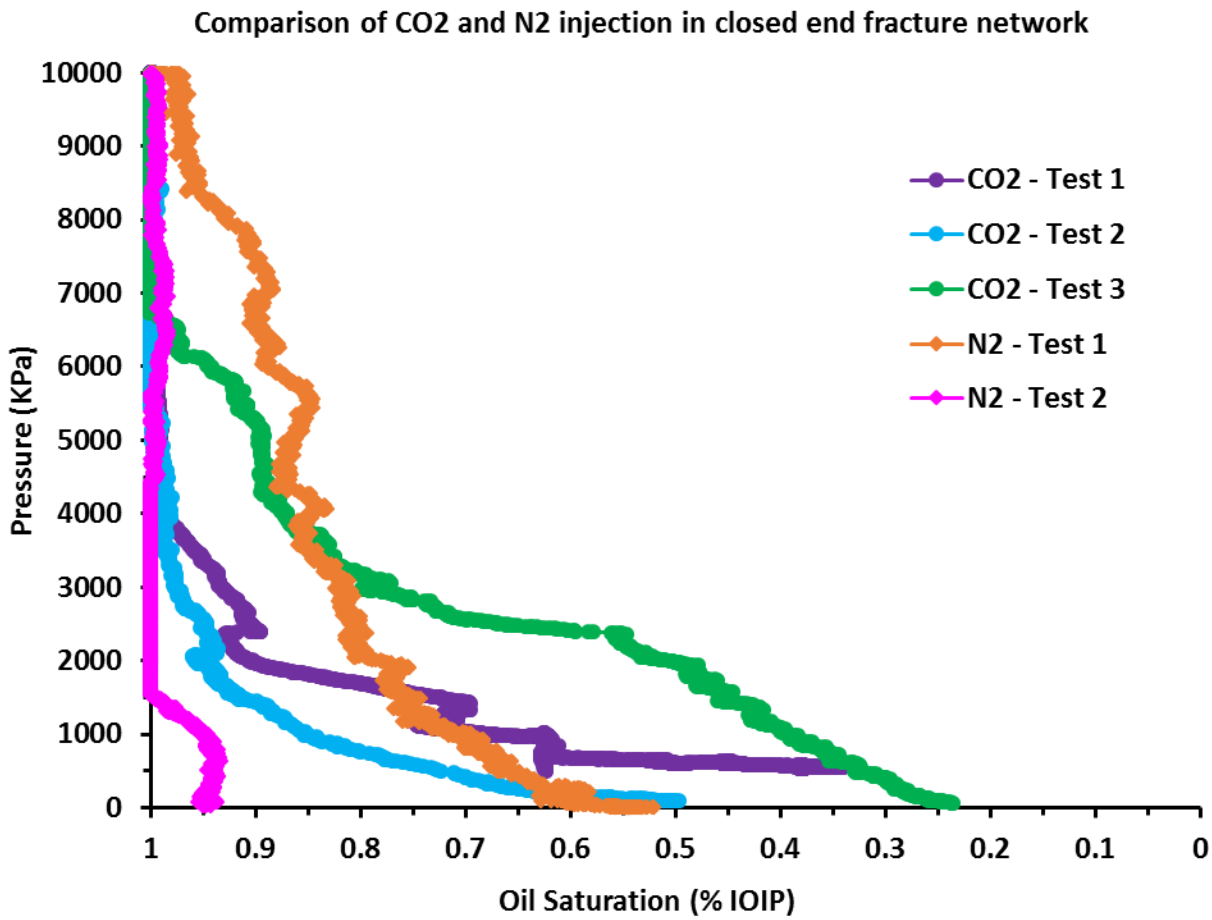

Fig. 13.22 Oil saturations during depressurization of CO_2 and N_2 in closed end fracture network.

LANL characterized the dynamics of bubble growth through time-lapse images of gas bubble nucleation and growth (Fig. 13.23). In the figures, t = 0 occurs at the start of bubble nucleation. The bubble starts as a round bubble with a diameter smaller than the fracture width. The bubble elongates to an oval shape when the hydraulic diameter becomes larger than the fracture width. Contours of the bubble growth at each time stage were traced and are shown as a series of outlines in different colors. Bubbles also shift locations as they can nucleate in one location and then migrate to another to continue growing. The bubbles also grow at different rates depending on local pressure changes, capillary pressure, and dissolved gas concentration. Fig. 13.24 illustrates a gas exsolution mechanism with bubble nucleation at multiple locations, growth locally, then migration and coalescence to form a single bubble. This mechanism results in a very fast growth rate since multiple bubbles merge to form one large connected gas bubble. Figs. 13.23 and 13.24 compare N_2 and CO_2 growth dynamics and show the relatively more rapid growth of CO_2.

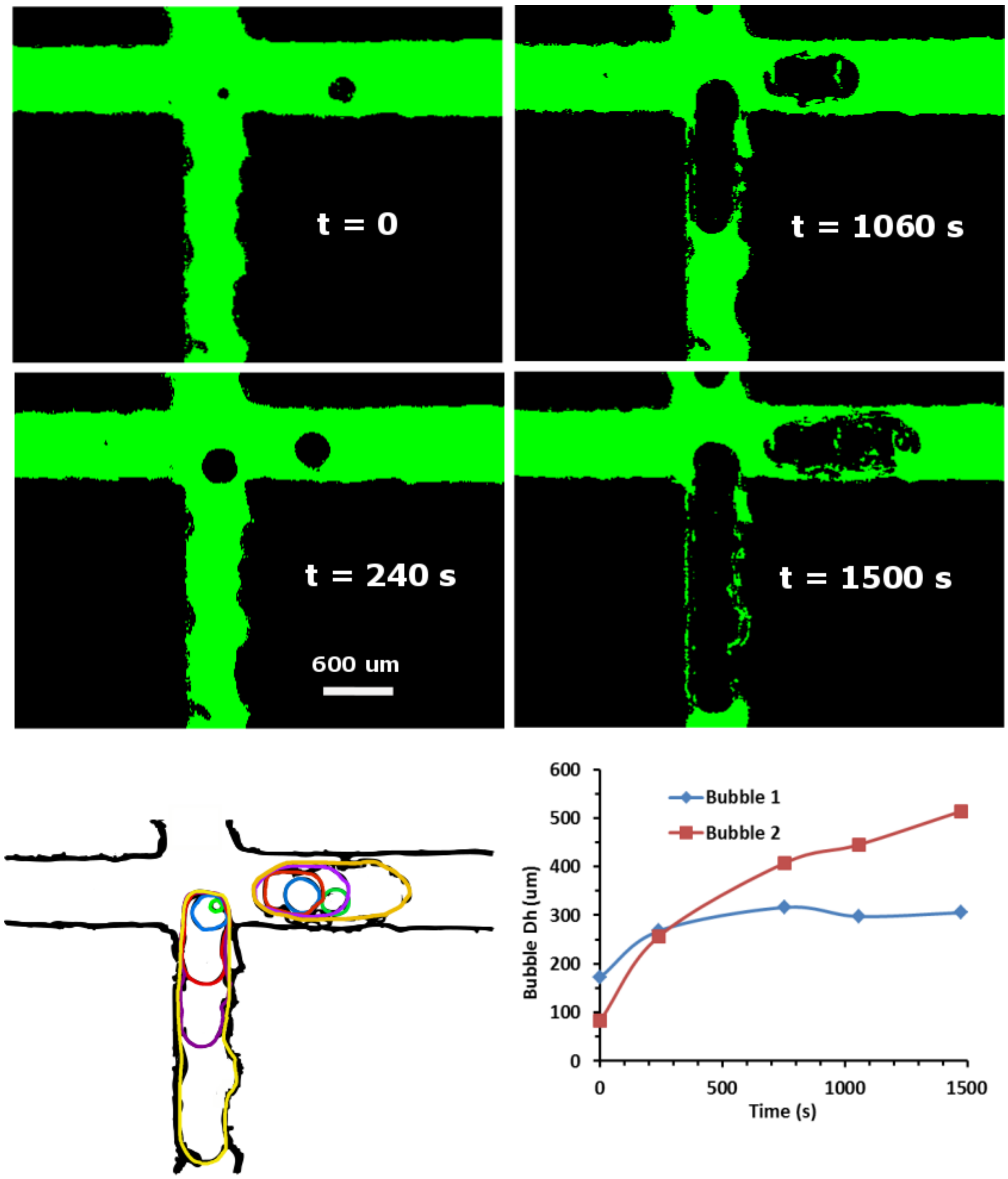

Fig. 13.23 Time-lapse image of gas bubble nucleation and growth in a N_2 experiment in a connected network. The upper figure shows images from the experiment. The lower-left image shows traces of bubble outlines as a function of time. The lower-right image shows the change in bubble hydraulic diameter (area divided by perimeter) with time.

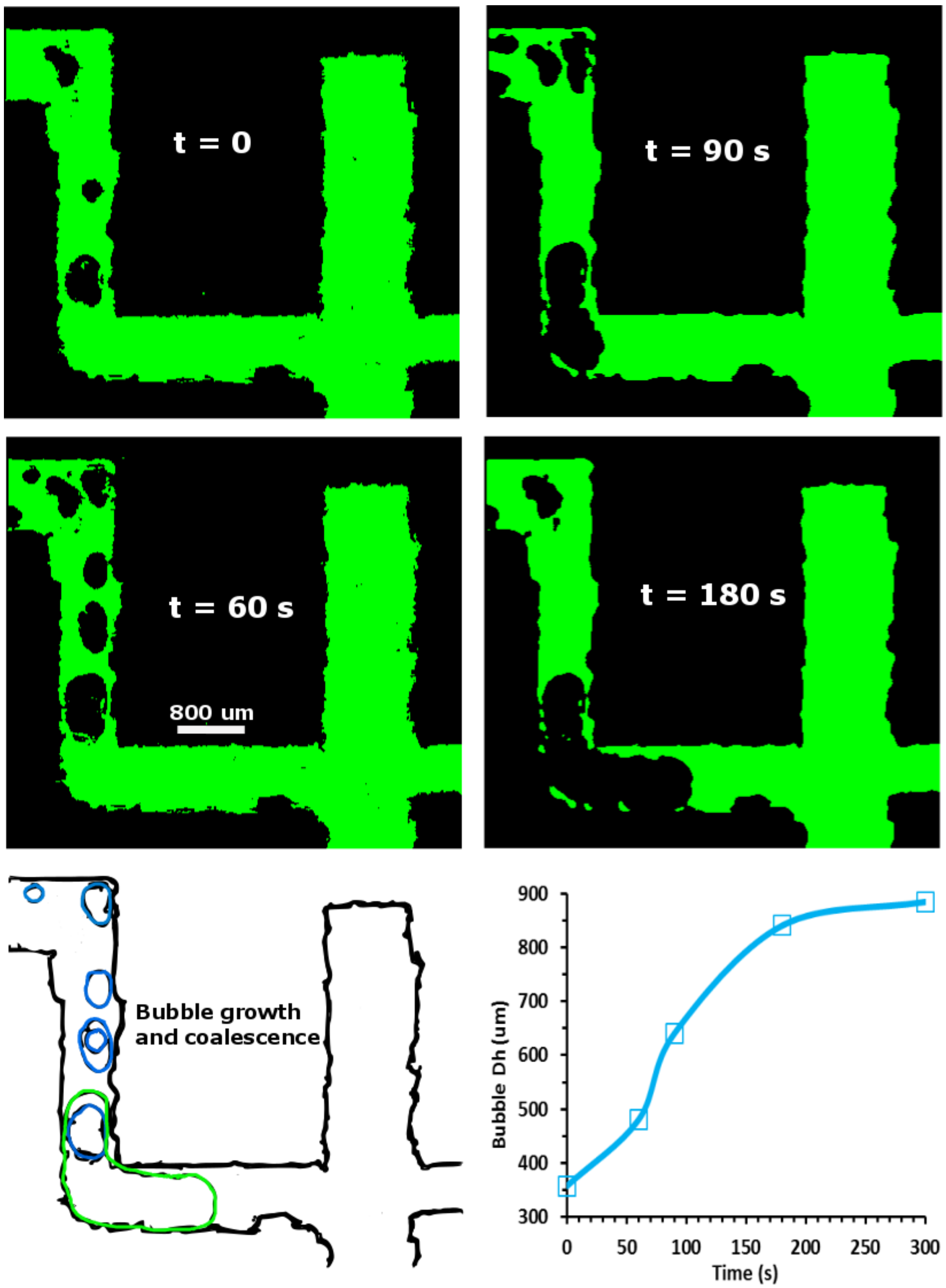

Fig. 13.24 Time-lapse image of gas bubble nucleation, growth, and coalescence in a CO_2 experiment in the dead-end fracture network. The upper figure shows images from the experiment. The lower-left image shows traces of bubble outlines as a function of time. The lower-right image shows the change in bubble hydraulic diameter (area divided by perimeter) with time.

The experimental results have been summarized in a manuscript that is being prepared for Applied Energy:

T. P. Nguyen, J. W. Carey, M. L. Porter and H. S. Viswanathan (in preparation) Analysis of the effectiveness of injection fluids in huff-and-puff method of enhanced oil recovery in shale fracture networks using microfluidic experiments. Intended for Applied Energy.

In addition, several other publications have presented results on multiphase flow processes involving CO_2 and N_2 in porous and fractured media:

47 Hyman, J.D, Jimenez-Martinez, J., Porter, M.L., Karra, S., Carey, J.W., and Viswanathan, H.S. 2016. *Understanding hydraulic fracturing: A multi-scale problem*. Philosophical Transactions of the Royal Society A. 374: 20150426. doi: 10.1098/rsta.2015.0426

48 Jimenez-Martinez, J., Porter, M.L., Hyman, J.D., Carey, J.W., and Viswanathan, H.S. 2015. *Mixing in a three-phase system: Enhanced production of oil-wet reservoirs by CO_2*. Geophysical Research Letters. doi: 10.1002/2015GL066787.

Appendix A – List of papers published from this project

1. Wan, T., Yu, Y., and Sheng, J.J. 2015. Experimental and numerical study of the EOR potential in liquid-rich shales by cyclic gas injection, Journal of Unconventional Oil and Gas Resources, 12, 56-67.
2. Yu, Y., Sheng, J.J., Barnes, W., and Mody, F. 2015. Evaluation of Cyclic Gas Injection EOR Performance on Shale Core Samples Using X-Ray CT Scanner, paper 407411 presented at the 2015 AIChE Annual Meeting, Salt Lake City, UT, 8-13 November.
3. Yu, Y., Li, L., and Sheng, J.J. 2016. Further Discuss the Roles of Soaking Time and Pressure Depletion Rate in Gas Huff-n-Puff Process in Fractured Liquid-rich Shale Reservoirs, paper SPE 181471 presented at the SPE Annual Technical Conference and Exhibition held in Dubai, UAE, 26–28 September 2016.
4. Yu, Y., and Sheng, J.J. 2015. An Experimental Study of the Potential of Improving Shale Oil Recovery by Gas-Flooding, paper 418166 presented at the 2015 AIChE Annual Meeting, Salt Lake City, UT, 8-13 November.
5. Yu, Y., and Sheng, J.J. 2016. Experimental Evaluation of Shale Oil Recovery from Eagle Ford Core Samples by Nitrogen Gas Flooding, paper SPE 179547 presented at the SPE Improved Oil Recovery Conference held in Tulsa, Oklahoma, USA, 11–13 April.
6. Yu, Y., Meng, X., and Sheng, J.J. 2016. Experimental and Numerical Evaluation of the Potential of Improving Oil Recovery from Shale Plugs by Nitrogen Gas Flooding, Journal of Unconventional Oil and Gas Resources, 15, 56-65.
7. Yu, Y., Li, L. and Sheng, J.J. 2017. A comparative experimental study of gas injection in shale plugs by flooding and huff-n-puff processes, Journal of Natural Gas Science and Engineering, 38, 195-202.
8. Yu, Y. and Sheng, J.J. 2016. Experimental Investigation of Light Oil Recovery from Fractured Shale Reservoirs by Cyclic Water Injection, paper SPE 180378 presented at the SPE Western Regional Meeting held in Anchorage, Alaska, USA, 23–26 May.
9. Yu, Y. and Sheng, J.J. 2017. A comparative experimental study of IOR potential in fractured shale reservoirs by cyclic water and nitrogen gas injection, J. of Petroleum Science and Engineering, 149, 844-850.
10. Li, L. and Sheng, J.J. 2016. Experimental Study of Core Size Effect on CH4 Huff-n-Puff Enhanced Oil Recovery in Liquid-rich Shale Reservoirs, Journal of Natural Gas Science and Engineering, 34, 1392-1402.
11. Li, L. and Sheng, J.J. 2017. Numerical analysis of cyclic CH_4 injection in liquid-rich shale reservoirs based on the experiments using different-diameter shale cores and crude oil, Journal of Natural Gas Science and Engineering, 39, 1-14.
12. Li, L., Zhang, Y., and Sheng, J.J. 2017. Effect of the Injection Pressure on Enhancing Oil Recovery in Shale Cores during the CO2 Huff-n-Puff Process When It Is above and below the Minimum Miscibility Pressure. Energy & Fuels, 31, 3856−3867.
13. Li, L. and Sheng, J.J. 2017. Upscale methodology for gas huff-n-puff process in shale oil reservoirs, Journal of Petroleum Science and Engineering, 153, 36-46.

14. Li, L., Sheng, J.J., and Sheng, J. 2016. Optimization of Huff-n-Puff Gas Injection to Enhance Oil Recovery in Shale Reservoirs, paper SPE 180219 presented at the SPE Low Perm Symposium held in Denver, Colorado, USA, 5–6 May.

15. Li, L., Sheng, J.J., Watson, M., Mody, F., and Barnes, W. 2015. Experimental and Numerical Upscale Study of Cyclic Methane Injection to Enhance Shale Oil Recovery, paper presented at the 2015 AIChE Annual Meeting, Salt Lake City, UT, 8-13 November.

16. Shen, Z. and Sheng, J.J. 2016. Experimental Study of Asphaltene Aggregation during CO2 and CH4 Injection in Shale Oil Reservoirs, paper SPE 179675 presented at the SPE Improved Oil Recovery Conference held in Tulsa, Oklahoma, USA, 11–13 April.

17. Shen, Z. and Sheng, J.J., 2017. Experimental study of permeability reduction and pore size distribution change due to asphaltene deposition during CO2 huff and puff injection in Eagle Ford shale, Asia-Pacific Journal of Chemical Engineering, 12(3), 381-390.

18. Shen, Z. and Sheng, J.J. 2017. Experimental and numerical study of permeability reduction caused by asphaltene precipitation and deposition during CO2 huff and puff injection in Eagle Ford shale, Fuel, 211, 432-445.

19. Meng, X., Sheng, J.J., and Yu, Y. 2017. Experimental and Numerical Study on Enhanced Condensate Recovery by Huff-n-Puff Gas Injection in Shale Gas Condensate Reservoirs, SPE Reservoir Evaluation & Engineering, May, 471-477, SPE 183645-PA.

20. Meng, X. and Sheng, J.J. 2016. Experimental and Numerical Study of Huff-n-Puff Gas Injection to Revaporize Liquid Dropout in Shale Gas Condensate Reservoirs, J. of Natural Gas Science and Engineering, 35, 444-454.

21. Meng, X. and Sheng, J.J. 2016. Experimental Study on Revaporization Mechanism of Huff-n-Puff Gas Injection to Enhance Condensate Recovery in Shale Gas Condensate Reservoirs, paper SPE 179537 presented at the SPE Improved Oil Recovery Conference held in Tulsa, Oklahoma, USA, 11–13 April.

22. Meng, X., Yu, Y., Sheng, J.J., Watson, W., and Mody, F. 2015. An Experimental Study on Huff-n-Puff Gas Injection to Enhance Condensate Recovery in Shale Gas Reservoirs, paper URTeC 2153322 presented at the Unconventional Resources Technology Conference held in San Antonio, Texas, USA, 20-22 July.

23. Meng, X., Sheng, J.J., and Yu, Y. 2015. Evaluation of Enhanced Condensate Recovery Potential in Shale Plays by Huff-n-Puff Gas Injection, paper SPE 177283 presented at the SPE Eastern Regional Meeting held in Morgantown, West Virginia, USA, 13–15 October.

24. Meng, X., Sheng, J.J. 2015. Simulation of Huff-n-Puff Gas Injection to Enhance Condensate Recovery in Fractured Shale Gas Reservoirs, paper 425710 presented at the 2015 AIChE Annual Meeting, Salt Lake City, UT, 8-13 November.

25. Meng, X., Sheng, J.J., and Yu, Y. 2015. Study on huff-n-puff gas injection to enhance condensate recovery in shale gas reservoirs, poster presented at the SPE Liquid-Rich Basins Conference – North America, Midland, Texas, 2-3 September; Honourable Mention.

26. Meng, X. and Sheng, J.J. 2016. Optimization of huff-n-puff gas injection in a shale gas condensate reservoir, Journal of Unconventional Oil and Gas Resources, 16, 34-44.

27. Sheng, J., Sheng, J.J. 2015. Optimization of Huff-n-Puff Gas Injection in Shale Condensate Reservoirs to Improve Liquid Oil Production, paper 425368 presented at the 2015 AIChE Annual Meeting, Salt Lake City, UT, 8-13 November.

28. Sharma, S. and Sheng, J.J. 2017. A comparative study of huff-n-puff gas and solvent injection in a shale gas condensate core, J. of Natural Gas Science and Engineering, 38, 549-565.

29. Sharma, S. and Sheng, J.J. 2017. A Comparative Study of Huff-n-Puff Gas and Solvent Injection in a Shale Gas Condensate Reservoir, J. of Natural Gas Science and Engineering, in print.

30. Sheng, J.J., Mody, F., Griffith, P.J., and Barnes, W.N. 2016. Potential to increase condensate oil production by huff-n-puff gas injection in a shale condensate reservoir, J. of Natural Gas Science and Engineering, 28, 46-51. DOI: 10.1016/j.jngse.2015.11.031

31. Sheng, J.J. 2017. Critical Review of Field EOR Projects in Shale and Tight Reservoirs, Journal of Petroleum Science and Engineering, 159, 654-665.

32. Jia, H. and Sheng, J.J. 2017. Discussion of the feasibility of air injection for enhanced oil recovery in shale oil reservoirs, Petroleum, 3, 249-257.

33. Jia, H. and Sheng, J.J. 2016. Numerical modeling on air injection in a light oil reservoir: Recovery mechanism and scheme optimization, Fuel, 172, 70-80.

34. Huang, S and Sheng, J.J. 2017. An innovative method to build a comprehensive kinetic model for air injection using TGA/DSC experiments, Fuel, 210, 98-106.

35. Huang, S. and Sheng, J.J. 2017. A practical method to obtain kinetic data from TGA (thermogravimetric analysis) experiments to build an air injection model for enhanced oil recovery, Fuel, 206, 199-209.

36. Huang, S. and Sheng, J.J. 2017. Discussion of thermal experiments' capability to screen the feasibility of air injection, Fuel, 195, 151-164.

37. Huang, S., Jia, H., and Sheng, J.J. 2016. Effect of shale core on combustion reactions of tight oil from Wolfcamp reservoir, Petroleum Science and Technology, 34(13), 1172-1179.

38. Huang, S., Jia, H., and Sheng, J.J. 2016. Exothermicity and oxidation behavior of tight oil with cuttings from the Wolfcamp shale reservoir, Petroleum Science and Technology, 34(21), 1735-1741.

39. Huang, S., Jia, H., and Sheng, J.J. 2016. Research on Oxidation Kinetics of Tight Oil of Wolfcamp Field, Petroleum Science and Technology, 34(10), 903-910.

40. Zhang, Y. and Sheng, J.J. 2016. Oxidation Kinetics Study of the Wolfcamp Light Oil, Petroleum Science and Technology, 34(13), 1180-1186.

41. Zhang, Y and Sheng, J.J. 2017. The mechanism of the oxidation of light oil, Petroleum Science and Technology, 35(12), 1224-1233.

42. Wang, X.-K.and Sheng, J.J. 2017. Effect of low-velocity non-Darcy flow on well production performance in shale and tight oil reservoirs, Fuel, 190, 41-46.

43. Wang, X.K. and Sheng, J.J. 2017. Discussion of liquid threshold pressure gradient, Petroleum, 3, 232-236.

44. Wang, X. and Sheng, J. 2017. Gas sorption and non-Darcy flow in shale reservoirs. Petroleum Science, 1-9. https://doi.org/10.1007/s12182-017-0180-3.

45. Wang, X. and Sheng, J.J. 2017. Understanding Oil and Gas Flow Mechanisms in Shale Reservoirs Using SLD–PR Transport Model, Transport in Porous Media, 119, 337-350. DOI 10.1007/s11242-017-0884-2

46. Porter, M. L., Jiménez-Martínez, J., Martinez, R., McCulloch, Q., Carey, J. W., and Viswanathan, H. (2015). Geo-material microfluidics at reservoir conditions for subsurface energy resource applications. Lab on a Chip, 15:4044–4053.

47. Hyman, J.D, Jimenez-Martinez, J., Porter, M.L., Karra, S., Carey, J.W., and Viswanathan, H.S. 2016. *Understanding hydraulic fracturing: A multi-scale problem*. Philosophical Transactions of the Royal Society A. 374: 20150426. doi: 10.1098/rsta.2015.0426

48. Jimenez-Martinez, J., Porter, M.L., Hyman, J.D., Carey, J.W., and Viswanathan, H.S. 2015. *Mixing in a three-phase system: Enhanced production of oil-wet reservoirs by* CO_2. Geophysical Research Letters. doi: 10.1002/2015GL066787.

National Energy Technology Laboratory

626 Cochrans Mill Road
P.O. Box 10940
Pittsburgh, PA 15236-0940

3610 Collins Ferry Road
P.O. Box 880
Morgantown, WV 26507-0880

13131 Dairy Ashford Road, Suite 225
Sugar Land, TX 77478

1450 Queen Avenue SW
Albany, OR 97321-2198

Arctic Energy Office
420 L Street, Suite 305
Anchorage, AK 99501

Visit the NETL website at:
www.netl.doe.gov

Customer Service Line:
1-800-553-7681

NATIONAL ENERGY TECHNOLOGY LABORATORY

U.S. DEPARTMENT OF ENERGY | NATIONAL ENERGY TECHNOLOGY LABORATORY